

Electronic Supplementary Information for:

## Rapid Post-Synthetic Modification of Porous Coordination Cages with Copper-Catalyzed Click Chemistry

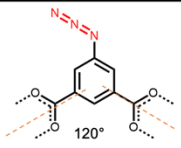
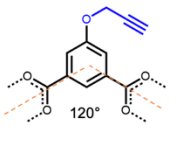
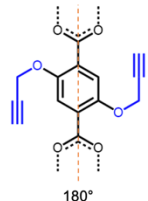
Michael R. Dworzak,<sup>γ,§</sup> Christine M. Montone,<sup>η,§</sup> Nicole I. Halaszynski, Glenn P. A. Yap,<sup>γ</sup>  
Christopher J. Kloxin,<sup>φ, λ,\*</sup> and Eric D. Bloch<sup>γ,η,\*</sup>  
\*email: edbloch@iu.edu; cjk@udel.edu

## List of Contents

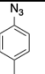


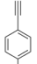
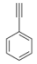
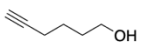
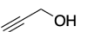
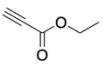
Formulas/nomenclature & Detailed Experimental Procedures	S3-9
<sup>1</sup> H NMR Spectra	S9-23
IR Spectra	S24-33
IR Kinetics Experiments	S34-36
UV-vis Spectroscopy	S37-42
Thermogravimetric Analysis (TGA)	S43-46
Gas Adsorption Measurements	S47-59
Mass Spectrometry	S59-60
Scanning Electron Microscopy Images	S61-67
Detailed Crystallographic Depictions and Information	S68-72
References	S72

## Compound names, structures, & abbreviations

**Table S1.** Starting materials of each cage and their resulting geometry, name, and abbreviations.

Ligand/Coordination Angle	Metal Salt	Cage Shape	Cage Name	Cage Abbreviation
	$\text{Co}(\text{NO}_3)_2 \cdot 6\text{H}_2\text{O}$	Box	$(\text{Co}_4\text{sc}4\text{a})_4(\mu_4\text{-OH})_4(5\text{-azido isophthalic acid})_8$	Co-N <sub>3</sub>
	$[\text{Cp}]_2\text{Zr}(\text{Cl})_2$	Window	$[\text{Zr}_{12}(\mu_3\text{-O})_4(\mu\text{-OH})_{12}(\text{Cp})_{12}(5\text{-azido isophthalic acid})_6]\text{Cl}_4$	Zr(5-N <sub>3</sub> )
	$\text{Co}(\text{NO}_3)_2 \cdot 6\text{H}_2\text{O}$	Box	$(\text{Co}_4\text{sc}4\text{a})_4(\mu_4\text{-OH})_4(5\text{-propargyl isophthalic acid})_8$	Co-ppgy
	$[\text{Cp}]_2\text{Zr}(\text{Cl})_2$	Window	$[\text{Zr}_{12}(\mu_3\text{-O})_4(\mu\text{-OH})_{12}(\text{Cp})_{12}(5\text{-propargyl isophthalic acid})_6]\text{Cl}_4$	Zr(5-ppgy)
	$[\text{Cp}]_2\text{Zr}(\text{Cl})_2$	Tetrahedron	$[\text{Zr}_{12}(\mu_3\text{-O})_4(\mu\text{-OH})_{12}(\text{Cp})_{12}(2,5\text{-dipropargyl terephthalic acid})_6]\text{Cl}_4$	Zr(2,5-dipgy)

**Table S1. (cont.)** List of small molecules and resulting cage after click reactions are complete.

Molecule Structure	Cage Target	Molecule Name	Abbreviation
	Zr(5-ppgy) Zr(2,5-dippgy)	<i>p</i> -azide toluene	N3Tol
	Co-ppgy Zr(5-ppgy) Zr(2,5-dippgy)	3-azide propan-1-ol	C3AP
	Co-ppgy Zr(5-ppgy) Zr(2,5-dippgy)	6-azide hexan-1-ol	C6AH
	Zr(5-N <sub>3</sub> )	Ethynyl toluene	EtTol
	Co-N <sub>3</sub>	Phenyl acetylene	CPA
	Zr(5-N <sub>3</sub> )	5-hexyn-1-ol	C6OH
	Co-N <sub>3</sub> Zr(5-N <sub>3</sub> )	Propargyl alcohol	CPrOH
	Co-N <sub>3</sub>	Ethyl propiolate	CEtPro

## Detailed Experimental Procedures

**Materials and Methods:** All reagents were obtained from commercial vendors and used without purification. For anhydrous procedures, solvents were obtained from a solvent system and stored over 4 Å sieves or in a nitrogen glovebox. All reactions and handling of materials were performed in air unless otherwise specified.

Thermogravimetric Analysis (TGA) were carried out from 30 °C to 600 °C at a 2 °C min<sup>-1</sup> heating rate with a TA Q5000 SA under a nitrogen flow. <sup>1</sup>H NMR spectra were obtained using a Bruker AV 400 MHz spectrometer and data obtained was manipulated in MestReNova NMR processor software. Cobalt cage acid digestions were performed by adding one drop of 35 wt. % DCI in D<sub>2</sub>O and 0.5 mL of DMSO-d<sub>6</sub> to a 4 mL vial containing 10 mg of cage. Zirconium cage digestions were performed by adding a solution of 10 mg CsF in 0.4 mL of D<sub>2</sub>O to a solution of 5 mg cage in 0.6 mL DMSO-d<sub>6</sub> and sonicating for 5 minutes. Infrared spectra were obtained using a Bruker ALPHA II ATR-IR instrument with OPUS data processing software. UV-Vis spectra were obtained using a Jasco V-770 spectral photometer and prepared with Jasco processing software. All mass spectra were obtained using an Acquity UPLC H-class/SQD2 single quadrupole instrument with a 2.5-minute LC-MS analysis program and analyzed with MassLynx software. Gas adsorption measurements were performed on either Micromeritics 3Flex or Tristar gas adsorption analyzers using 4.0 purity gases. Prior to measurements, samples were activated by heating under flowing nitrogen at 100 °C for 2 days. Low-pressure N<sub>2</sub> & CO<sub>2</sub> adsorption measurements were obtained on a Micromeritics Tristar II PLUS or Micromeritics Tristar 3000. BET surface areas were determined and have satisfied the first and second BET consistency criterion.<sup>1</sup>

X-Ray quality crystals were obtained via vapor diffusions unless otherwise noted. Vapor diffusion was performed by transferring 2 mL of mother liquor to a 4 mL scintillation vial after the reaction has cooled. That vial was then placed inside a sealed 20 mL scintillation vial containing



4 mL of ethyl acetate (EtOAc) unless otherwise noted. The sealed apparatus was then allowed to remain undisturbed until x-ray quality crystals were grown.

**Synthesis of *p*-tert-butylthiacalix[4]arene (TC4A)<sup>2</sup>:** To a 1 L round-bottom flask, *p*-tert-butylphenol (64.5 g, 0.43 mol), elemental sulfur (27.5 g, 0.86 mol), NaOH (8.86 g, 0.215 mol), and tetraethylene glycol dimethyl ether (19 mL) were added and stirred under a flow of nitrogen. The mixture was heated to 230 °C over 4 h and held at this temperature overnight. The mixture was allowed to cool to room temperature, yielding a dark-brown solid to which toluene (35 mL) and 4 M H<sub>2</sub>SO<sub>4</sub> (78 mL) were added. The flask was then sonicated for 30 min, and the solubilized material was transferred to a separatory funnel. The organic phase was collected, and MeOH (400 mL) was added, precipitating the product as a light-brown powder that could be isolated by vacuum filtration. This process was repeated until all of the initially generated solid was dissolved. The collected product was dried at 120 °C for 24 h prior to use. (Yield: 16.6 g, 21.5 %) <sup>1</sup>H NMR (400 MHz, DMSO-d<sub>6</sub>) δ = 9.60 (s, 4H), 7.64 (s, 8H), 1.22 (s, 36H).

**Synthesis of *p*-tert-butylsulfonylcalix[4]arene (SC4A)<sup>3</sup>:** In a 1 L round-bottom flask, TC4A (7 g, 46.7 mmol) and sodium perborate tetrahydrate (14 g, 91.0 mmol) were added to a mixture of chloroform (210 mL) and acetic acid (350 mL). The resultant solution was heated with stirring at 50 °C for 18 h. After the solution cooled to room temperature, H<sub>2</sub>O (300 mL) was added, and the solution was transferred to a separatory funnel. The organic layer was collected, and the solvent was removed via rotary evaporation before an excess of Et<sub>2</sub>O was added; the precipitated white solid was collected via vacuum filtration. The product was dried at 120 °C for 24 h prior to use. (Yield: 4.55 g, 55.2 %) <sup>1</sup>H NMR (400 MHz, DMSO-d<sub>6</sub>) δ = 7.98 (s, 8H), 1.27 (m, 36H).

**Synthesis of 5-Propargyl Isophthalic Acid:** was adapted from a previously reported procedure.<sup>4</sup> To a 250 mL round bottom flask, dimethyl 5-hydroxy isophthalate (5 g, 23.8 mmol) and potassium carbonate (5 g, 36.2 mmol) were added and solvated in DMF (100 mL). The solution was cooled to 0°C before the dropwise addition of propargyl bromide (7.7 mL, 71.5 mmol). Upon complete addition, the solution was allowed to warm to room temperature and allowed to stir for 4 hours. The solution was then poured into 500 mL H<sub>2</sub>O and the precipitate collected via vacuum filtration and dried in an oven at 60°C for 24 hours to yield dimethyl 5-propargyl isophthalate. <sup>1</sup>H NMR (400 MHz, CDCl<sub>3</sub>) δ = 8.33 (t, 1H), 7.83 (d, 2H), 4.78 (s, 2H), 3.94 (s, 6H), 2.55 (s, 1H). Dimethyl 5-propargyl isophthalate (5.1 g, 20.5 mmol) and sodium methoxide were then solvated in a 1:1 THF/MeOH solution (160 mL) and H<sub>2</sub>O (160 mL). The mixture was allowed to stir overnight at 85°C. The organic solvent was then removed via rotary evaporation and HCl was added slowly until a pH of 2 was reached. The precipitate was then collected via vacuum filtration, washed with water 3x and dried in an oven at 120°C for 24 hours. <sup>1</sup>H NMR (600 MHz, DMSO-d<sub>6</sub>) δ = 8.11 (t, 1H), 7.71 (d, 2H), 4.94 (s, 2H), 3.62 (s, 1H).

**Synthesis of 5-Azide Isophthalic Acid:** was adapted from a previously reported procedure.<sup>5</sup> To a HCl solution (6 N, 250 mL) 5-amino isophthalic acid was added (5 g, 27.6 mmol) and cooled to 0°C. The suspension was stirred for 30 minutes at 0°C before a 0°C solution of NaNO<sub>2</sub> in H<sub>2</sub>O (1.75 g, 25.4 mmol in 25 mL) was slowly added to the reaction mixture. The mixture was stirred

for an additional 30 minutes at 0°C before a 0°C solution of NaN<sub>3</sub> in H<sub>2</sub>O (1.58 g, 24.3 mmol in 25 mL) was added dropwise upon which the solution bubbled vigorously. The solution was then allowed to warm to room temperature before stirring overnight. The white precipitate was then collected via vacuum filtration and washed with H<sub>2</sub>O 3x before being dried in an oven at 60°C for 24 hours. <sup>1</sup>H NMR (400 MHz, DMSO-d<sub>6</sub>) δ = 13.56 (s, 2H), 8.23 (t, 1H), 7.73 (d, 2H).

**Synthesis of p-azide toluene:** To a 500 mL round bottom flask p-toluidine (3.6 g, 33.6 mmol) was added and dissolved in H<sub>2</sub>O (100 mL). The flask was immersed in a NaCl/ice water bath and allowed to stir for 20 minutes. To this, concentrated HCl (8 mL) and a solution of 1.52 g (22.0 mmol) sodium nitrite in H<sub>2</sub>O was added and allowed to stir for an additional 30 minutes. After this time a solution of sodium azide in H<sub>2</sub>O (1.58 g, 24.3 mmol in 10 mL) was added dropwise. Upon the addition of azide, the solution bubbled vigorously. The reaction was then removed from the ice bath and allowed to stir at room temperature for 14 hours. The product was then extracted 3x with chloroform and concentrated under vacuum to yield a dark amber oil. The product was used without further purification. <sup>1</sup>H NMR (400 MHz, CDCl<sub>3</sub>) δ = 7.18 (d, 2H), 7.01 (d, d2), 2.41 (s, 3H).

**Synthesis of 3-azide 1-propanol:** 3-bromo 1-propanol (3.4 g, 24.3 mmol) was added to a mixture of 3:10 H<sub>2</sub>O:acetone. To this, sodium azide (3.65 g 56 mmol) in H<sub>2</sub>O was added dropwise and allowed to stir for 14 hours at 50 C. Excess acetone was removed under reduced pressure. The remaining slurry was extracted twice with dichloromethane, the organic fractions were combined and washed 3x with H<sub>2</sub>O, dried with magnesium sulfate, and finally concentrated under reduced pressure to yield a pale yellow liquid. The product was used without further purification. <sup>1</sup>H NMR (400 MHz, DMSO-d<sub>6</sub>) δ = 4.55 (t, 1H), 3.47 (m, 5H), 1.60 (m, 2H).

**Synthesis of 6-azide 1-hexanol:** 6-bromo 1-hexanol (2.4 g, 13.3 mmol) was added to a mixture of 3:10 H<sub>2</sub>O:acetone. To this, sodium azide (1.82 g 28 mmol) in H<sub>2</sub>O was added dropwise and allowed to stir for 14 hours at 50 C. Excess acetone was removed under reduced pressure. The remaining slurry was extracted twice with dichloromethane, the organic fractions were combined and washed 3x with H<sub>2</sub>O, dried with magnesium sulfate, and finally concentrated under reduced pressure to yield a clear, colorless liquid. The product was used without further purification. <sup>1</sup>H NMR (400 MHz, DMSO-d<sub>6</sub>) δ = 4.41 (t, 1H), 3.39 (m, 5H), 1.40 (m, 8H).

**Synthesis of 2,5-dipropargyl terephthalic acid:** To a 250mL round bottom flask, dimethyl-2,5-dihydroxy terephthalate (4 g, 17.7mmol) and potassium carbonate (4 g, 28.9mmol) were added and solvated with DMF (100 mL). The flask was then placed in an ice bath and allowed to stir for 20 minutes. Once cold, propargyl bromide (80% in toluene) (20 mL, 214.5 mmol) was added dropwise, maintaining the temperature below 4 °C. The solution was then removed from the ice bath and allowed to stir at room temperature for an additional 18 hours. The reaction mixture was then poured into H<sub>2</sub>O (500 mL), poured over a frit, and washed with additional H<sub>2</sub>O. The product was used for the next step without purification. Dimethyl 2,5-dipropargyl terephthalate (3.5 g, 11.6 mmol) and sodium methoxide (2 g, 37 mmol) was added to a 250 mL round bottom flask and solvated in a 1:1:2 mixture of EtOH:THF:H<sub>2</sub>O (100 mL). The solution was heated at reflux (85°C) for 12 hours. The reaction was cooled then concentrated under vacuum, poured into H<sub>2</sub>O (50 mL) and acidified with 6M HCl until a pH of <1 was reached. The product was then poured over a frit,

washed with additional H<sub>2</sub>O, and dried in an oven at 80 °C for 24 hours. <sup>1</sup>H NMR (400 MHz, DMSO-d<sub>6</sub>) δ = 7.44 (s, 2H), 4.81 (s, 4H), 3.67 (s, 2H).

**Synthesis of (Co<sub>4</sub>sc4a)<sub>4</sub>(μ<sup>4</sup>-OH)<sub>4</sub>(5-propargyl isophthalic acid)<sub>8</sub> [Co-ppgy]:** To a 20 mL scintillation vial, Co(NO<sub>3</sub>)<sub>2</sub>·6H<sub>2</sub>O (145 mg, 0.5 mmol), 5-propargyl isophthalic acid (72.7 mg, 0.33 mmol), and SC4A (85 mg, 0.1 mmol) were added and solvated in DMF (10 mL). The vial was then heated to 100 °C in a dry bath for 24 hours before cooling slowly to room temperature. Diethyl ether was then added to the reaction mixture to precipitate a pink-red amorphous solid. The material was then solvent exchanged and washed five times with MeOH at 12-hour intervals before being dried under vacuum. The material was activated for gas adsorption measurements at 100 °C under flow of N<sub>2</sub>.

**Synthesis of (Co<sub>4</sub>sc4a)<sub>4</sub>(μ<sup>4</sup>-OH)<sub>4</sub>(5-azido isophthalic acid)<sub>8</sub> [Co-N<sub>3</sub>]:** To a 20 mL scintillation vial, Co(NO<sub>3</sub>)<sub>2</sub>·6H<sub>2</sub>O (145 mg, 0.5 mmol), 5-azide isophthalic acid (68.3 mg, 0.33 mmol), and SC4A (85 mg, 0.1 mmol) were added and solvated in DMF (10 mL). The vial was then heated to 100 °C in a dry bath for 24 hours before cooling slowly to room temperature. Diethyl ether was then added to the reaction mixture to precipitate a red-brown amorphous solid. The material was then solvent exchanged and washed five times with MeOH at 12-hour intervals before being dried under vacuum. The material was activated for gas adsorption measurements at 100 °C under flow of N<sub>2</sub>.

**Synthesis of [Zr<sub>12</sub>(μ<sup>3</sup>-O)<sub>4</sub>(μ-OH)<sub>12</sub>(Cp)<sub>12</sub>(5-azido isophthalic acid)<sub>6</sub>]Cl<sub>4</sub> [Zr(5-N<sub>3</sub>)]:** To a 20 mL scintillation vial, zirconocene dichloride (150 mg, 0.51 mmol) and 5-azido isophthalic acid (50 mg, 0.24 mmol) were added and solvated with 10 mL of dry DMF. To this, H<sub>2</sub>O (1 mL) was added, and the solution sonicated until the solution was homogeneous. The vial was heated to 45 °C in a dry bath and kept at temperature for 10 hours, after which was allowed to cool slowly to room temperature. X-ray quality crystals formed as the reaction progressed. Crystalline material was solvent exchanged 3 times with fresh DMF and three times with chloroform, waiting at least 8 hours between each solvent exchange before being dried under vacuum.

**Synthesis of [Zr<sub>12</sub>(μ<sup>3</sup>-O)<sub>4</sub>(μ-OH)<sub>12</sub>(Cp)<sub>12</sub>(5-propargyl isophthalic acid)<sub>6</sub>]Cl<sub>4</sub> [Zr(5-ppgy)]:** To a 20 mL scintillation vial, 150 mg zirconocene dichloride (150 mg, 0.51 mmol) and 5-propargyl isophthalic acid (50 mg, 0.23 mmol) were added and solvated in dry DMF (10 mL). To this, H<sub>2</sub>O (1 mL) was added, and the solution sonicated until the solution was homogenous. The vial was heated to 45 °C in a dry bath and kept at temperature for 10 hours, after which was allowed to cool slowly to room temperature. X-ray quality crystals formed as the reaction progressed. Crystalline material was solvent exchanged 3 times with fresh DMF and then with chloroform, whereby the material dissolves. Product is obtained by precipitation with excess EtOAc, and then washed several times with EtOAc before being dried under vacuum.

**Synthesis of [Zr<sub>12</sub>(μ<sup>3</sup>-O)<sub>4</sub>(μ-OH)<sub>12</sub>(Cp)<sub>12</sub>(2,5-dipropargyl terephthalic acid)<sub>6</sub>]Cl<sub>4</sub> [Zr(2,5-dipgy)]:** To a 20 mL scintillation vial, zirconocene dichloride (150 mg, 0.51 mmol) and 2,5-dipropargyl terephthalic acid (50 mg, 0.18 mmol) were added and solvated in dry DMF (10 mL). To this, H<sub>2</sub>O (1 mL) was added, and the solution sonicated until the solution was homogenous. The vial was heated to 65 °C in a dry bath and kept at temperature for 8 hours, after which was

allowed to cool slowly to room temperature. X-ray quality crystals formed as the reaction progressed. Crystalline material was solvent exchanged 3 times with fresh DMF and three times with chloroform, waiting at least 8 hours between each solvent exchange before being dried under vacuum.

**Representative cobalt cage click reaction:** To a 20 mL scintillation vial, cage material (200 mg) was added along with  $\text{CuSO}_4 \cdot 2.5\text{H}_2\text{O}$  (7 mg) and sodium ascorbate (63 mg) followed by solvation in DMF (20 mL). After sonication, an alkyne or azide functionalized molecule was added (16 equiv.). The reaction was allowed to heat at 65 °C for 48 hours. Upon cooling to room temperature, the mother liquor was decanted away from any precipitate in the reaction vessel and product material was precipitated out of solution with excess diethyl ether. The product was then isolated via centrifuge and washed 3 times with additional diethyl ether before drying under vacuum.

**Representative zirconium cage click reaction:** Cage material (50 mg) was dissolved in dry DMF (20 mL), to which trimethylamine (70  $\mu\text{L}$ ) and an alkyne or azide functionalized molecule (100  $\mu\text{L}$ ) were added. The solution was capped and sparged with nitrogen for 10 minutes. To the solution, a mixture of  $\text{CuI}$  in dry acetonitrile (2 mg in 2 mL) was injected maintaining an air-free solution. The reaction was allowed to proceed at room temperature for 14 hours. The product was then isolated by precipitation with excess diethyl ether, centrifuged, then washed 3 times with additional diethyl ether before drying under vacuum.

**Synthesis of Co-ppgy-3AP:** To a 20 mL scintillation vial, Co-III(5-Propargyl) (200 mg, 0.036 mmol) was added and solvated in DMF (20 mL). To the mixture, sodium ascorbate (63 mg, 0.32 mmol),  $\text{CuSO}_4 \cdot 6\text{H}_2\text{O}$  (7 mg, 0.028 mmol), and 3-azido propanol (53.6  $\mu\text{L}$ , 0.58 mmol) were added and sonicated for 5 minutes. The reaction mixture was then allowed to stand at 60 °C for 2 days. The mother liquor was then decanted away from remaining sodium ascorbate and  $\text{Cu}(0)$  and the clicked product was precipitated with an excess of diethyl ether. The product was collected via centrifuge and washed three times with diethyl ether before being dried under vacuum on a schlenk line.

**Synthesis of Co-ppgy-6AH:** To a 20 mL scintillation vial, Co-III(5-Propargyl) (200 mg, 0.036 mmol) was added and solvated in DMF (20 mL). To the mixture, sodium ascorbate (63 mg, 0.32 mmol),  $\text{CuSO}_4 \cdot 6\text{H}_2\text{O}$  (7 mg, 0.028 mmol), and 6-azido hexanol (83.1 mg, 0.58 mmol) were added and sonicated for 5 minutes. The reaction mixture was then allowed to stand at 60 °C for 2 days. The mother liquor was then decanted away from remaining sodium ascorbate and  $\text{Cu}(0)$  and the clicked product was precipitated with an excess of diethyl ether. The product was collected via centrifuge and washed three times with diethyl ether before being dried under vacuum on a schlenk line.

**Synthesis of Co- $\text{N}_3$ -PrOH:** To a 20 mL scintillation vial, Co-III(5- $\text{N}_3$ ) (200 mg, 0.033 mmol) was added and solvated in DMF (20 mL). To the mixture, sodium ascorbate (63 mg, 0.32 mmol),  $\text{CuSO}_4 \cdot 6\text{H}_2\text{O}$  (7 mg, 0.028 mmol), and propargyl alcohol (30.6  $\mu\text{L}$ , 0.53 mmol) were added and sonicated for 5 minutes. The reaction mixture was then allowed to stand at 60 °C for 2 days. The mother liquor was then decanted away from remaining sodium ascorbate and  $\text{Cu}(0)$  and the

clicked product was precipitated with an excess of diethyl ether. The product was collected via centrifuge and washed three times with diethyl ether before being dried under vacuum on a schlenk line.

**Synthesis of Co-N<sub>3</sub>-EP:** To a 20 mL scintillation vial, Co-III(5-N<sub>3</sub>) (200 mg, 0.033 mmol) was added and solvated in DMF (20 mL). To the mixture, sodium ascorbate (63 mg, 0.32 mmol), CuSO<sub>4</sub>·6H<sub>2</sub>O (7 mg, 0.028 mmol), and ethyl propiolate (53.8 μL, 0.53 mmol) were added and sonicated for 5 minutes. The reaction mixture was then allowed to stand at 60 °C for 2 days. The mother liquor was then decanted away from remaining sodium ascorbate and Cu(0) and the clicked product was precipitated with an excess of diethyl ether. The product was collected via centrifuge and washed three times with diethyl ether before being dried under vacuum on a schlenk line.

**Synthesis of Co-N<sub>3</sub>-PA:** To a 20 mL scintillation vial, Co-III(5-N<sub>3</sub>) (200 mg, 0.033 mmol) was added and solvated in DMF (20 mL). To the mixture, sodium ascorbate (63 mg, 0.32 mmol), CuSO<sub>4</sub>·6H<sub>2</sub>O (7 mg, 0.028 mmol), and phenyl acetylene (58.3 μL, 0.53 mmol) were added and sonicated for 5 minutes. The reaction mixture was then allowed to stand at 60 °C for 2 days. The mother liquor was then decanted away from remaining sodium ascorbate and Cu(0) and the clicked product was precipitated with an excess of diethyl ether. The product was collected via centrifuge and washed three times with diethyl ether before being dried under reduced pressure.

### **<sup>1</sup>H NMR Spectra**

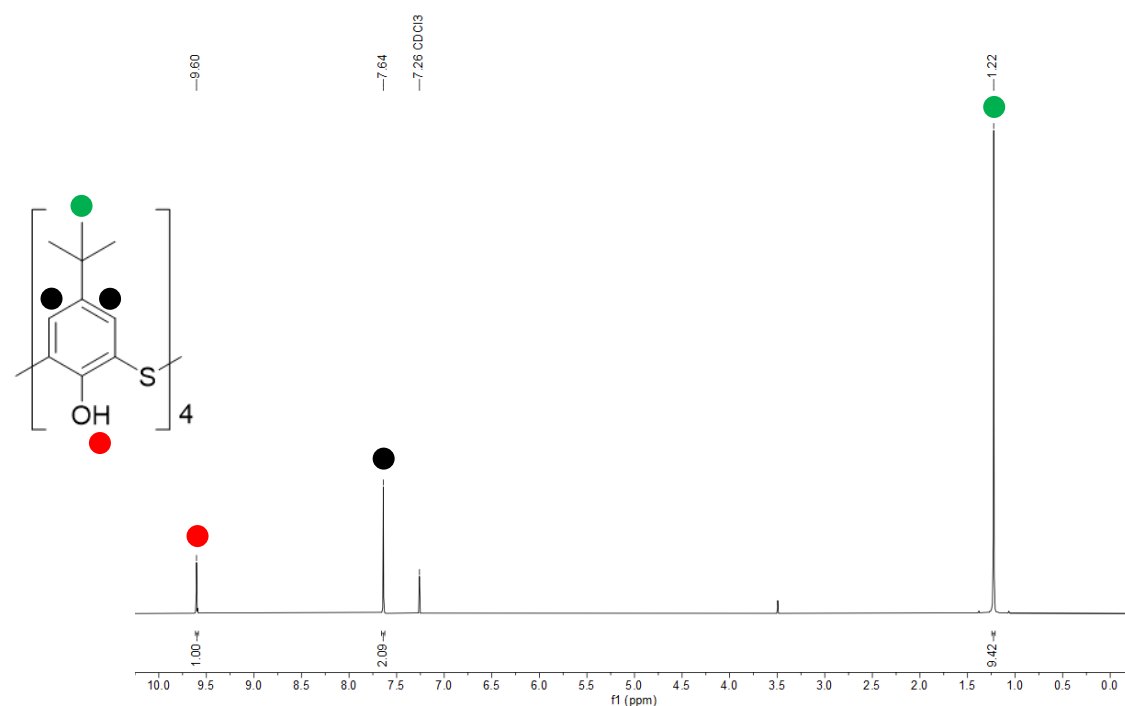


**Figure S1.** <sup>1</sup>H-NMR (400 MHz, DMSO-d<sub>6</sub>) spectrum of *p*-*tert*-butylthiacalix[4]arene.

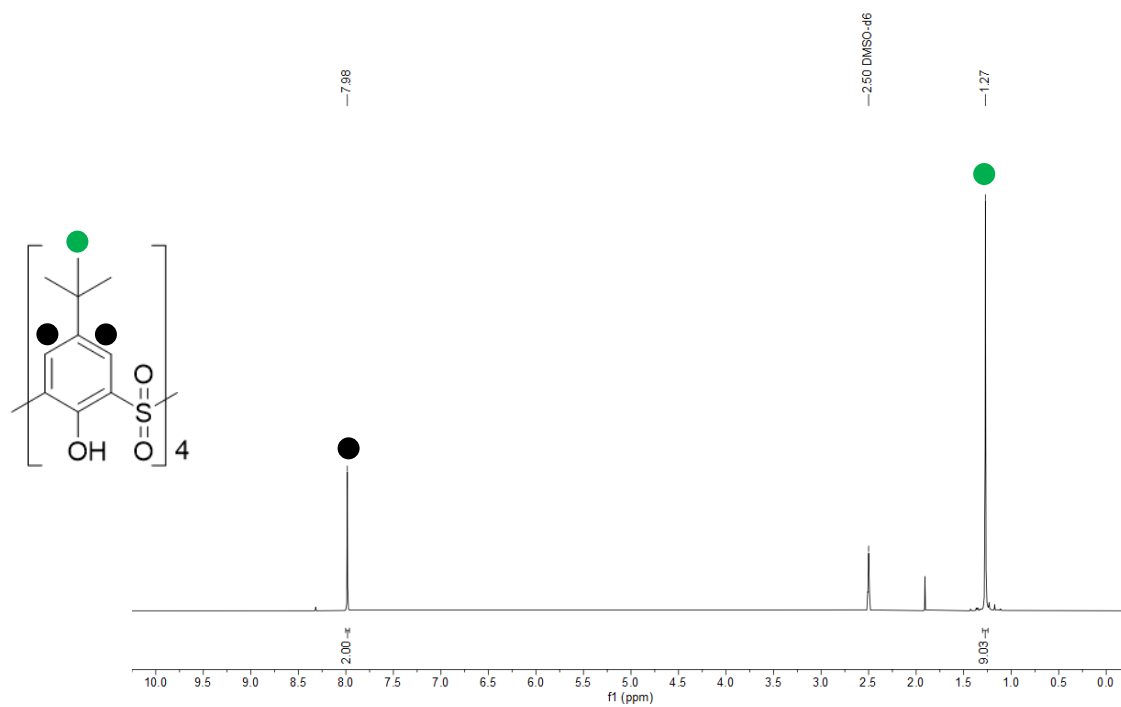


**Figure S2.**  $^1\text{H}$ -NMR (400 MHz, DMSO- $d_6$ ) spectrum of *p*-*tert*-butylsulfonylcalix[4]arene

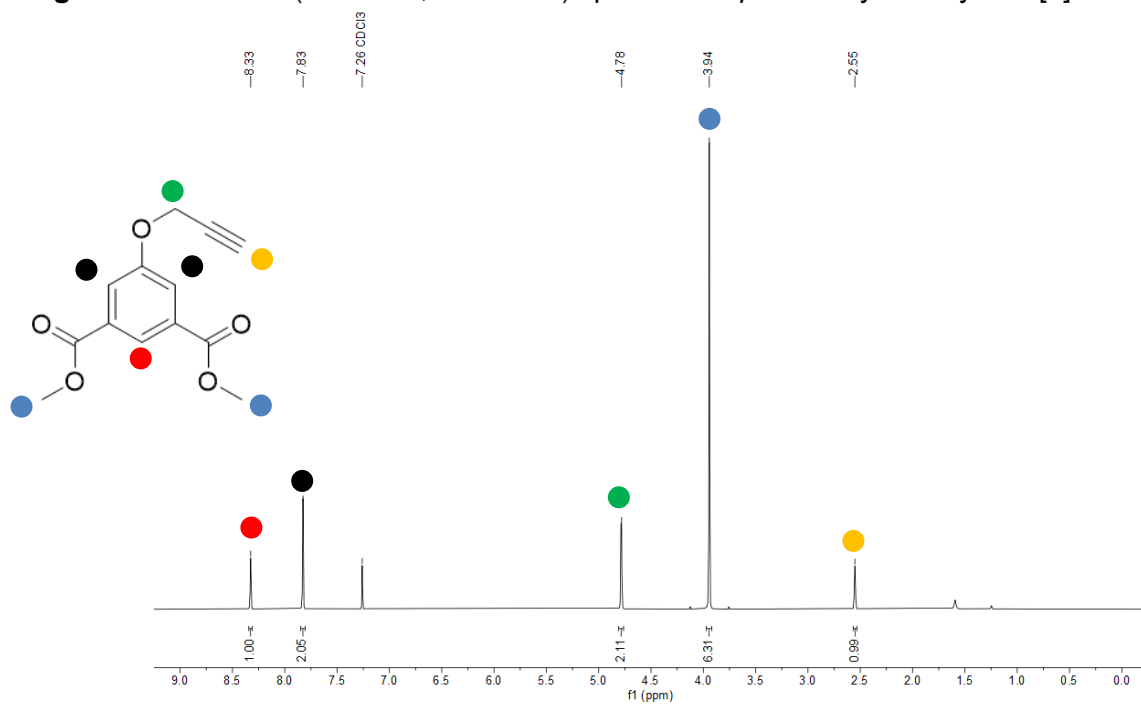


**Figure S3.**  $^1\text{H}$ -NMR (400 MHz, DMSO- $d_6$ ) dimethyl 5-propargyl isophthalate.

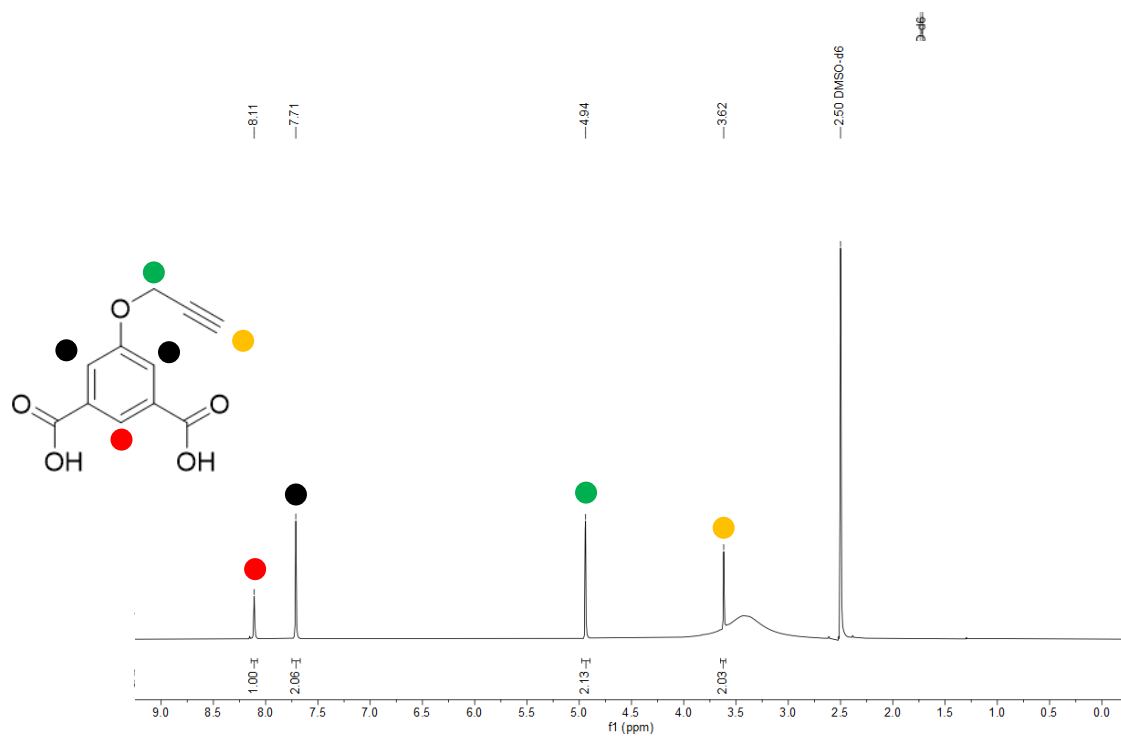


**Figure S4.** <sup>1</sup>H-NMR (600 MHz, DMSO-d<sub>6</sub>) spectrum of 5-propargyl bdc.

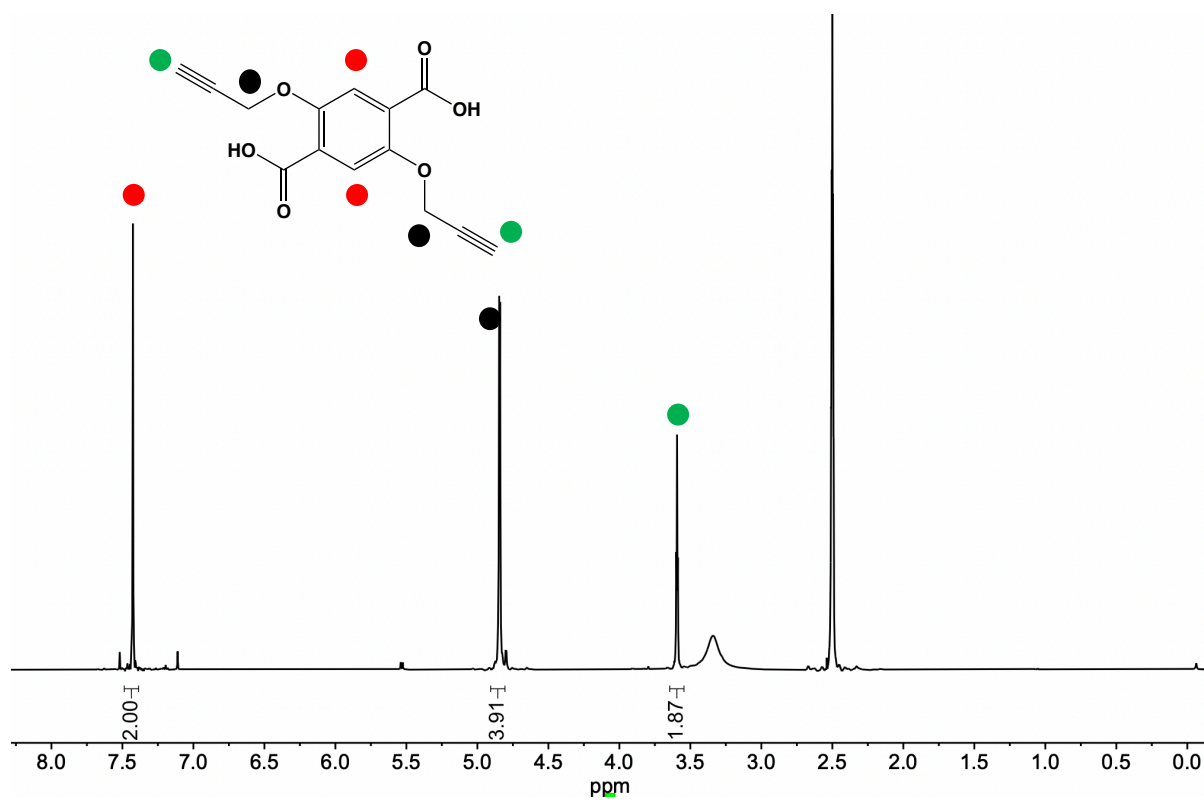


**Figure S5.** <sup>1</sup>H-NMR (600 MHz, DMSO-d<sub>6</sub>) spectrum of 2,5-dipropargyl bdc.

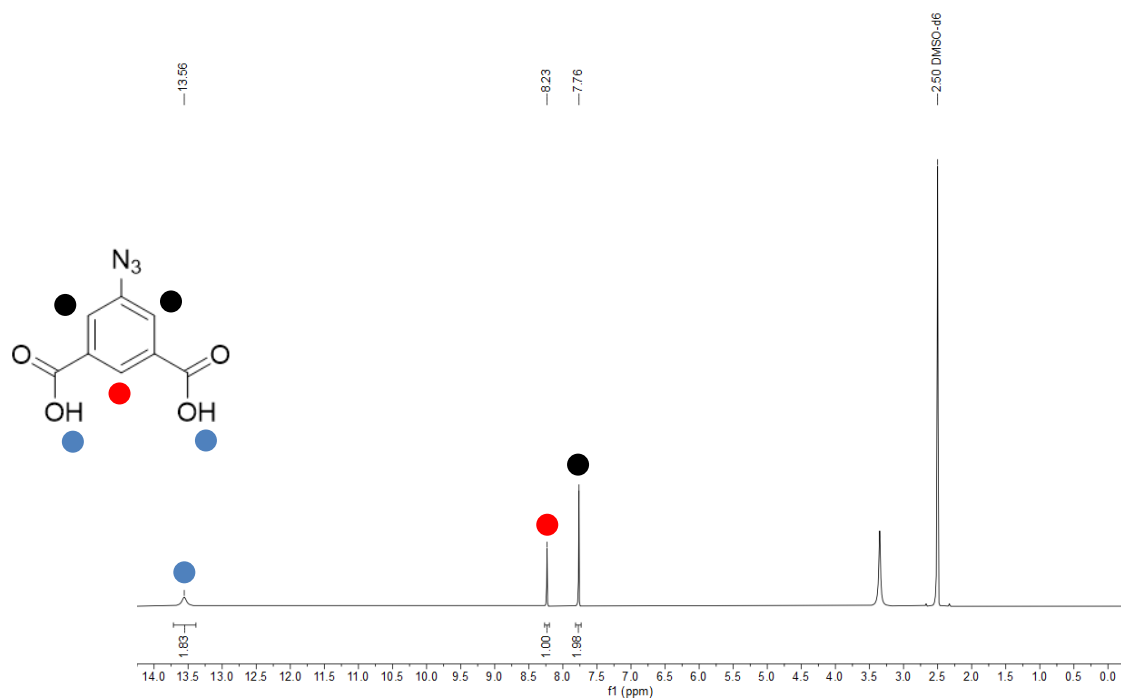


**Figure S6.**  $^1\text{H}$ -NMR (400 MHz,  $\text{DMSO-d}_6$ ) spectrum of 5- $N_3$  bdc.

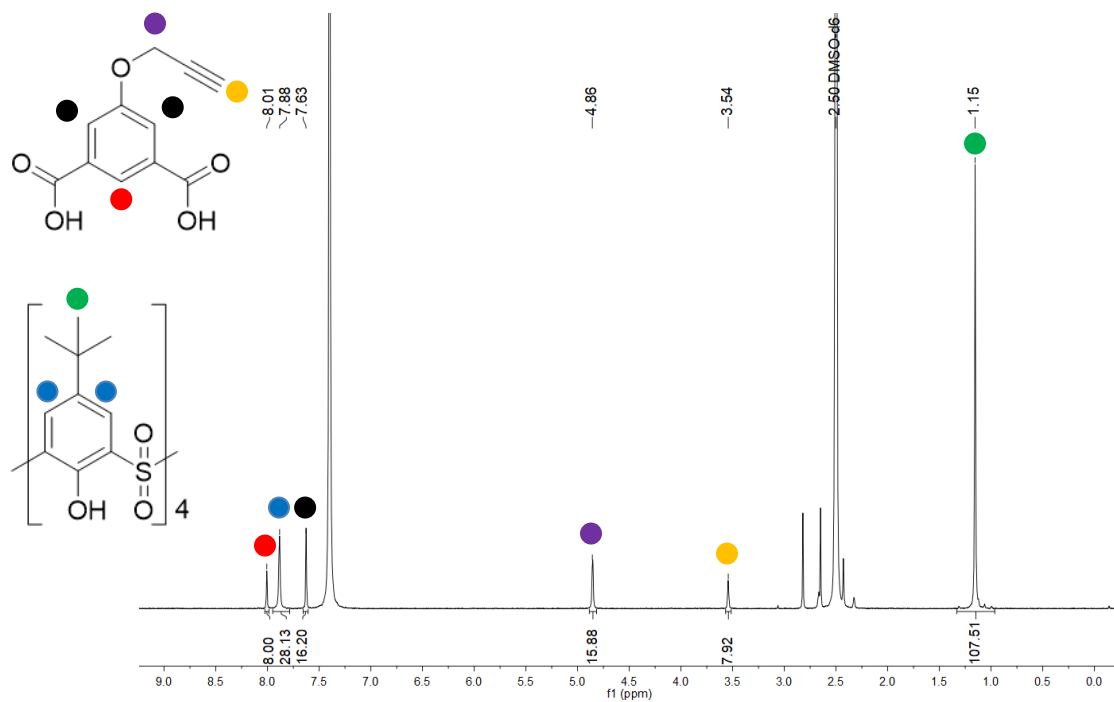


**Figure S7.**  $^1\text{H}$ -NMR (400MHz,  $\text{DMSO-d}_6$ ) spectrum of digested Co-ppgy.



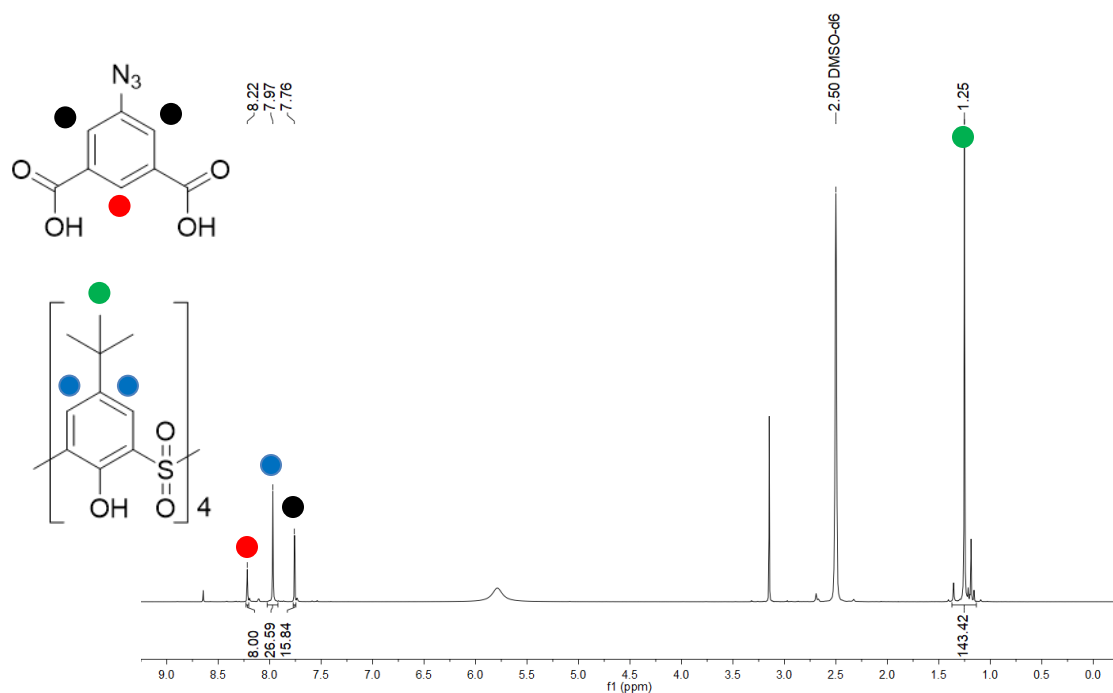


**Figure S8.** <sup>1</sup>H-NMR (400MHz, DMSO-d<sub>6</sub>) spectrum of digested Co-N<sub>3</sub>.

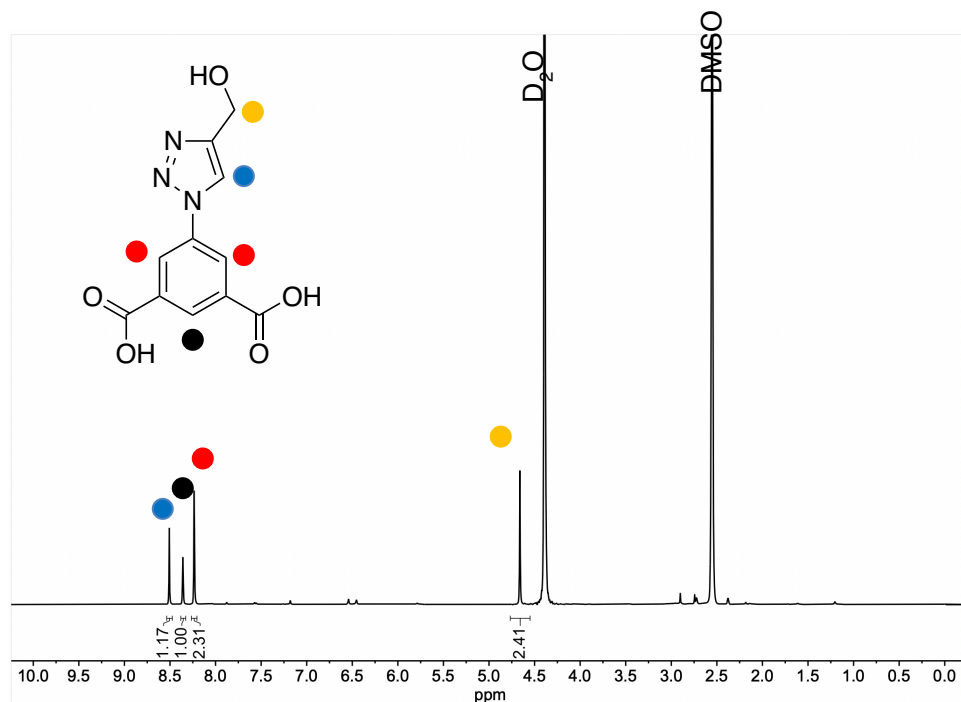


**Figure S9.** Digested <sup>1</sup>H-NMR (400 MHz, DMSO-d<sub>6</sub>/D<sub>2</sub>O) spectrum of Zr(5-N<sub>3</sub>) cage after click reaction with propargyl alcohol.

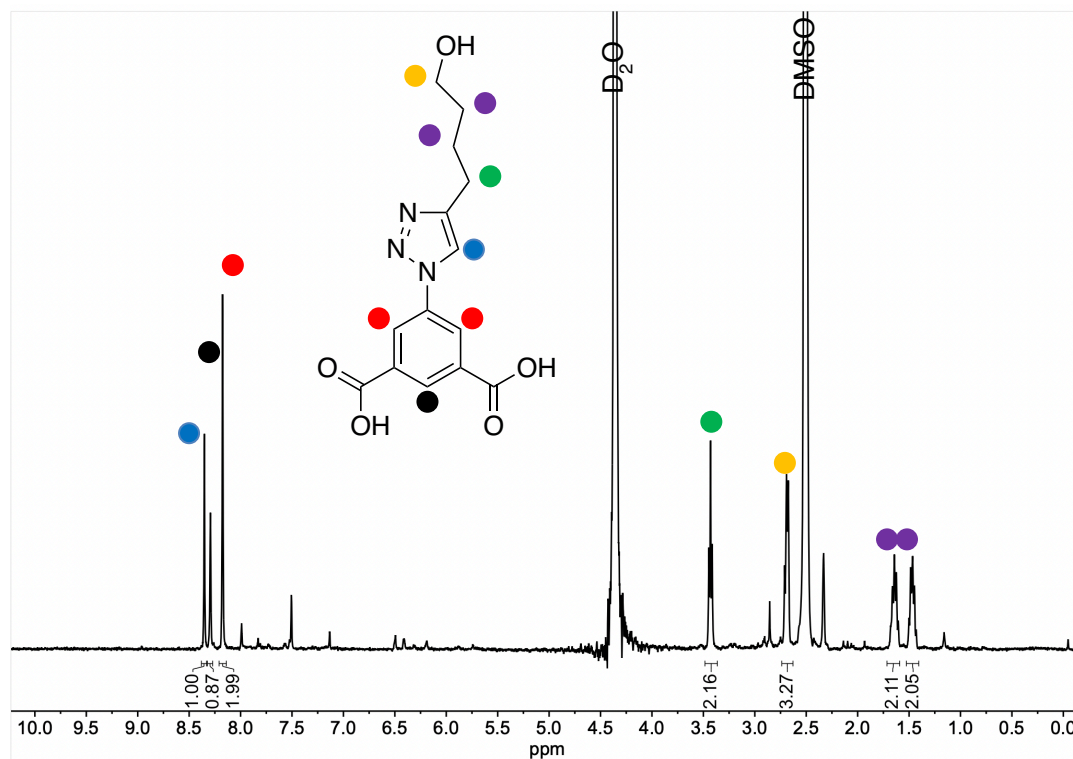


**Figure S10.** Digested  $^1\text{H}$ -NMR (400 MHz,  $\text{DMSO-d}_6/\text{D}_2\text{O}$ ) spectrum of  $\text{Zr}(5\text{-N}_3)$  cage after click reaction with 5-hexyn-1-ol.

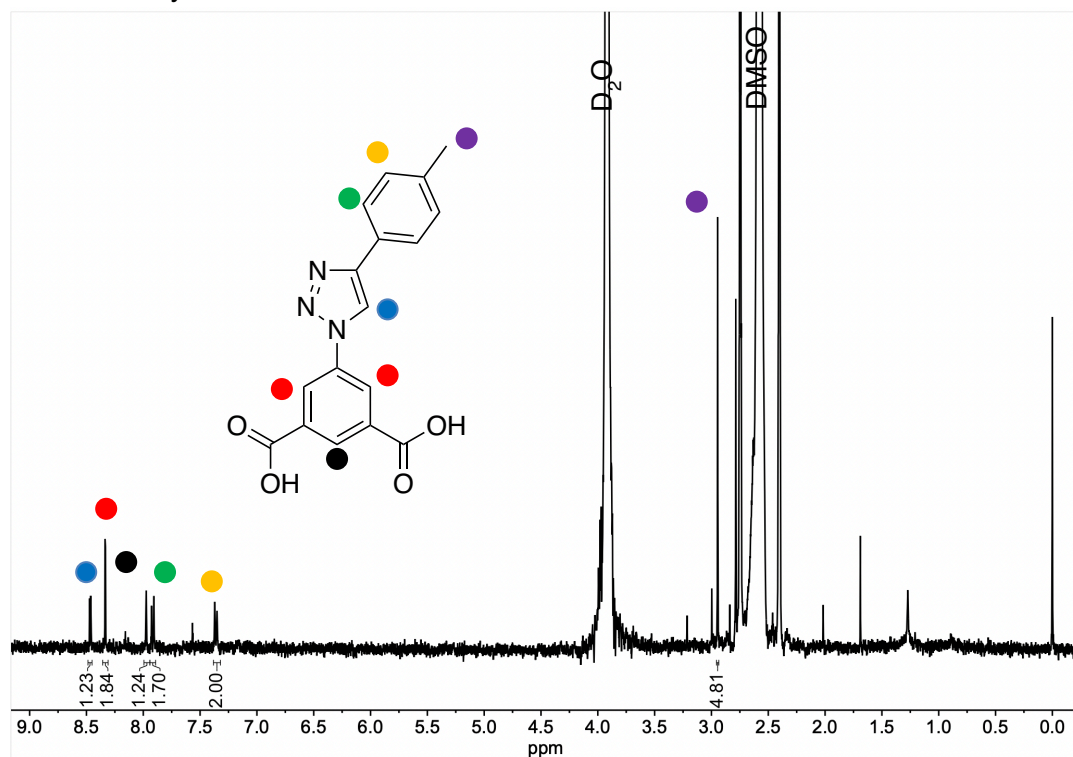


**Figure S11.** Digested  $^1\text{H}$ -NMR (400 MHz,  $\text{DMSO-d}_6/\text{D}_2\text{O}$ ) spectrum of  $\text{Zr}(5\text{-N}_3)$  cage after click reaction with ethynyl toluene.

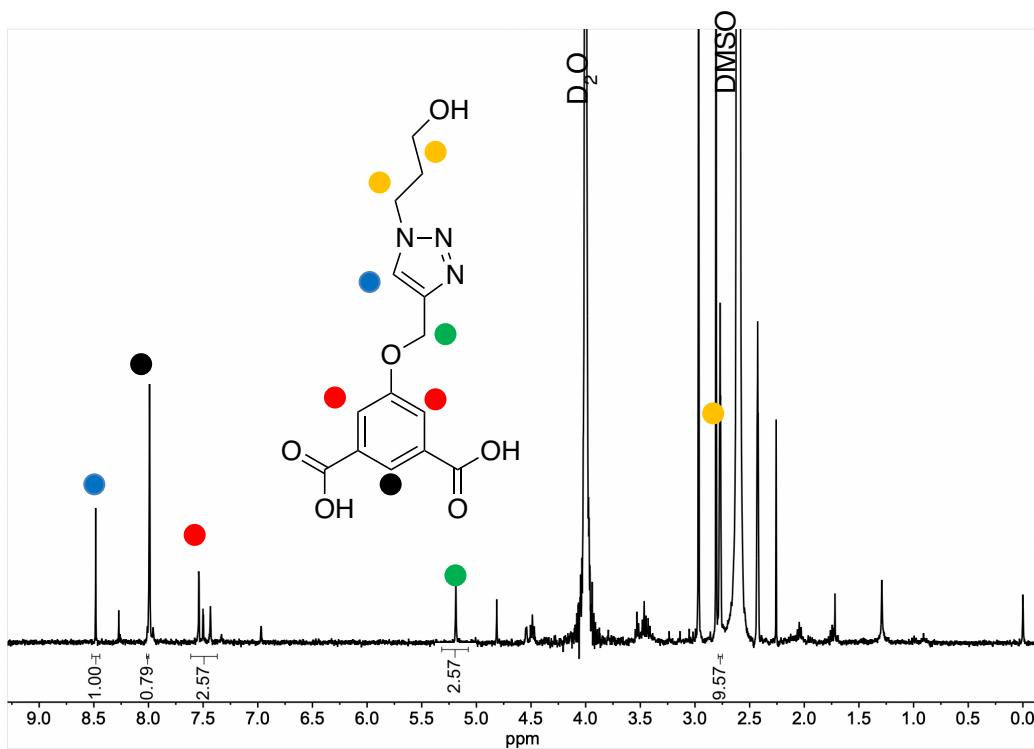


**Figure S12.** Digested  $^1\text{H}$ -NMR (400 MHz,  $\text{DMSO-d}_6/\text{D}_2\text{O}$ ) spectrum of  $\text{Zr}(\text{5-ppgy})$  cage after click reaction with 3-azide 1-propanol.

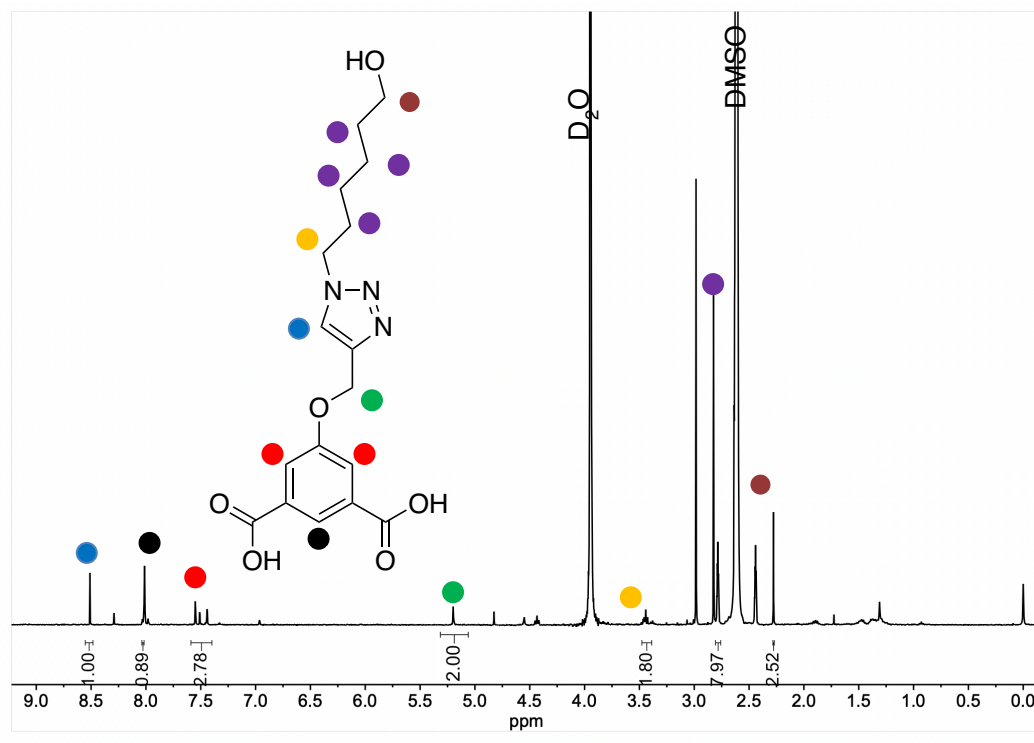


**Figure S13.** Digested  $^1\text{H}$ -NMR (400 MHz,  $\text{DMSO-d}_6/\text{D}_2\text{O}$ ) spectrum of  $\text{Zr}(\text{5-ppgy})$  cage after click reaction with 6-azide 1-hexanol.

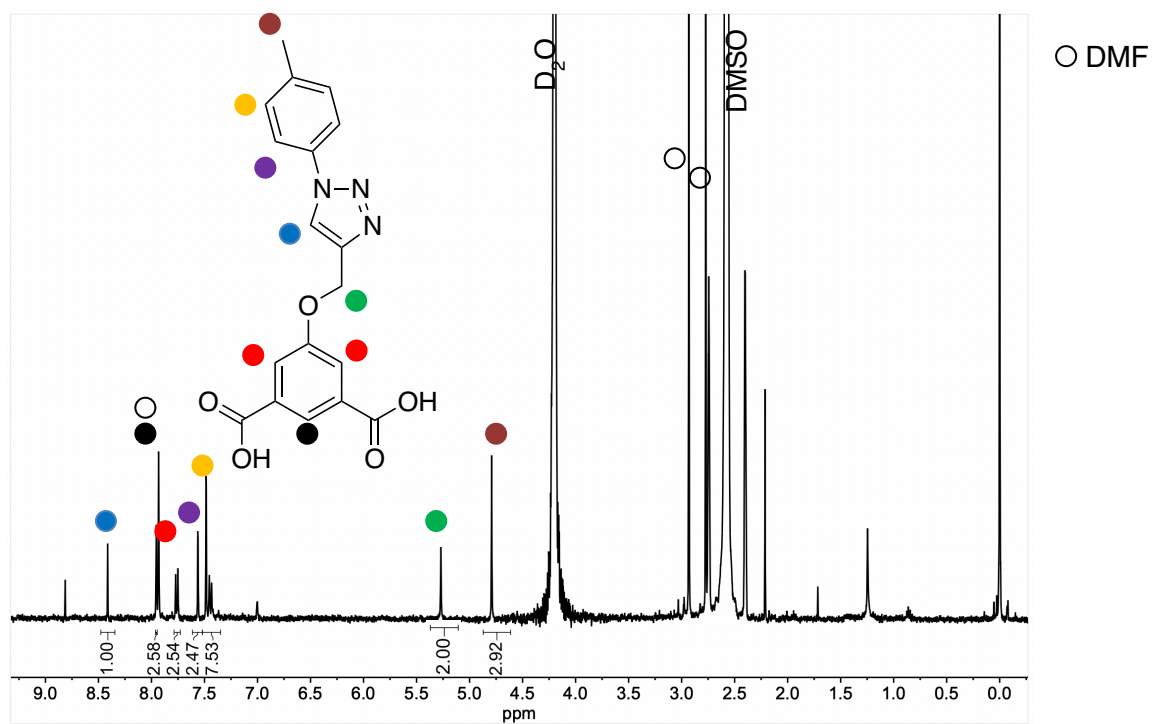


**Figure S14.** Digested  $^1\text{H-NMR}$  (400 MHz,  $\text{DMSO-d}_6/\text{D}_2\text{O}$ ) spectrum of  $\text{Zr(5-ppgy)}$  cage after click reaction with p-azide toluene.

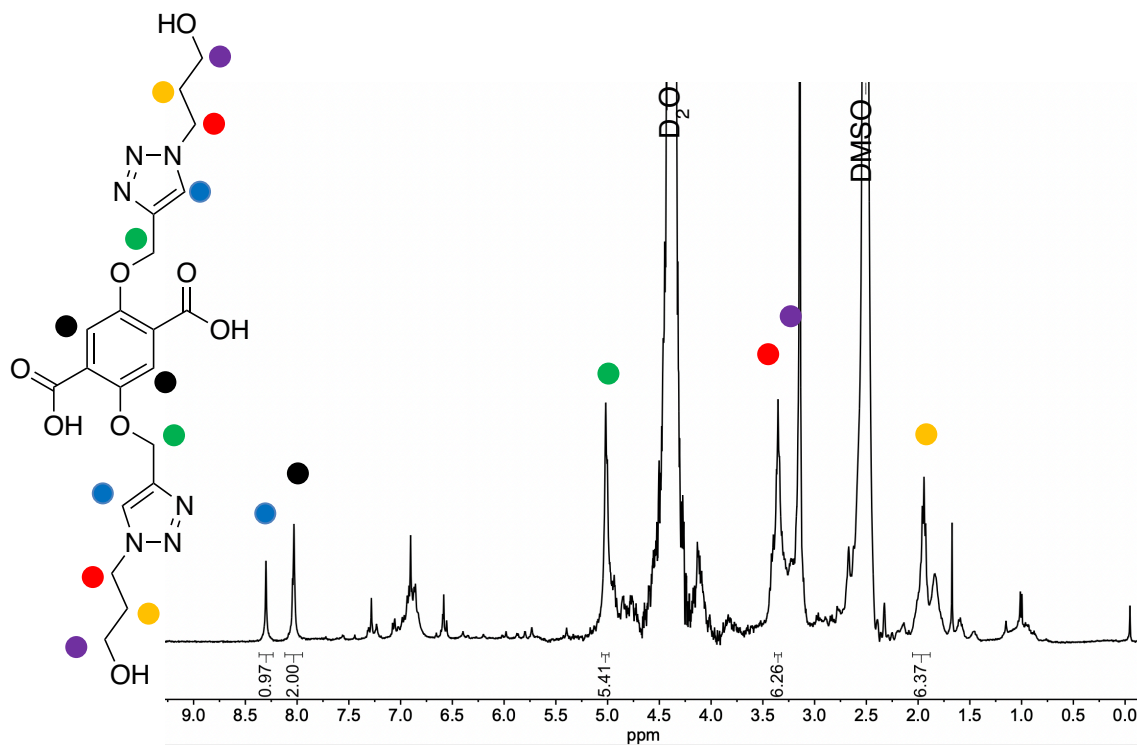


**Figure S15.** Digested  $^1\text{H}$ -NMR (400 MHz, DMSO- $d_6$ /D $_2$ O) spectrum of Zr(2,5-dippgy) cage after incomplete click reaction with 3-azide 1-propanol.

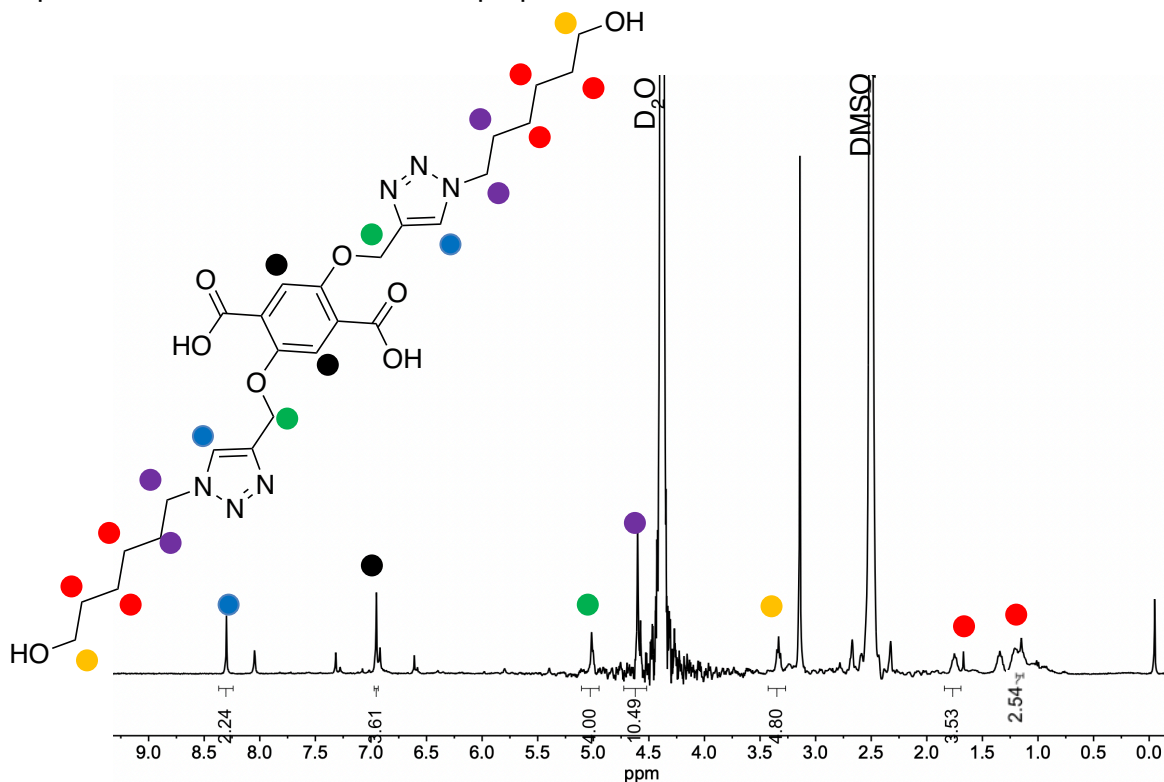


**Figure S16.** Digested  $^1\text{H}$ -NMR (400 MHz, DMSO- $d_6$ /D $_2$ O) spectrum of Zr(2,5-dippgy) cage after click reaction with 6-azide 1-hexanol.

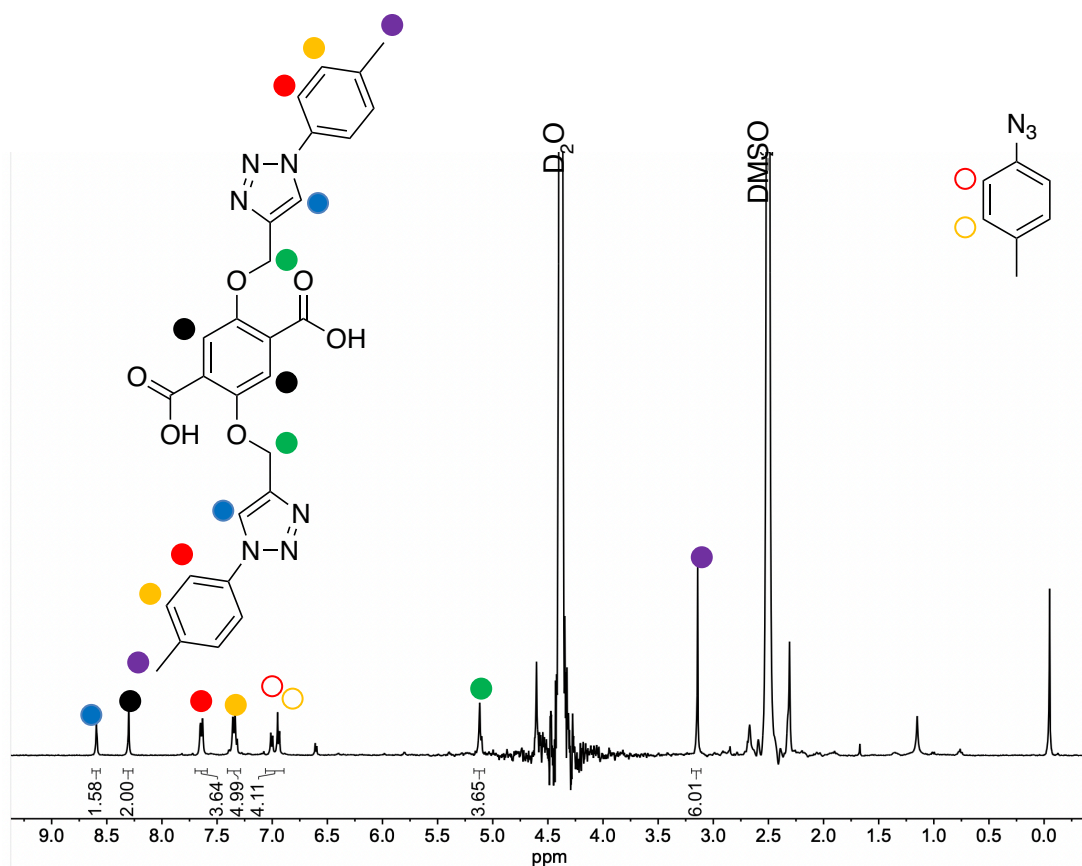


**Figure S17.** Digested  $^1\text{H}$ -NMR (400 MHz,  $\text{DMSO-d}_6/\text{D}_2\text{O}$ ) spectrum of Zr(2,5-dippgy) cage after click reaction with p-azide toluene.

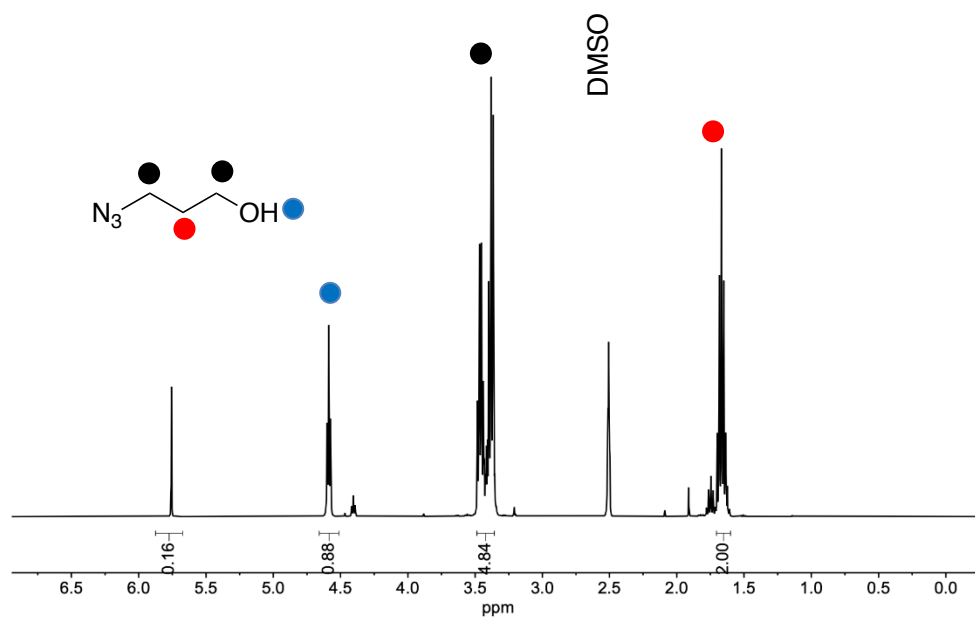


**Figure S18.**  $^1\text{H}$ -NMR (400 MHz,  $\text{DMSO-d}_6$ ) spectrum of 3-azide 1-propanol.

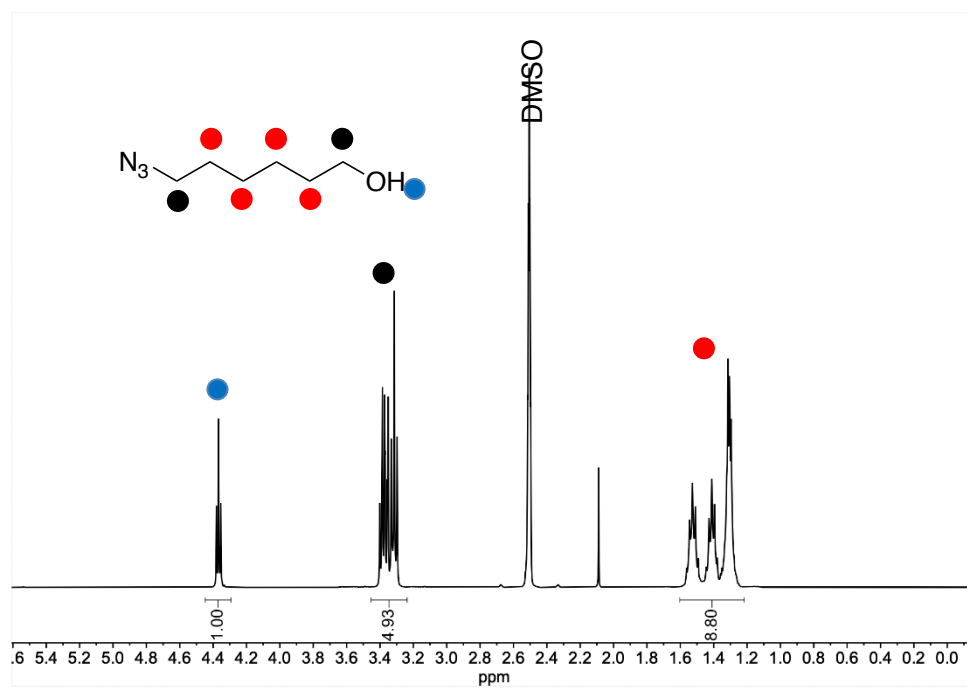


**Figure S19.**  $^1\text{H}$ -NMR (400 MHz,  $\text{DMSO-d}_6$ ) spectrum of 6-azide 1-hexanol.

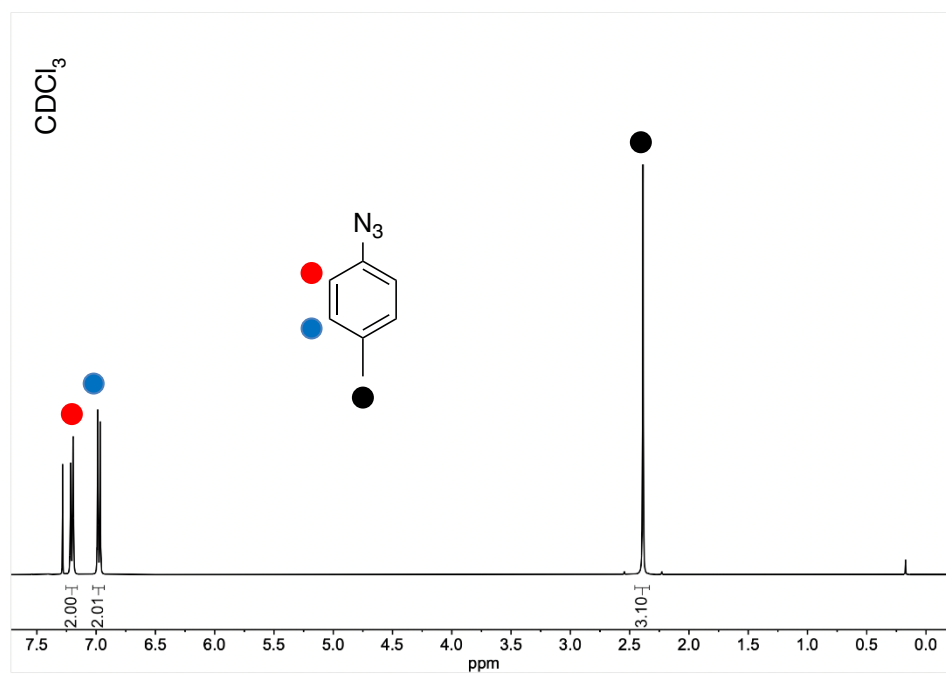


**Figure S20.**  $^1\text{H}$ -NMR (400 MHz,  $\text{CDCl}_3$ ) spectrum of p-azide toluene.



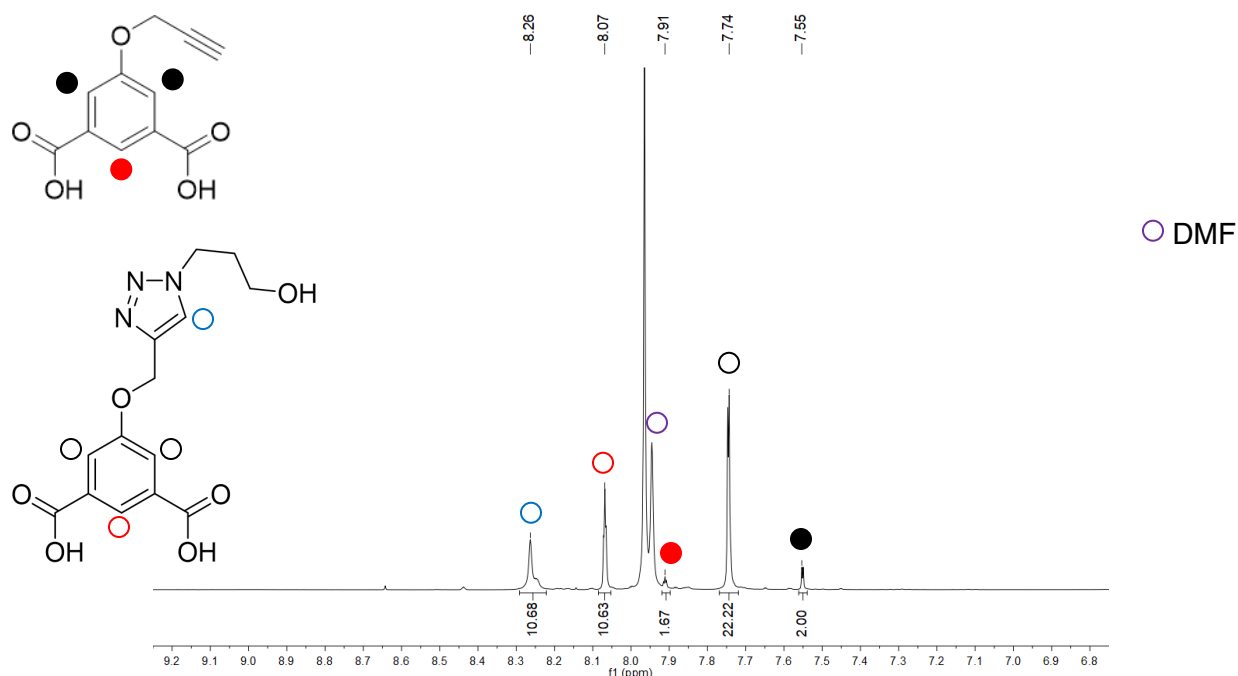


**Figure S21.** Digested  $^1\text{H}$ -NMR (400 MHz,  $\text{DMSO-d}_6$ ) spectrum of Co-ppgy after being allowed to react with 3-azido propanol for 1 hour at 60 °C. showing 91.7 % conversion based on the ratio between the aromatic protons in the product and starting material (black).

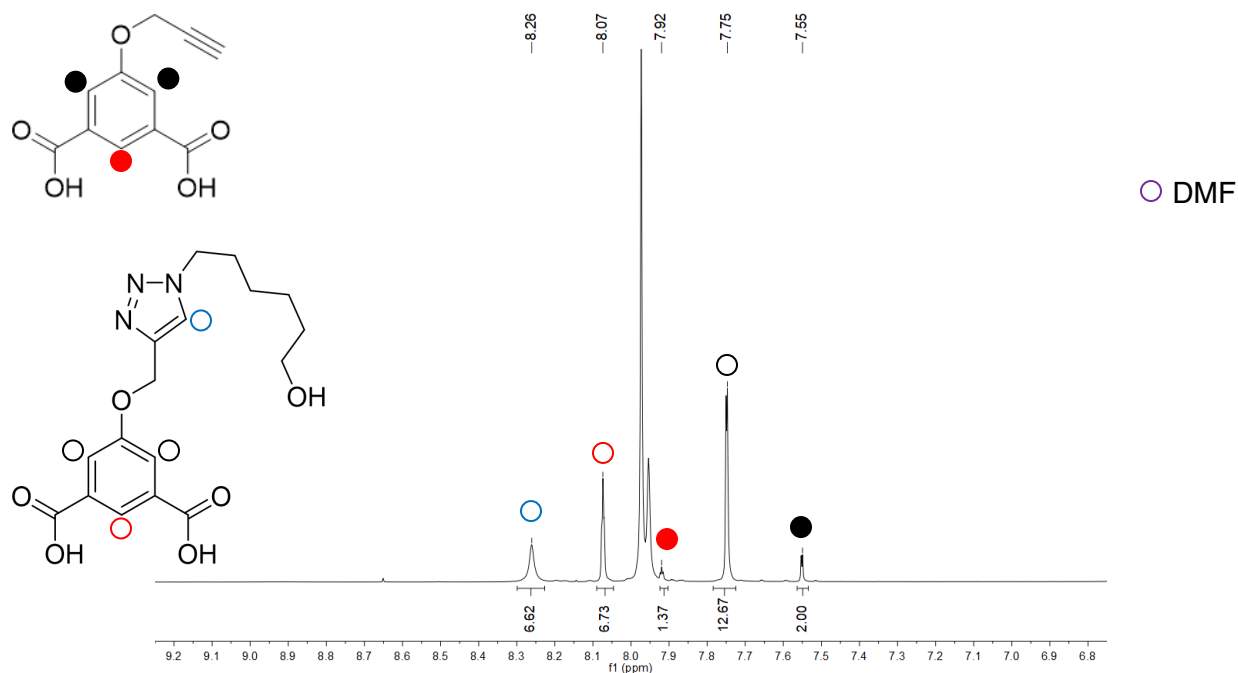


**Figure S22.** Digested  $^1\text{H}$ -NMR (400 MHz,  $\text{DMSO-d}_6$ ) spectrum of Co-ppgy after being allowed to react with 6-azido hexanol for 1 hour at 60 °C. showing 86.4 % conversion based on the ratio between the aromatic protons in the product and starting material (black).



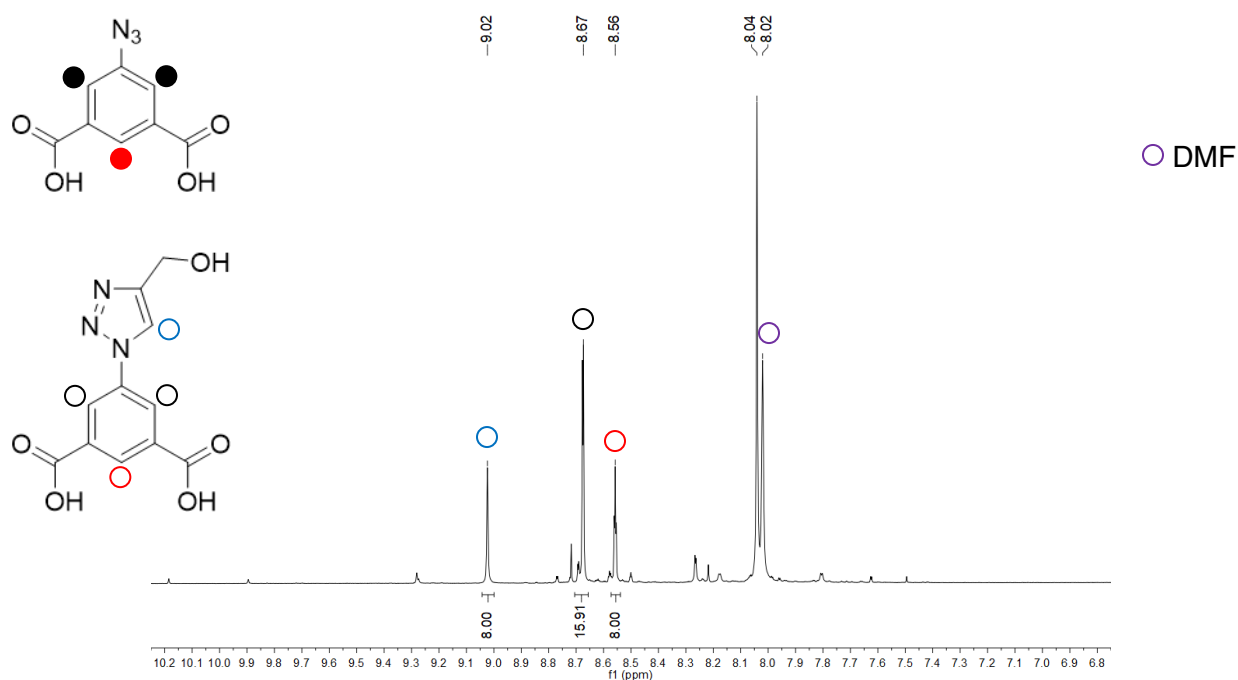


**Figure S23.** Digested  $^1\text{H}$ -NMR (400 MHz,  $\text{DMSO-d}_6$ ) spectrum of  $\text{Co-N}_3$  after being allowed to react with propargyl alcohol for 1 hour at 60 °C. showing full conversion based on the ratio between the newly formed triazole peak and lack of the previously present isophthalate peak.

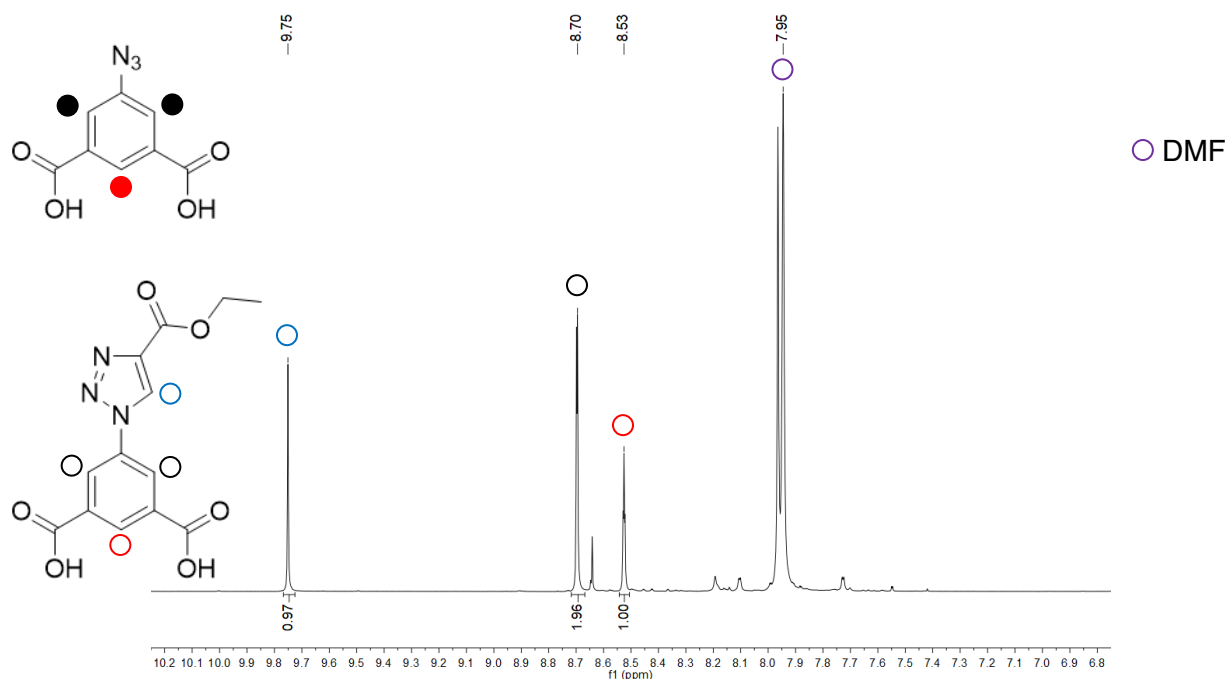


**Figure S24.** Digested  $^1\text{H}$ -NMR (400 MHz,  $\text{DMSO-d}_6$ ) spectrum of  $\text{Co-N}_3$  after being allowed to react with ethyl propiolate for 1 hour at 60 °C. showing full conversion based on the ratio between the newly formed triazole peak and the lack of previously present isophthalate peak.

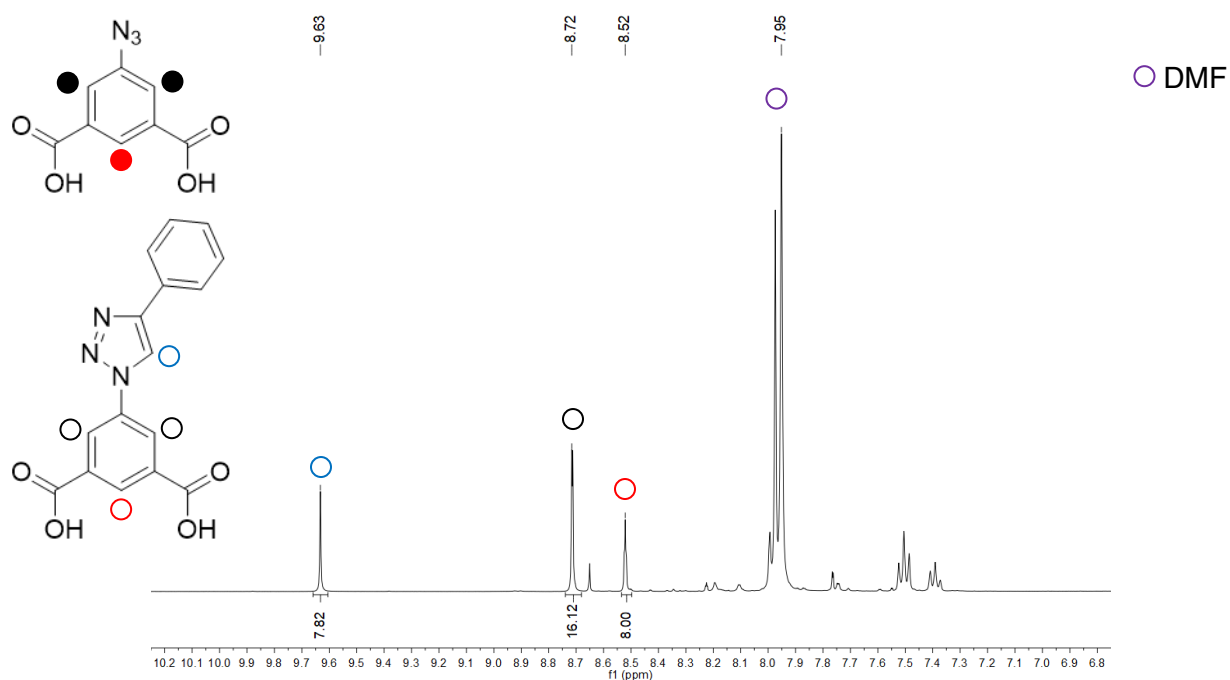


**Figure S25.** Digested  $^1\text{H}$ -NMR (400 MHz,  $\text{DMSO-d}_6$ ) spectrum of  $\text{Co-N}_3$  after being allowed to react with phenyl acetylene for 1 hour at  $60^\circ\text{C}$  showing virtually full conversion based on the ratio between the newly formed triazole peak and the previously present isophthalate peak.

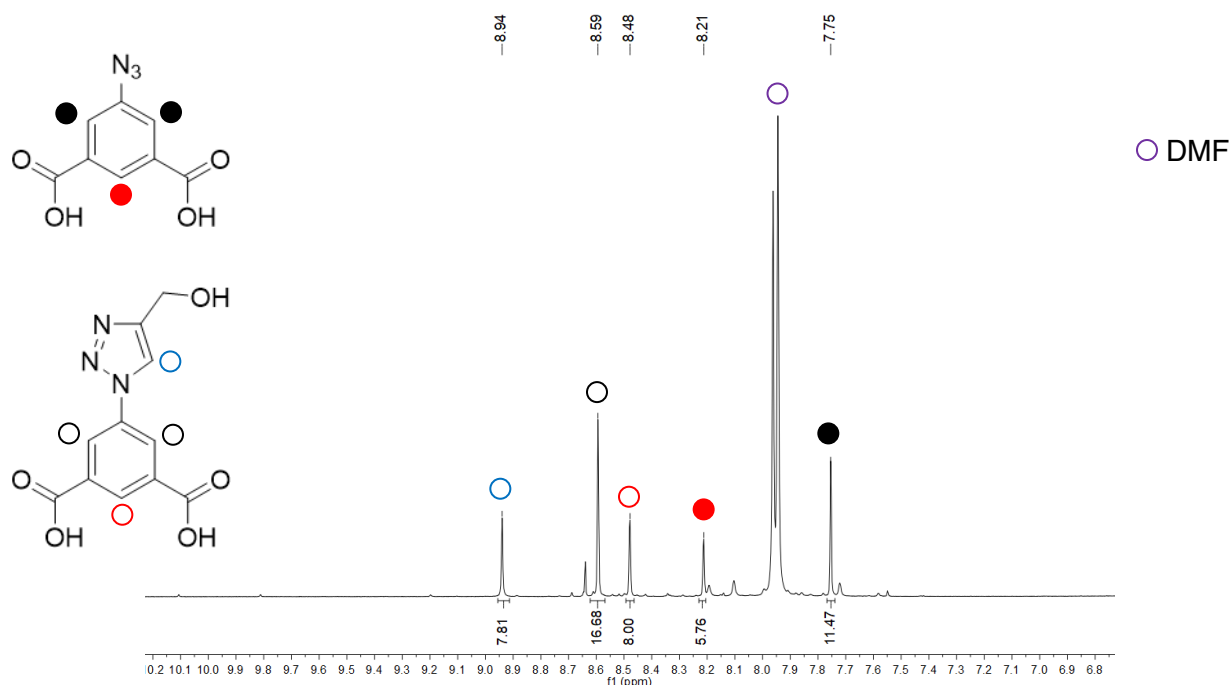


**Figure S26.** Digested  $^1\text{H}$ -NMR (400 MHz,  $\text{DMSO-d}_6$ ) spectrum of  $\text{Co-N}_3$  after being allowed to react with propargyl alcohol for 180 minutes at  $35^\circ\text{C}$ . showing a percent conversion of 59.3 % based on the ratio between the aromatic protons in the product and starting material (black).

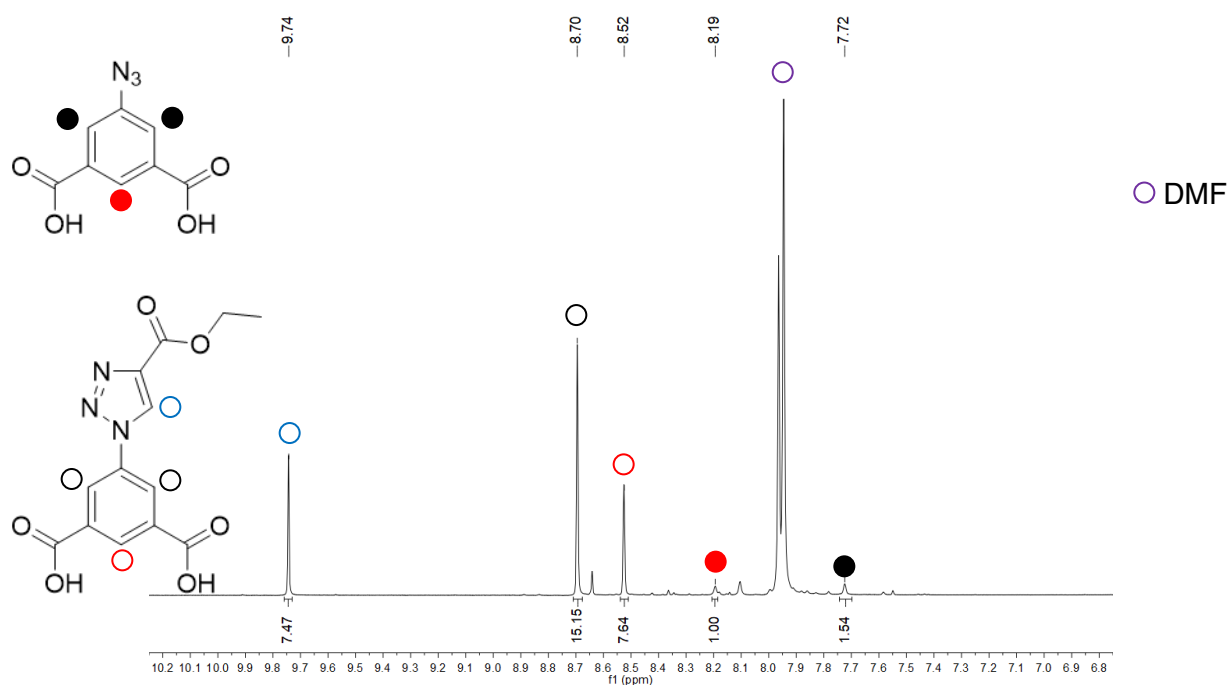


**Figure S27.** Digested  $^1\text{H}$ -NMR (400 MHz,  $\text{DMSO-d}_6$ ) spectrum of  $\text{Co-N}_3$  after being allowed to react with ethyl propiolate for 180 minutes at  $35^\circ\text{C}$  showing a percent conversion of 90.8 % based on the ratio between the aromatic protons in the product and starting material (black).

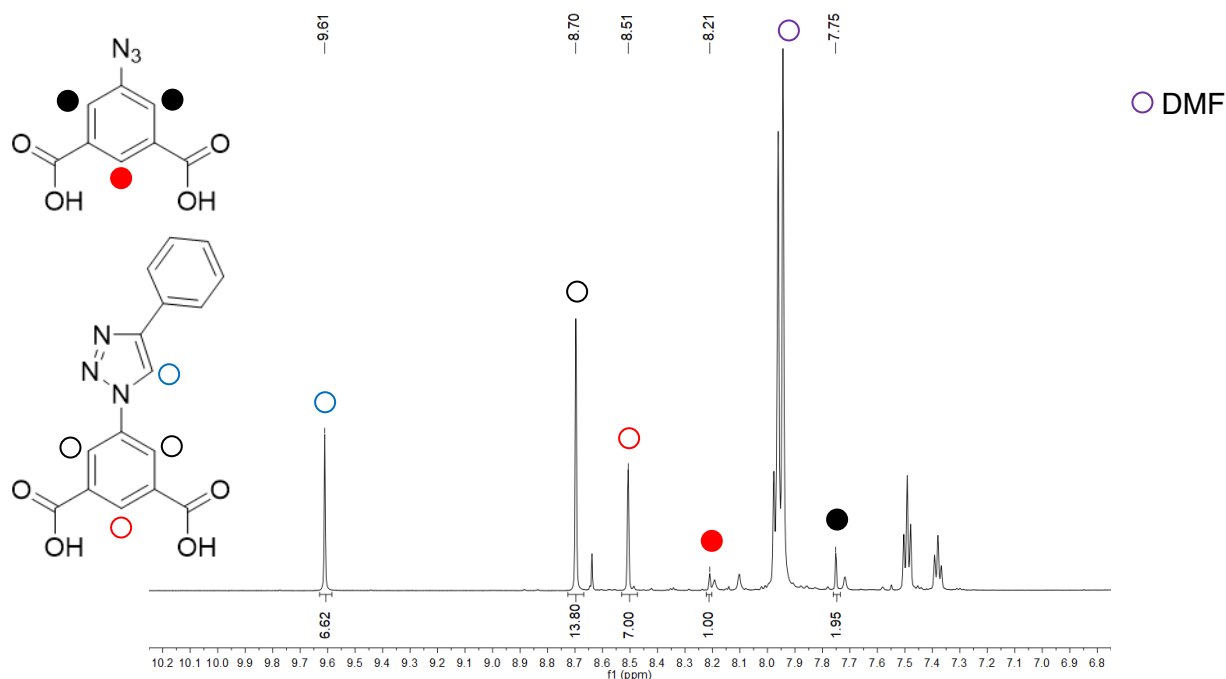


**Figure S28.** Digested  $^1\text{H}$ -NMR (400 MHz,  $\text{DMSO-d}_6$ ) spectrum of  $\text{Co-N}_3$  after being allowed to react with phenyl acetylene for 180 minutes at  $35^\circ\text{C}$  showing a percent conversion of 87.6 % based on the ratio between the aromatic protons in the product and starting material (black).

## IR Spectra

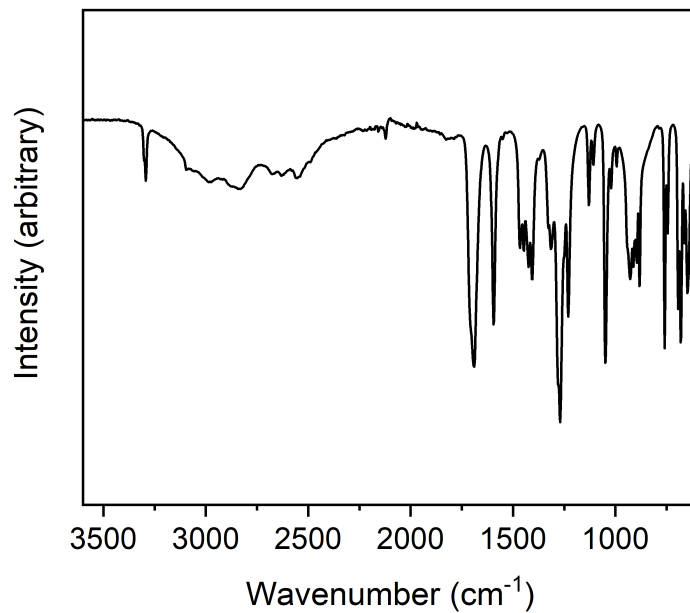


**Figure S29.** IR spectrum of 5-propargyl bdc.

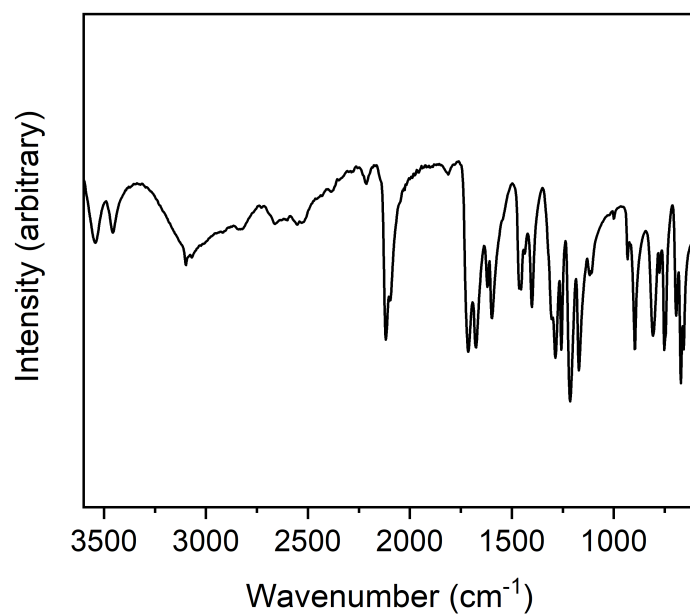


**Figure S30.** IR spectrum of 5-azide bdc.

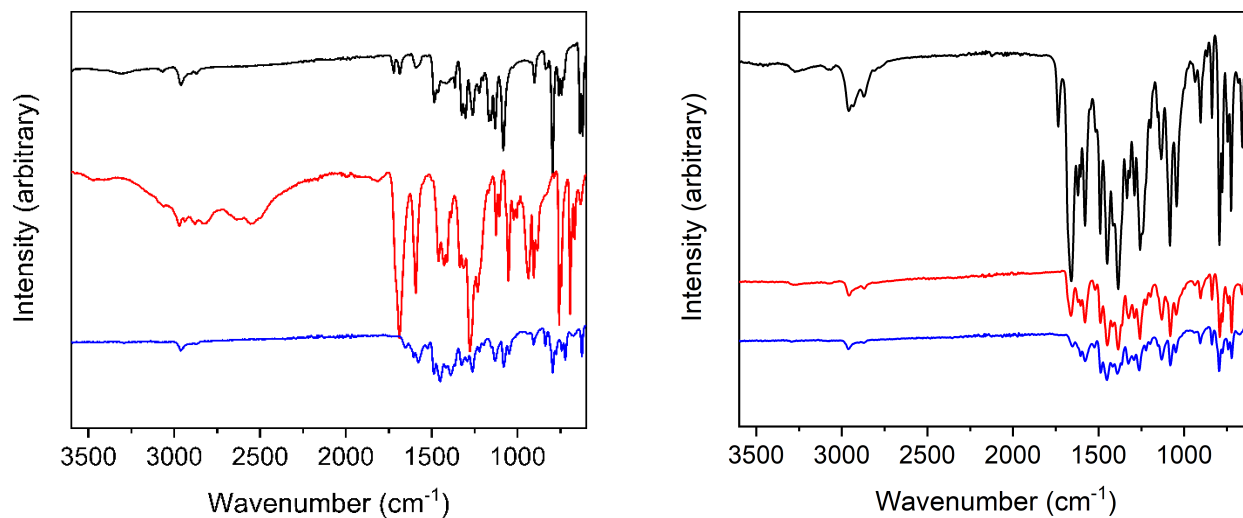


**Figure S31.** (Left) IR spectra of PTBSC4A (black), 5-propargyl isophthalic acid (red), and Co-ppgy activated at 100°C (blue). (Right) IR spectra of Co-ppgy as synthesized (black), solvent exchanged with MeOH (red), and activated at 100°C (blue).

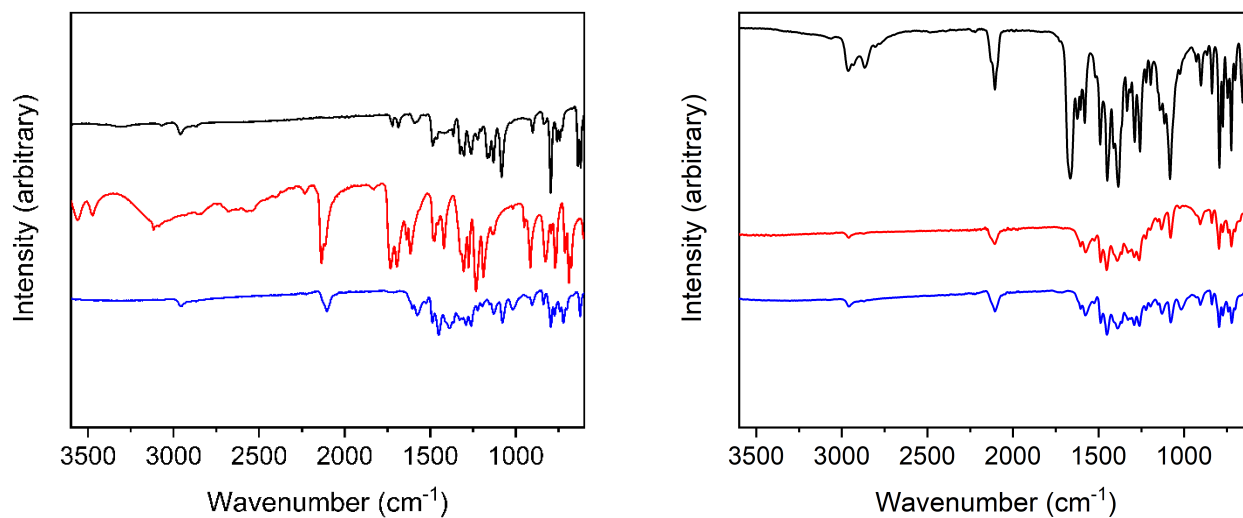


**Figure S32.** (Left) IR spectra of PTBSC4A (black), 5-N<sub>3</sub> isophthalic acid (red), and Co-N<sub>3</sub> activated at 100°C (blue). (Right) IR spectra of Co-N<sub>3</sub> as synthesized (black), solvent exchanged with MeOH (red), and activated at 100°C (blue).

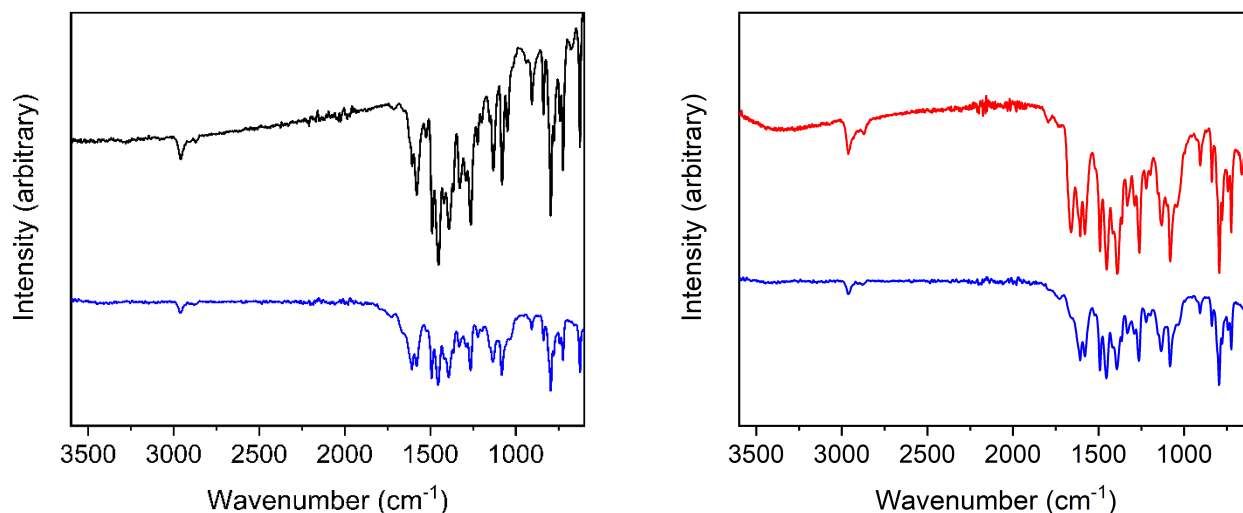


**Figure S33.** (Left) IR spectra of Co-ppgy activated at 100°C (black) and Co-ppgy-3AP activated at 100°C (blue). (Right) IR spectra of Co-ppgy-3AP solvent exchanged with MeOH (red) and activated at 100°C (blue).

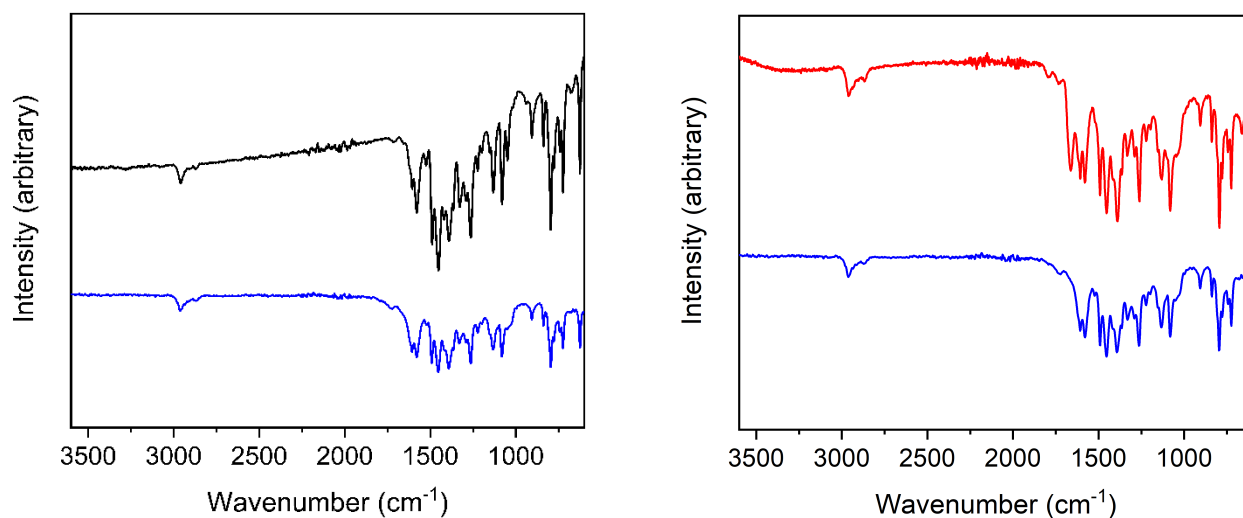


**Figure S34.** (Left) IR spectra of Co-ppgy activated at 100°C (black) and Co-ppgy-6AH activated at 100°C (blue). (Right) IR spectra of Co-ppgy-6AH solvent exchanged with MeOH (red) and activated at 100°C (blue).

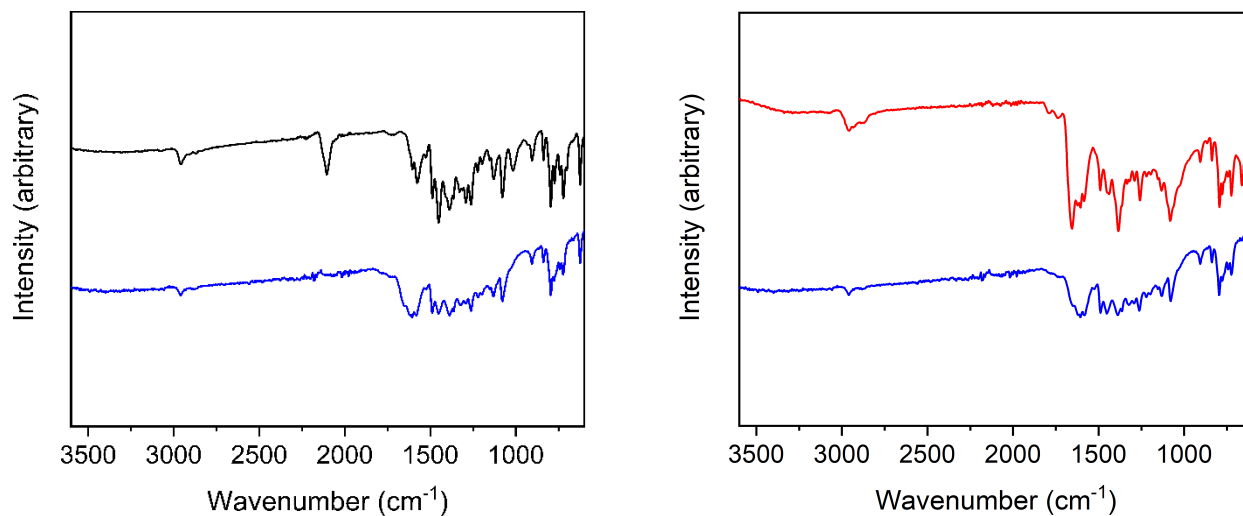


**Figure S35.** (Left) IR spectra of Co-N<sub>3</sub> activated at 100°C (black) and Co-N<sub>3</sub>-PrOH activated at 100°C (blue). (Right) IR spectra of Co-N<sub>3</sub>-PrOH solvent exchanged with MeOH (red) and activated at 100°C (blue).

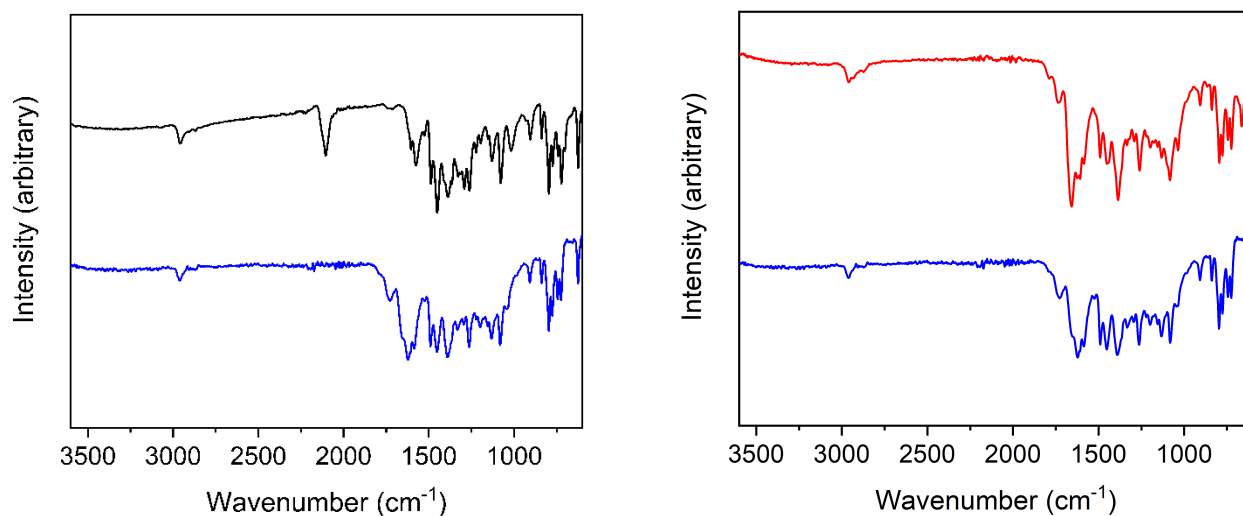


**Figure S36.** (Left) IR spectra of Co-N<sub>3</sub> activated at 100°C (black) and Co-N<sub>3</sub>-EP activated at 100°C (blue). (Right) IR spectra of Co-N<sub>3</sub>-EP solvent exchanged with MeOH (red) and activated at 100°C (blue).

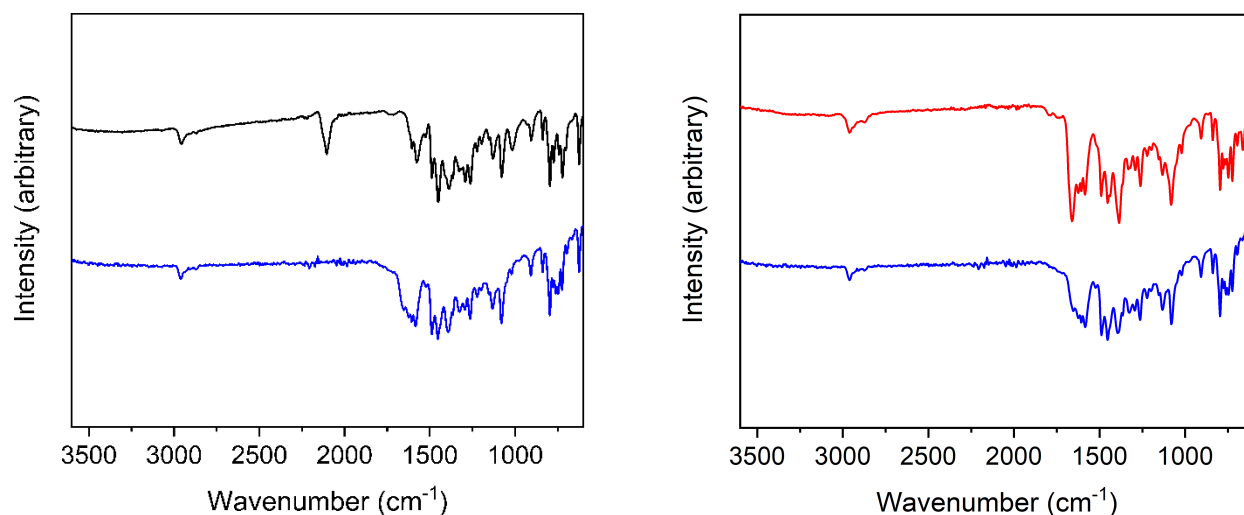


**Figure S37.** (Left) IR spectra of Co-N<sub>3</sub> activated at 100°C (black) and Co-N<sub>3</sub>-PA activated at 100°C (blue). (Right) IR spectra of Co-N<sub>3</sub>-PA solvent exchanged with MeOH (red) and activated at 100°C (blue).

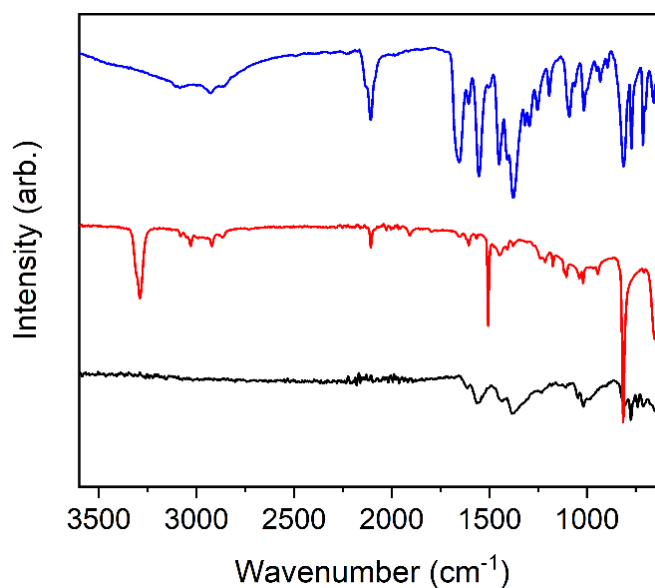


**Figure S38.** IR spectra of Zr(5-N<sub>3</sub>) cage before (blue) and after (black) click reaction with ethynyl toluene (red).



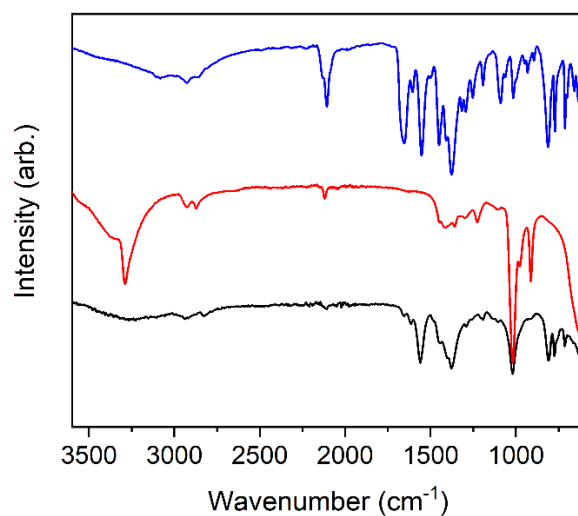


**Figure S39.** IR spectra of Zr(5-N<sub>3</sub>) cage before (blue) and after (black) click reaction with propargyl alcohol (red).

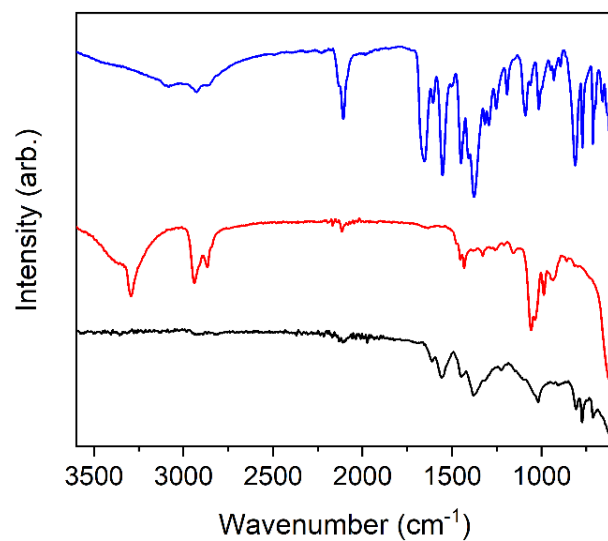


**Figure S40.** IR spectra of Zr(5-N<sub>3</sub>) cage before (blue) and after (black) click reaction with 5-hexyn-1-ol (red).

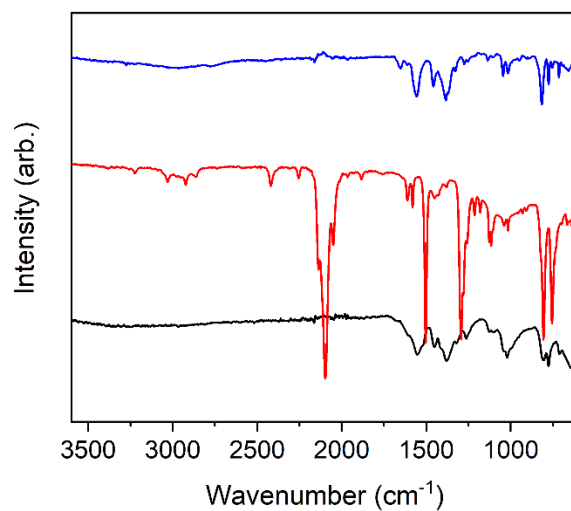


**Figure S41.** IR spectra of Zr(5-ppgy) cage before (blue) and after (black) click reaction with p-azide toluene (red).

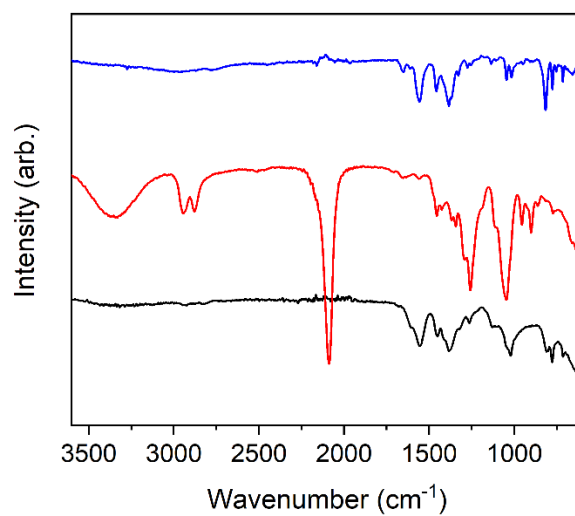


**Figure S42.** IR spectra of Zr(5-ppgy) cage before (blue) and after (black) click reaction with 3-azide 1-propanol (red).

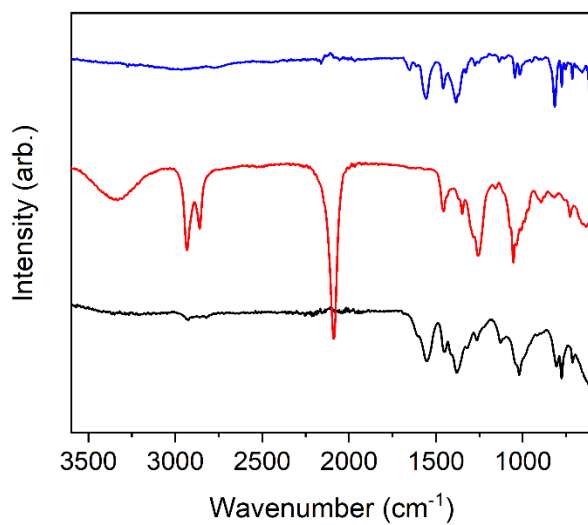


**Figure S43.** IR spectra of Zr(5-ppgy) cage before (blue) and after (black) click reaction with 6-azide 1-hexanol (red).

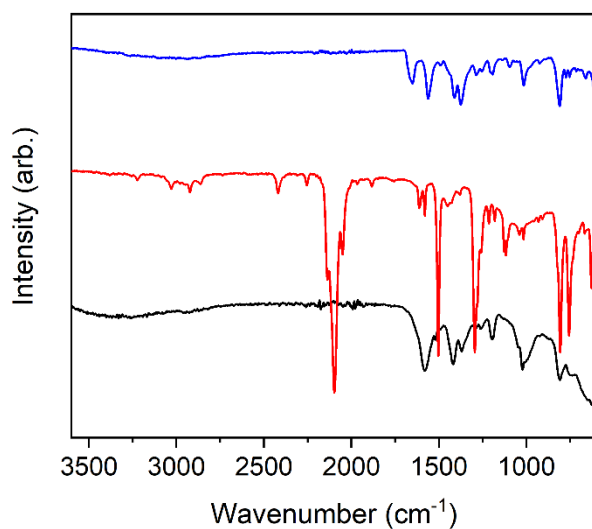


**Figure S44.** IR spectra of Zr(2,5-dippgy) cage before (blue) and after (black) click reaction with p-azide toluene (red).

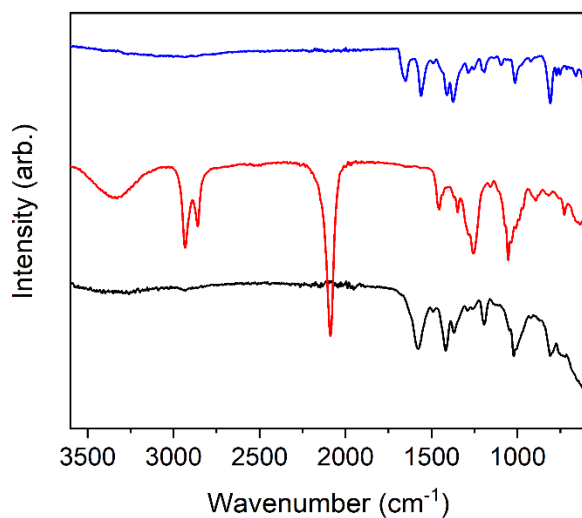


**Figure S45.** IR spectra of Zr(2,5-dippgy) cage before (blue) and after (black) click reaction with 6-azide 1-hexanol (red).

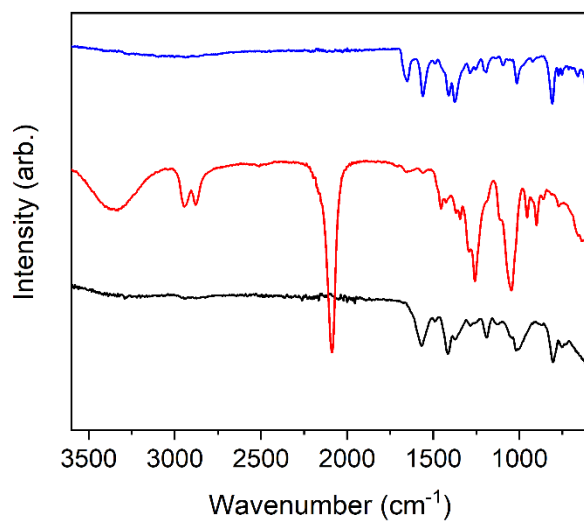


**Figure S46.** IR spectra of Zr(2,5-dippgy) cage before (blue) and after (black) click reaction with 3-azide 1-propanol (red).

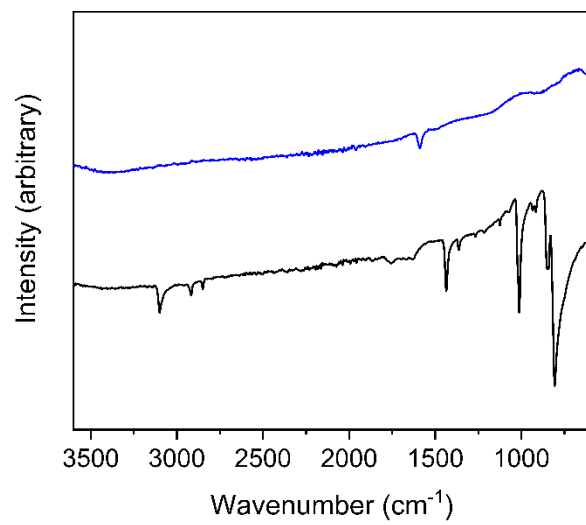


**Figure S47.** IR spectra of ZrCl<sub>4</sub> (black) & [Cp<sub>2</sub>]ZrCl<sub>2</sub> (blue).

### Kinetic Monitoring via IR

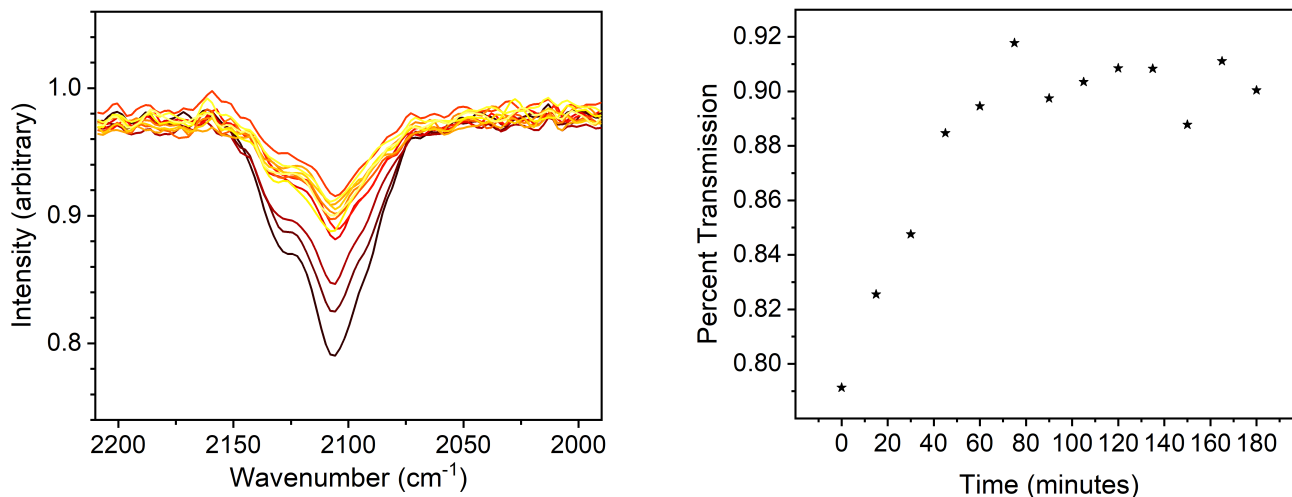


**Figure S48.** Left: Azide IR stretch from 2200 to 2000  $\text{cm}^{-1}$  of  $\text{Co-N}_3$  as it reacts with propargyl alcohol yielding  $\text{Co-N}_3\text{-PrOH}$ , monitored from 0 minutes (dark red) to 180 minutes (yellow). Right: Percent transmission of the azide stretch observed in the IR spectra versus time.

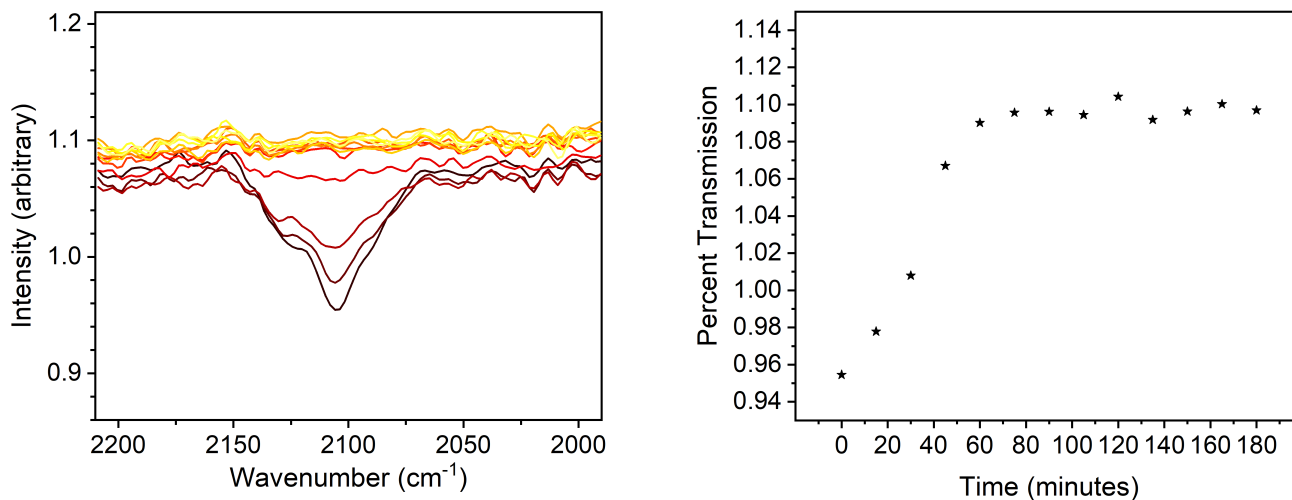


**Figure S49.** Left: Azide IR stretch from 2200 to 2000  $\text{cm}^{-1}$  of  $\text{Co-N}_3$  as it reacts with ethyl propiolate yielding  $\text{Co-N}_3\text{-EP}$ , monitored from 0 minutes (dark red) to 180 minutes (yellow). Right: Percent transmission of the azide stretch observed in the IR spectra versus time.

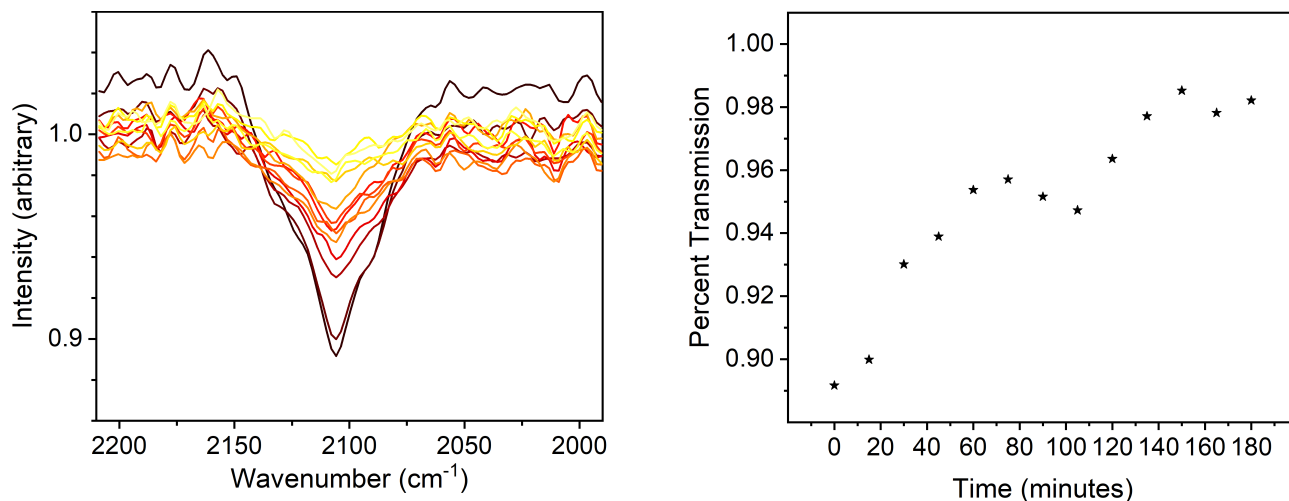


**Figure S50.** Left: Azide IR stretch from 2200 to 2000  $\text{cm}^{-1}$  of  $\text{Co-N}_3$  as it reacts with phenyl acetylene yielding  $\text{Co-N}_3\text{-PA}$ , monitored from 0 minutes (dark red) to 180 minutes (yellow). Right: Percent transmission of the azide stretch observed in the IR spectra versus time.

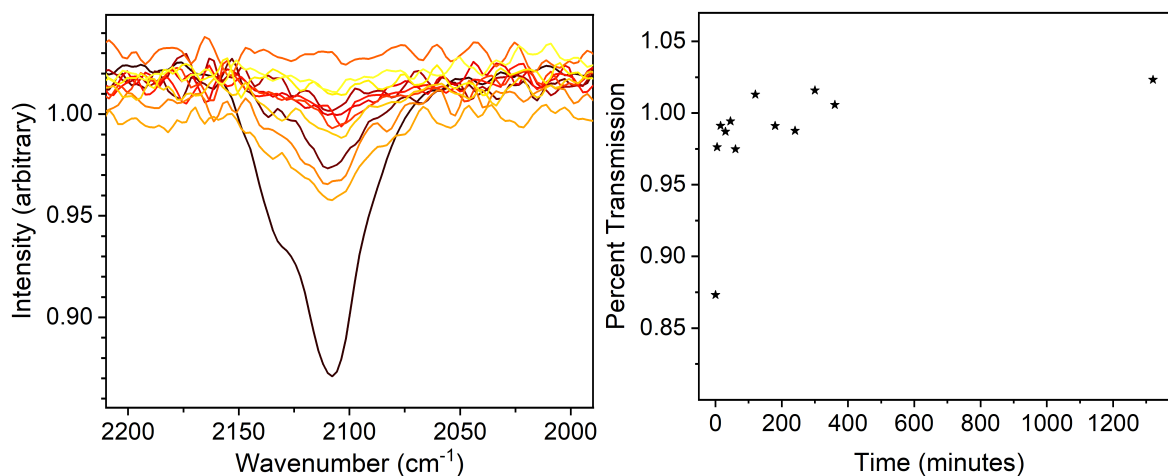


**Figure S51.** Left: Azide IR stretch from 2200 to 2000  $\text{cm}^{-1}$  of  $\text{Zr(5-N}_3\text{)}$  as it reacts with 5-hexyn-1-ol monitored from 0 minutes (dark red) to 1200 minutes (yellow). Right: Percent transmission of the azide stretch observed in the IR spectra versus time.

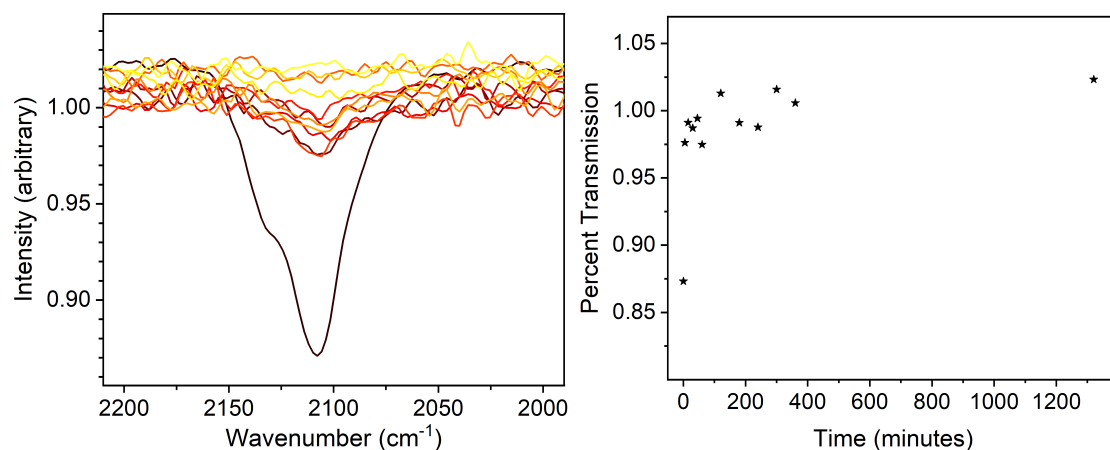


**Figure S52.** Left: Azide IR stretch from 2200 to 2000  $\text{cm}^{-1}$  of  $\text{Zr}(5\text{-N}_3)$  as it reacts with ethynyl toluene monitored from 0 minutes (dark red) to 1200 minutes (yellow). Right: Percent transmission of the azide stretch observed in the IR spectra versus time.

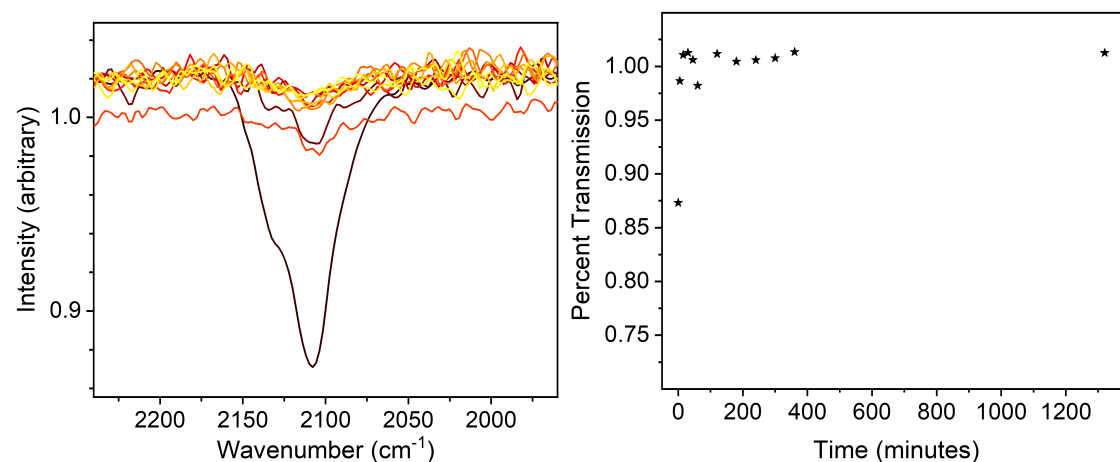


**Figure S53.** Left: Azide IR stretch from 2200 to 2000  $\text{cm}^{-1}$  of  $\text{Zr}(5\text{-N}_3)$  as it reacts with propargyl alcohol monitored from 0 minutes (dark red) to 1200 minutes (yellow). Right: Percent transmission of the azide stretch observed in the IR spectra versus time.



### UV-Vis Experiments

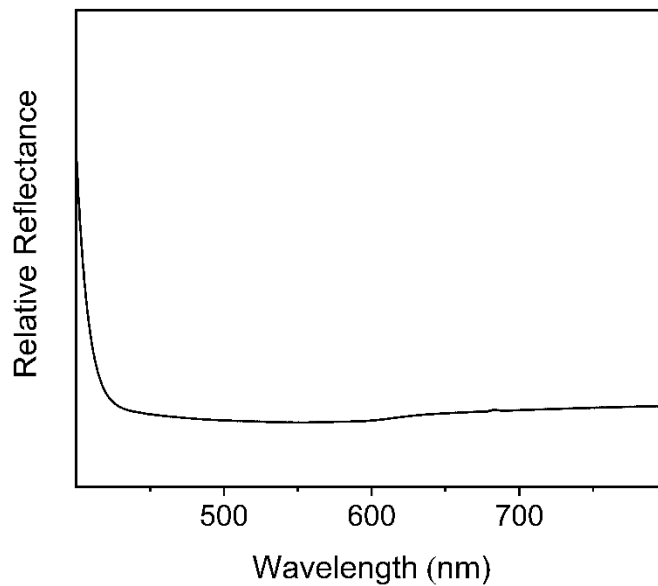


**Figure S54.** UV-Vis spectrum of *p*-tert-butylsulfonylcalix[4]arene solvated in DMF at a concentration of 1 mM.

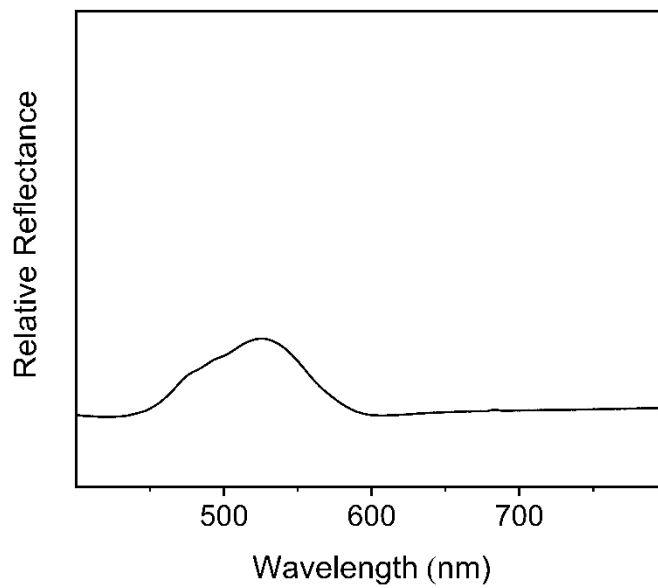


**Figure S55.** UV-Vis spectrum of  $\text{Co}(\text{NO}_3)_2$  solvated in DMF at a concentration of 5.46 mM.

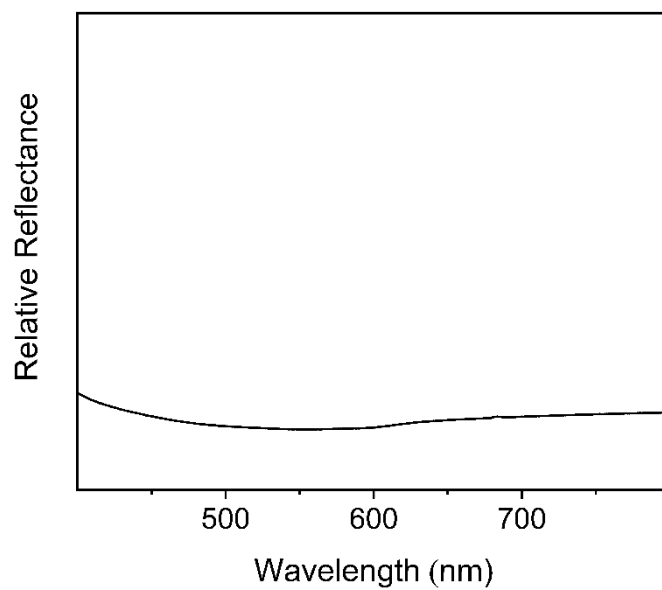


**Figure S56.** UV-Vis spectrum of 5-Propargyl bdc solvated in DMF at a concentration of 4.54 mM.

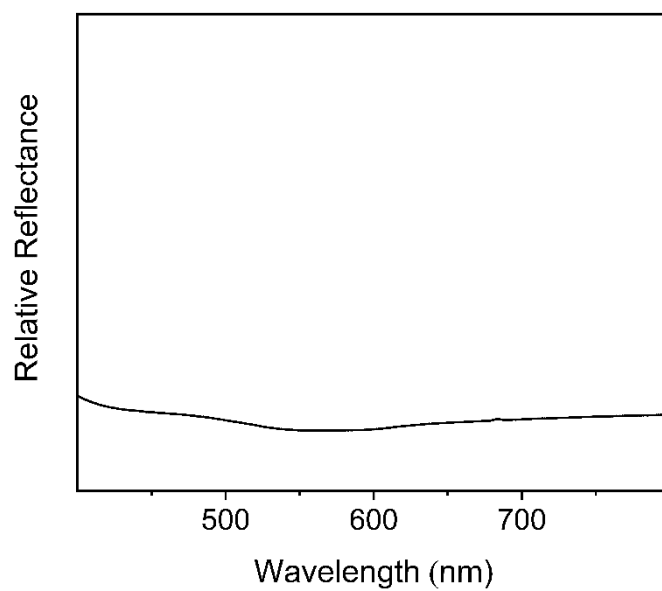


**Figure S57.** UV-Vis spectrum of 5-N<sub>3</sub> bdc solvated in DMF at a concentration of 4.83 mM.

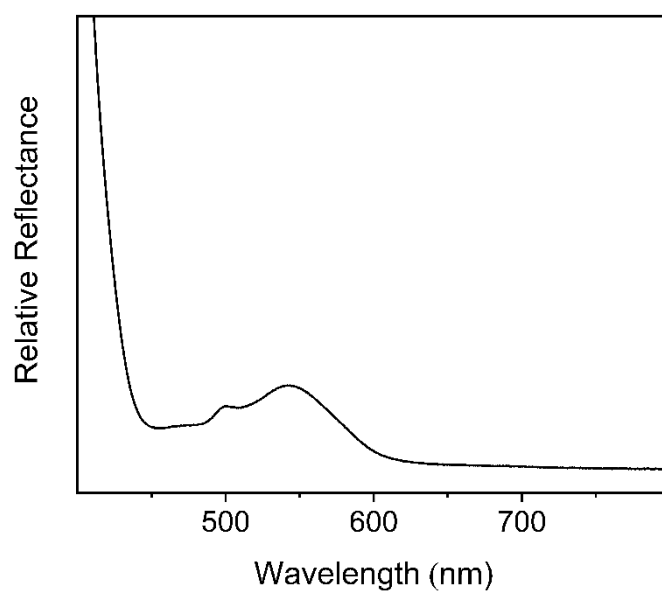


**Figure S58.** UV-Vis spectrum of Co-ppgy solvated in DMF at a concentration of 0.01 mM.

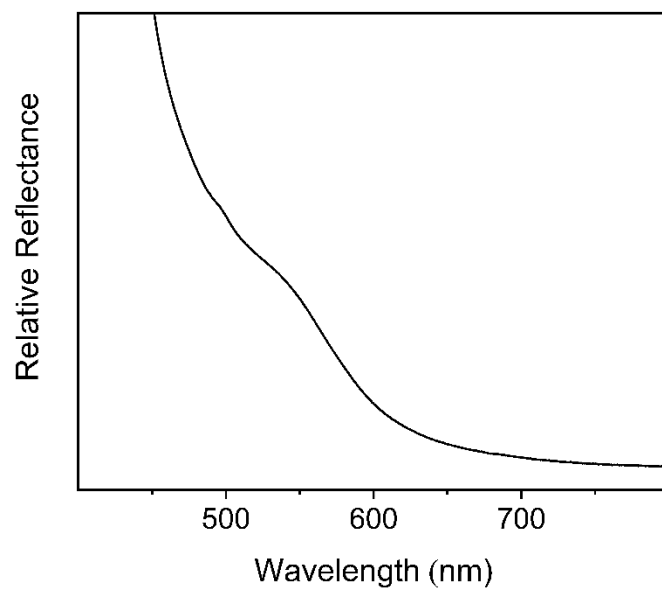


**Figure S59.** UV-Vis spectrum of Co-N<sub>3</sub> solvated in DMF at a concentration of 0.01 mM.

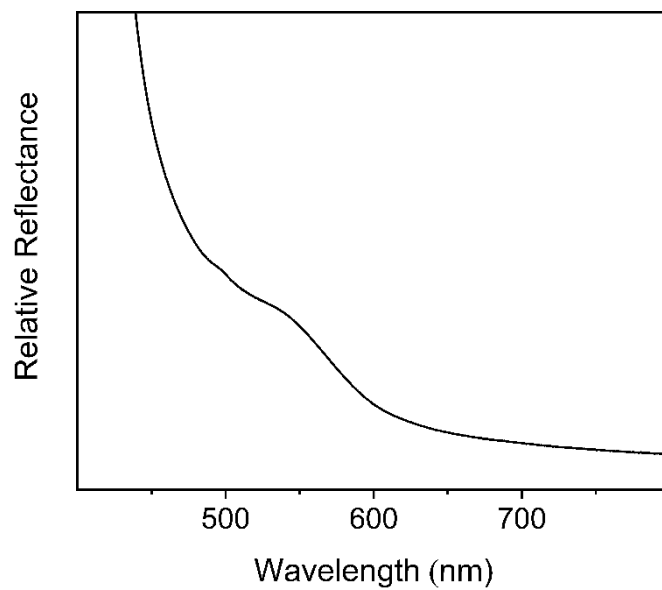


**Figure S60.** UV-Vis spectrum of Co-ppgy-3AP solvated in DMF at a concentration of 0.01 mM.

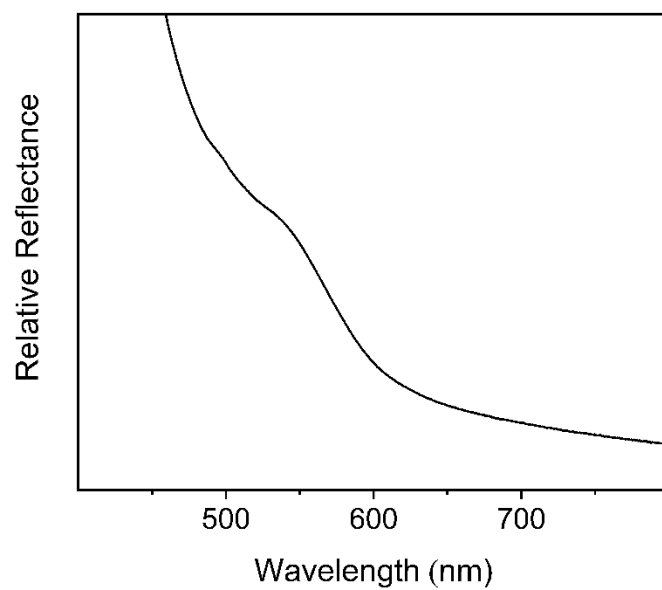


**Figure S61.** UV-Vis spectrum of Co-ppgy-6AP solvated in DMF at a concentration of 0.01 mM.

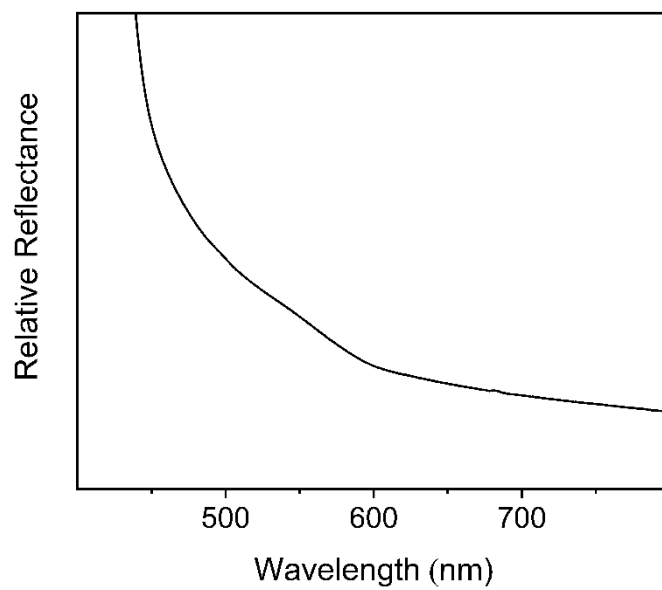


**Figure S62.** UV-Vis spectrum of Co-N<sub>3</sub>-PrOH solvated in DMF at a concentration of 0.01 mM.

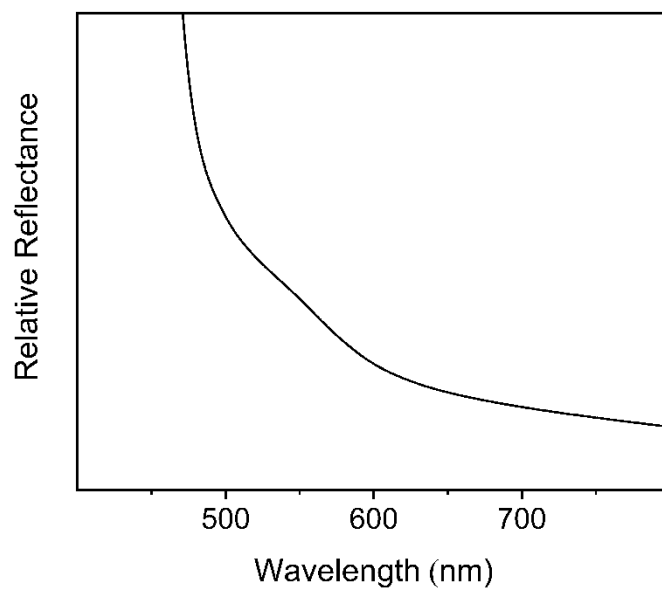


**Figure S63.** UV-Vis spectrum of Co-N<sub>3</sub>-EP solvated in DMF at a concentration of 0.01 mM.

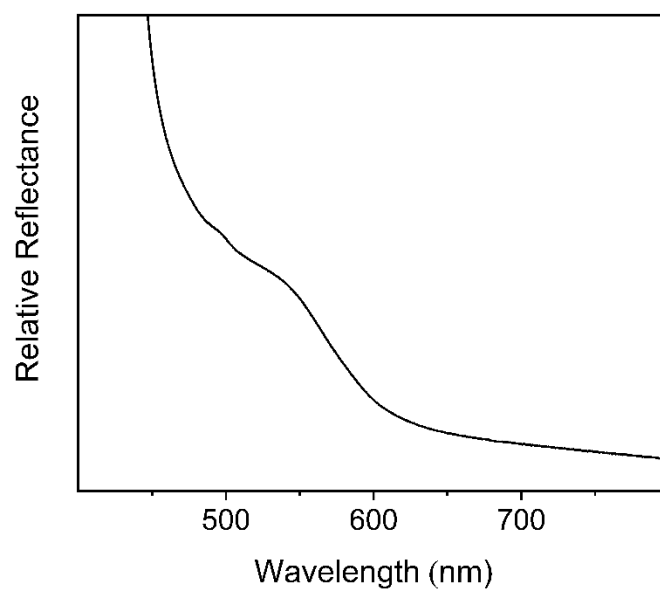


**Figure S64.** UV-Vis spectrum of Co-N<sub>3</sub>-PA solvated in DMF at a concentration of 0.01 mM.

### Thermogravimetric Analysis (TGA)

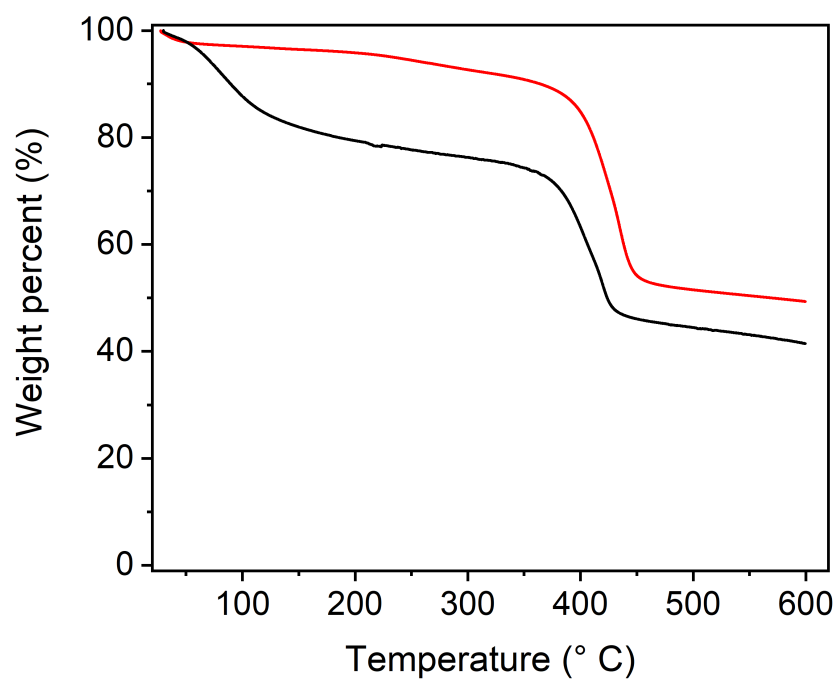


**Figure S65.** TGA of Co-ppgy as synthesized (black) and solvent exchanged with MeOH (red).

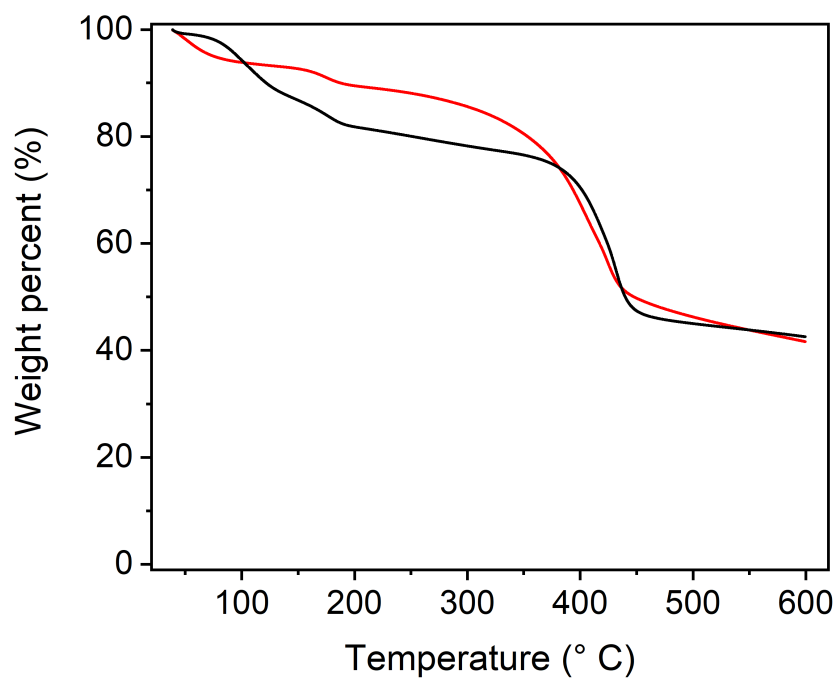


**Figure S66.** TGA of Co-N<sub>3</sub> as synthesized (black) and solvent exchanged with MeOH (red).

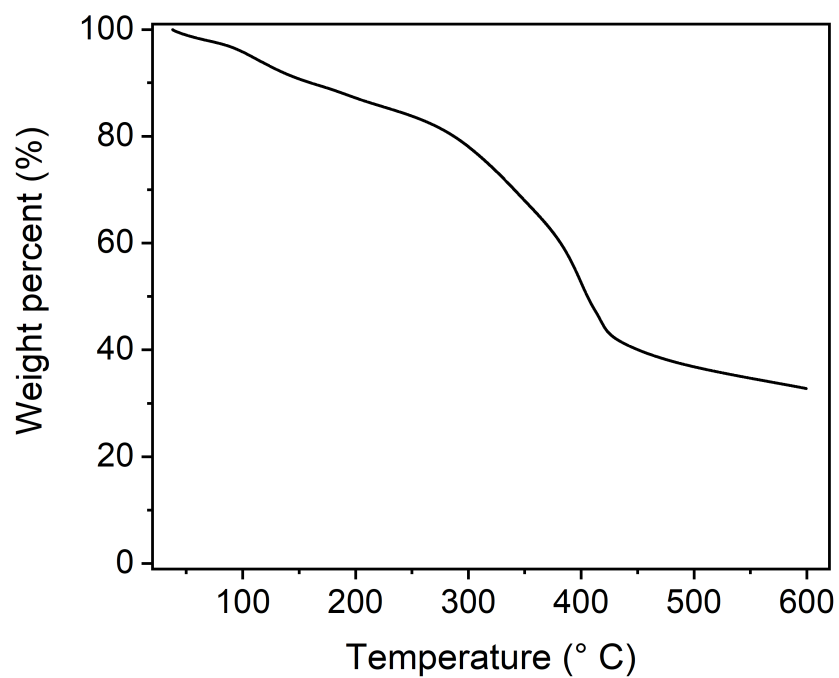


**Figure S67.** TGA of Co-ppgy-3AP solvent exchanged with MeOH.

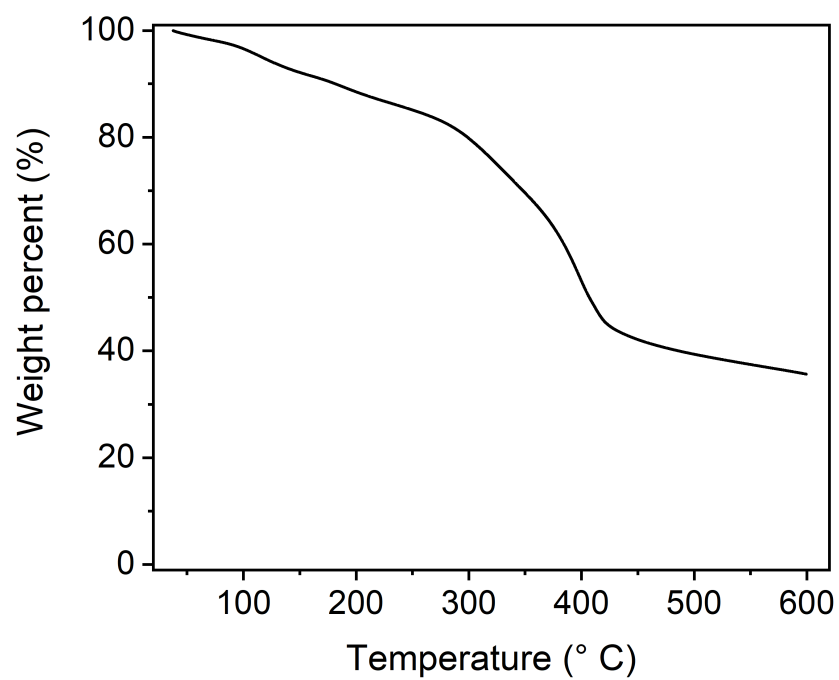


**Figure S68.** TGA of Co-ppgy-6AH solvent exchanged with MeOH.



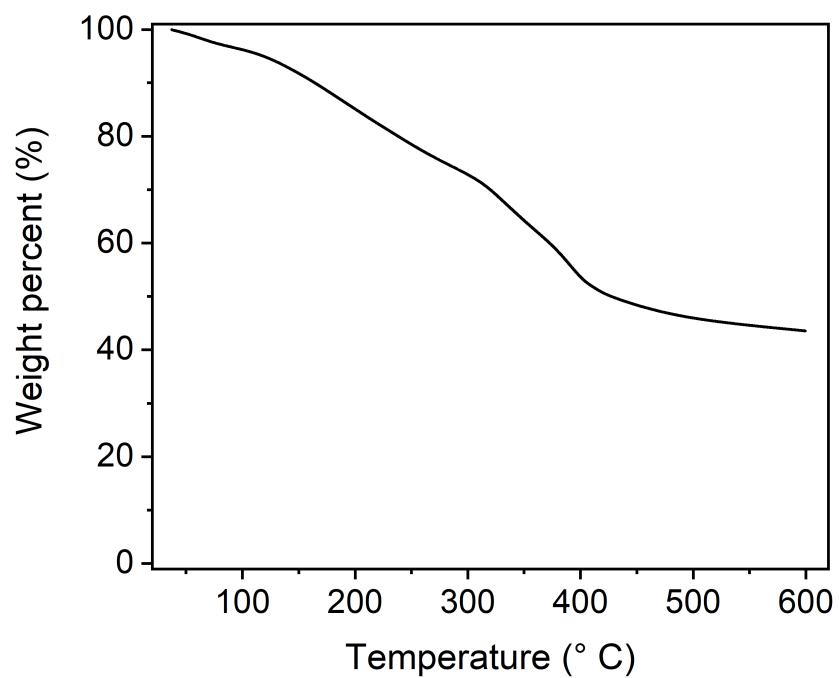


**Figure S69.** TGA of Co-N<sub>3</sub>-PrOH solvent exchanged with MeOH.

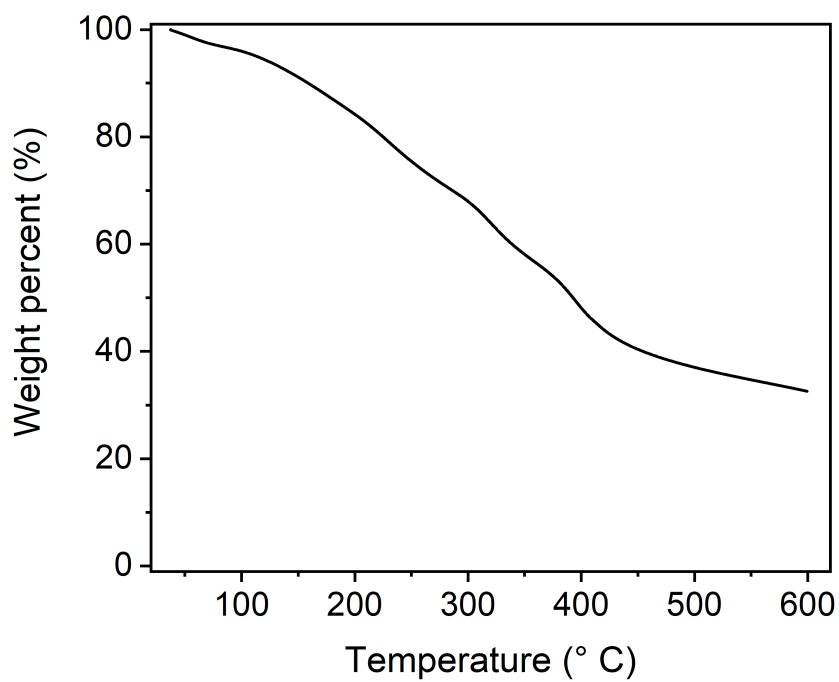


**Figure S70.** TGA of Co-N<sub>3</sub>-EP solvent exchanged with MeOH.

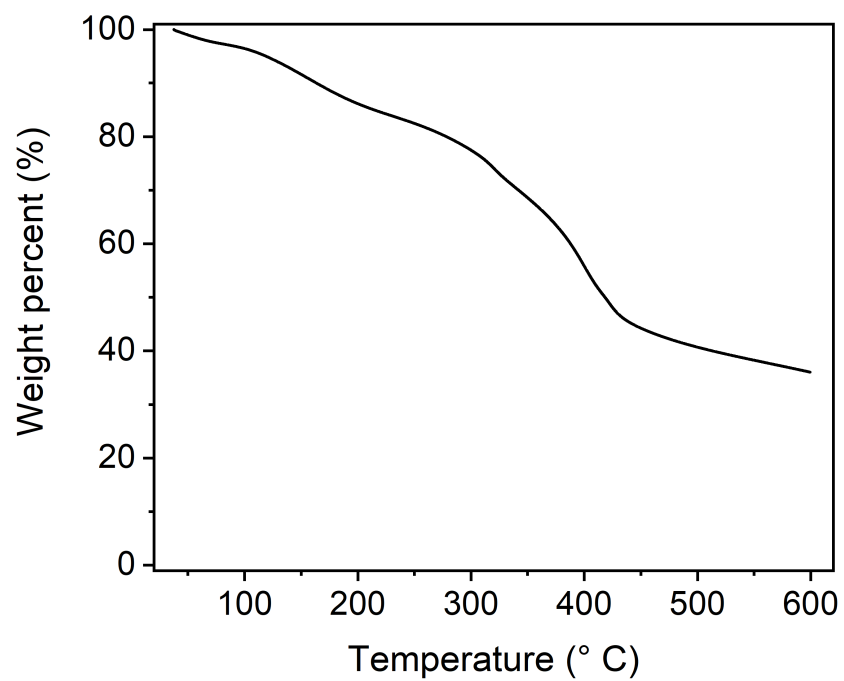


**Figure S71.** TGA of Co-N<sub>3</sub>-PA solvent exchanged with MeOH.

## Gas Adsorption Measurements

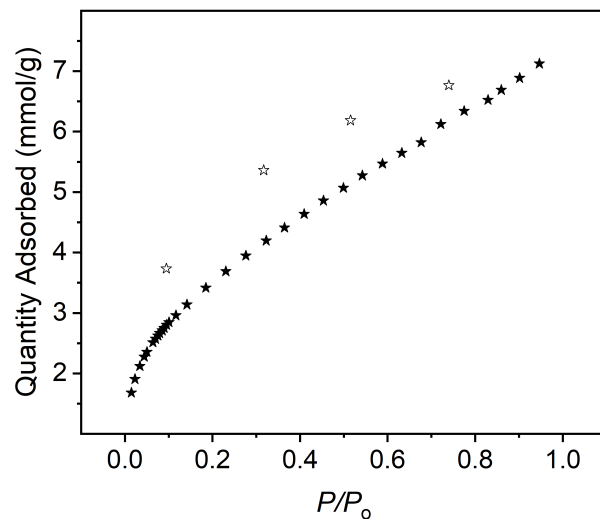


**Figure S72.** CO<sub>2</sub> adsorption (solid red stars) and desorption (hollow red stars) 195 K for Co-ppgy.

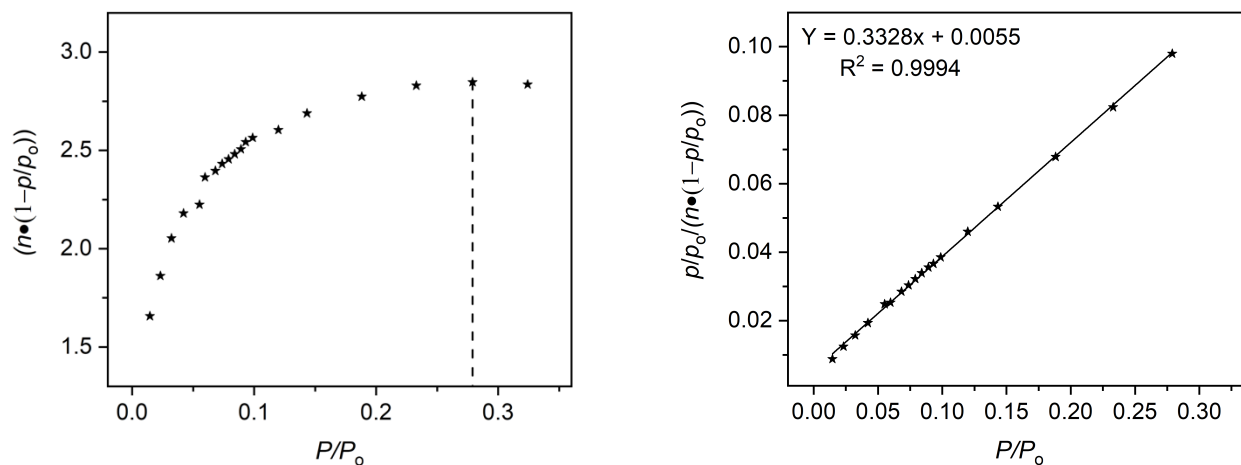


**Figure S73.** Left: Plot of  $n(1-P/P_0)$  vs.  $P/P_0$  to determine the maximum  $P/P_0$  used in the BET linear fit according to the first BET consistency criterion for CO<sub>2</sub> adsorption at 195 K for the Co-ppgy. Bottom right: The slope of the best fit line for  $P/P_0 < 0.279$  is 0.3328 and the y-intercept is 0.0055, which satisfies the second BET consistency criterion. This results in a measured surface area of 308 m<sup>2</sup>/g to CO<sub>2</sub>.

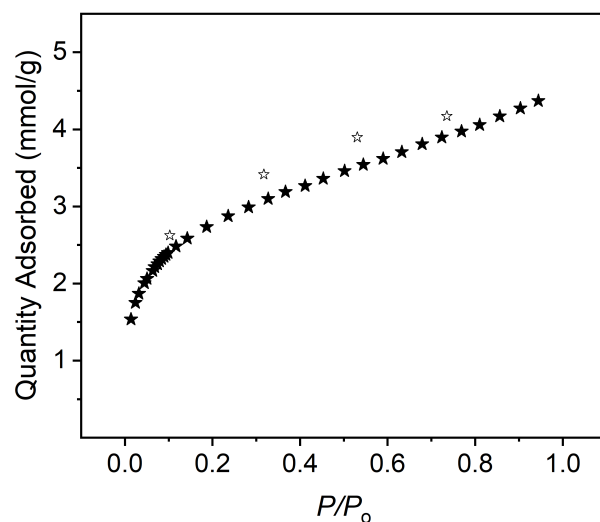


**Figure S74.** CO<sub>2</sub> adsorption (solid black stars) and desorption (hollow black stars) at 195 K for Co-N<sub>3</sub>.

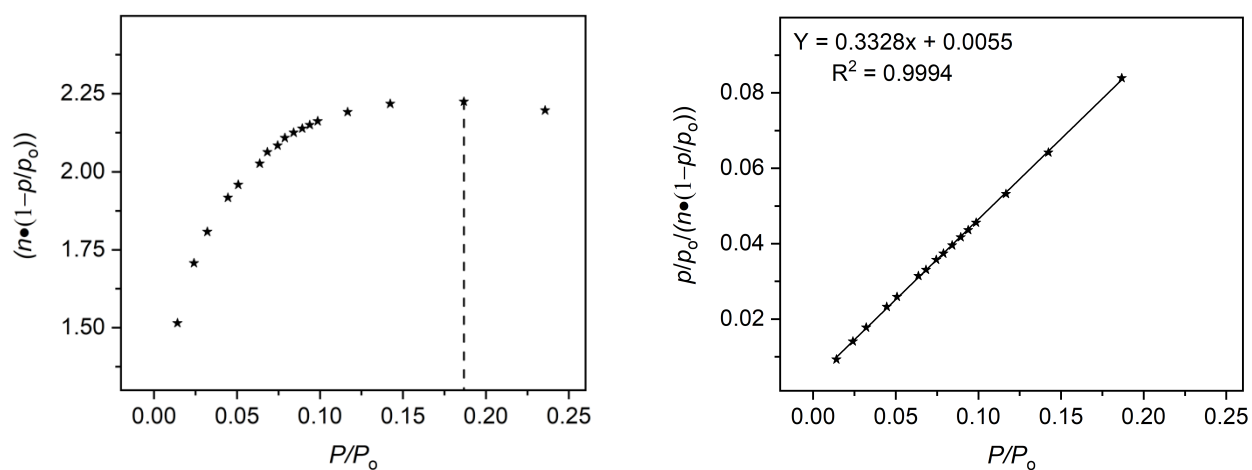


**Figure S75.** Left: Plot of  $n(1-P/P_0)$  vs.  $P/P_0$  to determine the maximum  $P/P_0$  used in the BET linear fit according to the first BET consistency criterion for N<sub>2</sub> adsorption at 195 K for the Co-N<sub>3</sub>. Right: The slope of the best fit line for  $P/P_0 < 0.1867$  is 0.4262 and the y-intercept is 0.0039, which satisfies the second BET consistency criterion. This results in a measured surface area of 240 m<sup>2</sup>/g to CO<sub>2</sub>.

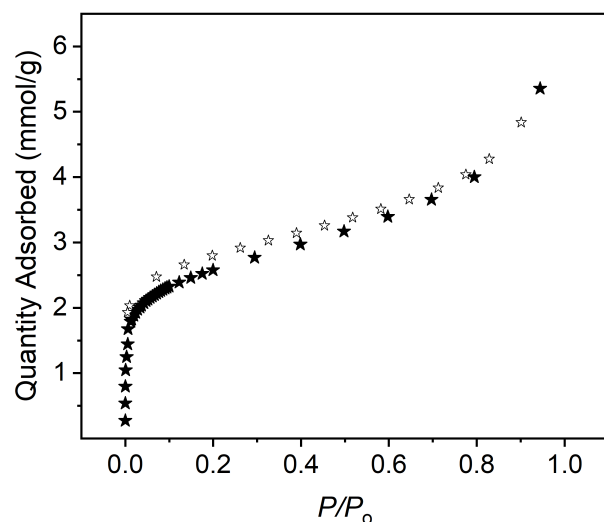


**Figure S76.** N<sub>2</sub> adsorption (solid black stars) and desorption (hollow black stars) at 77 K for Co-ppgy-3AP.

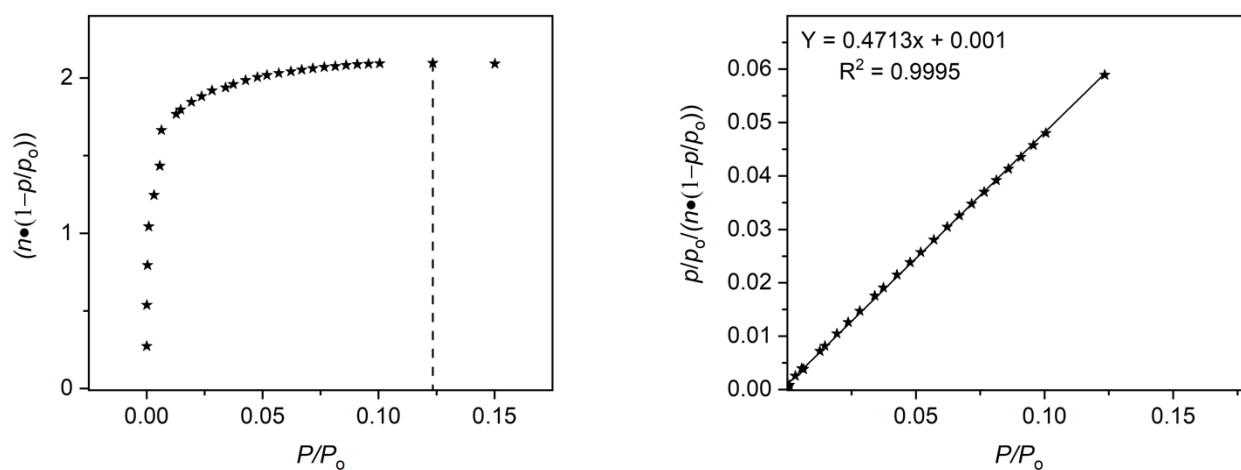


**Figure S77.** Top left: Plot of  $n(1-P/P_0)$  vs.  $P/P_0$  to determine the maximum  $P/P_0$  used in the BET linear fit according to the first BET consistency criterion for N<sub>2</sub> adsorption at 77 K for the Co-ppgy-3AP. Top right: The slope of the best fit line for  $P/P_0 < 0.1227$  is 0.471 and the y-intercept is 0.001, which satisfies the second BET consistency criterion. This results in a measured surface area of 207 m<sup>2</sup>/g to N<sub>2</sub>.

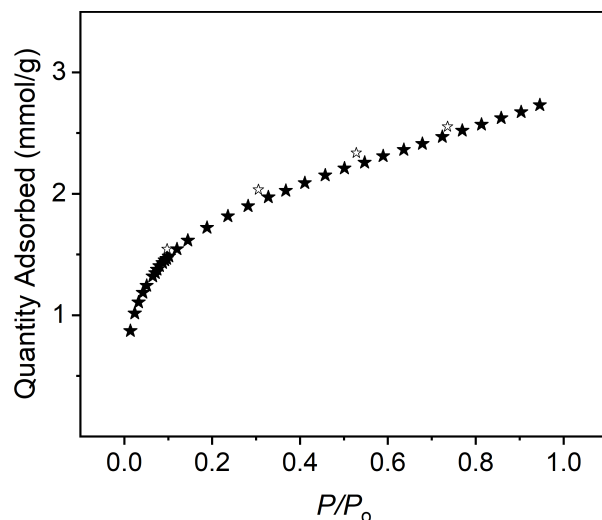


**Figure S78.** CO<sub>2</sub> adsorption (solid black stars) and desorption (hollow black stars) at 195 K for Co-ppgy-3AP.

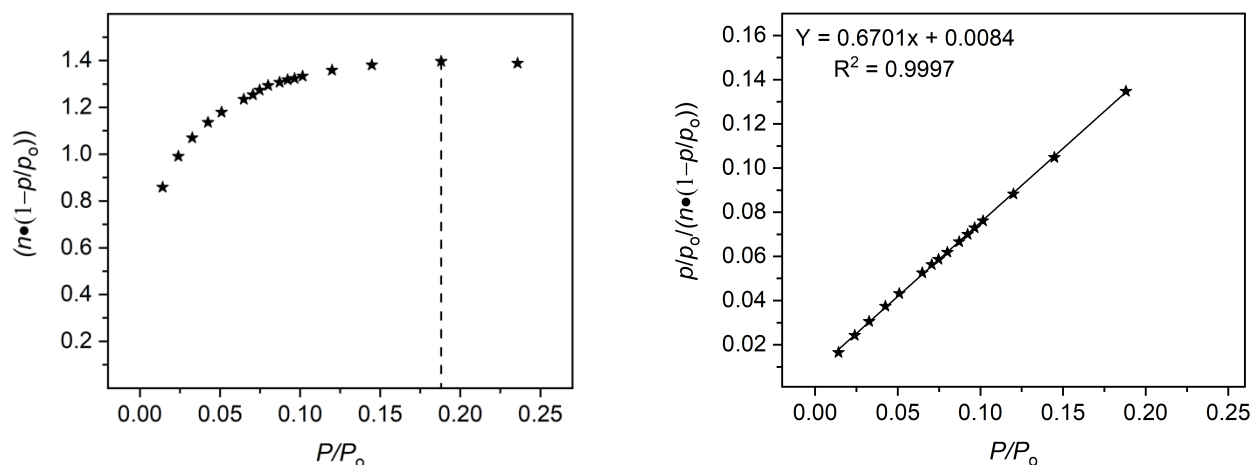


**Figure S79.** Top left: Plot of  $n(1-P/P_0)$  vs.  $P/P_0$  to determine the maximum  $P/P_0$  used in the BET linear fit according to the first BET consistency criterion for CO<sub>2</sub> adsorption at 195 K for the Co-ppgy-3AP. Top right: The slope of the best fit line for  $P/P_0 < 0.1881$  is 0.6701 and the y-intercept is 0.0084, which satisfies the second BET consistency criterion. This results in a measured surface area of 153 m<sup>2</sup>/g to CO<sub>2</sub>.

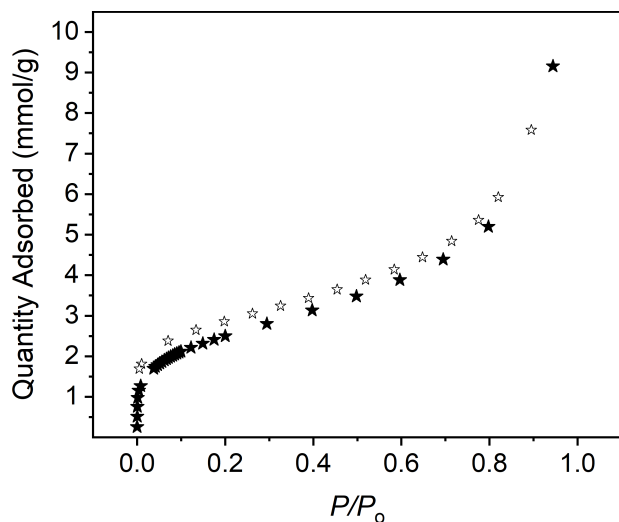


**Figure S80.** N<sub>2</sub> adsorption (solid black stars) and desorption (hollow black stars) at 77 K for Co-ppgy-6AH.

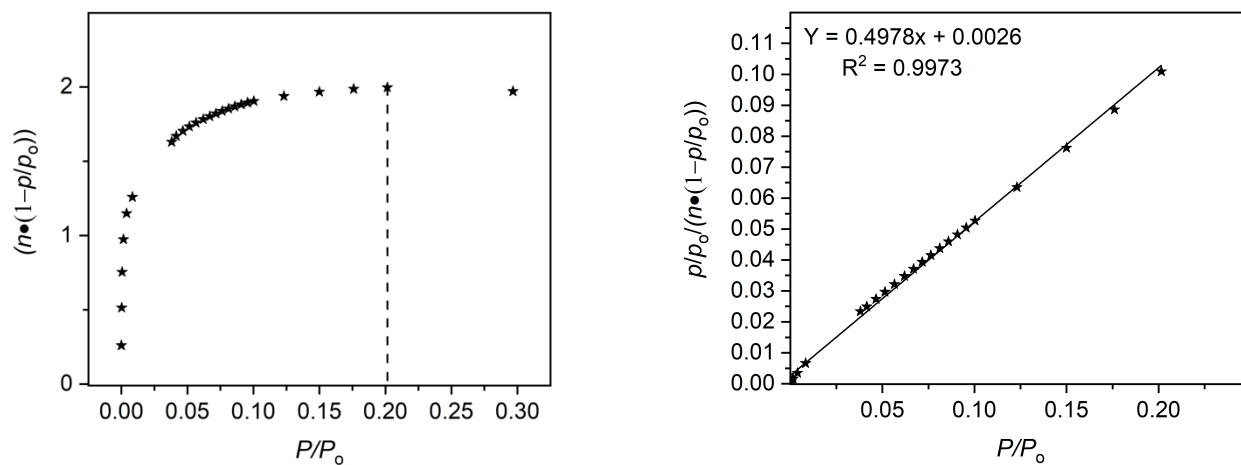


**Figure S81.** Top left: Plot of  $n(1-P/P_0)$  vs.  $P/P_0$  to determine the maximum  $P/P_0$  used in the BET linear fit according to the first BET consistency criterion for N<sub>2</sub> adsorption at 77 K for the Co-ppgy-6AH. Top right: The slope of the best fit line for  $P/P_0 < 0.2015$  is 0.4978 and the y-intercept is 0.0026, which satisfies the second BET consistency criterion. This results in a measured surface area of 196 m<sup>2</sup>/g to N<sub>2</sub>.

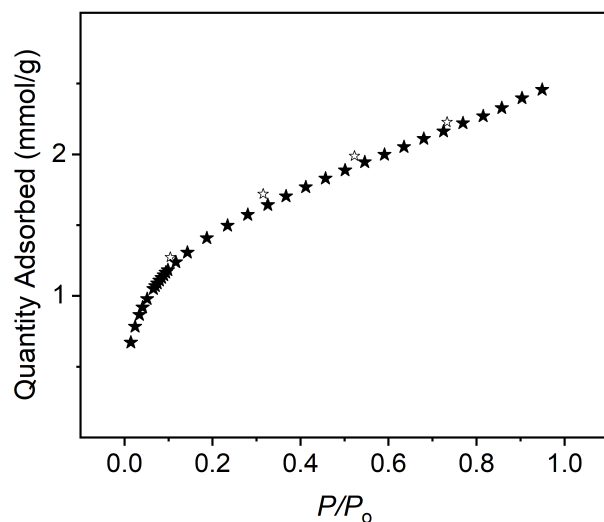


**Figure S82.** CO<sub>2</sub> adsorption (solid black stars) and desorption (hollow black stars) at 195 K for Co-ppgy-6AH).

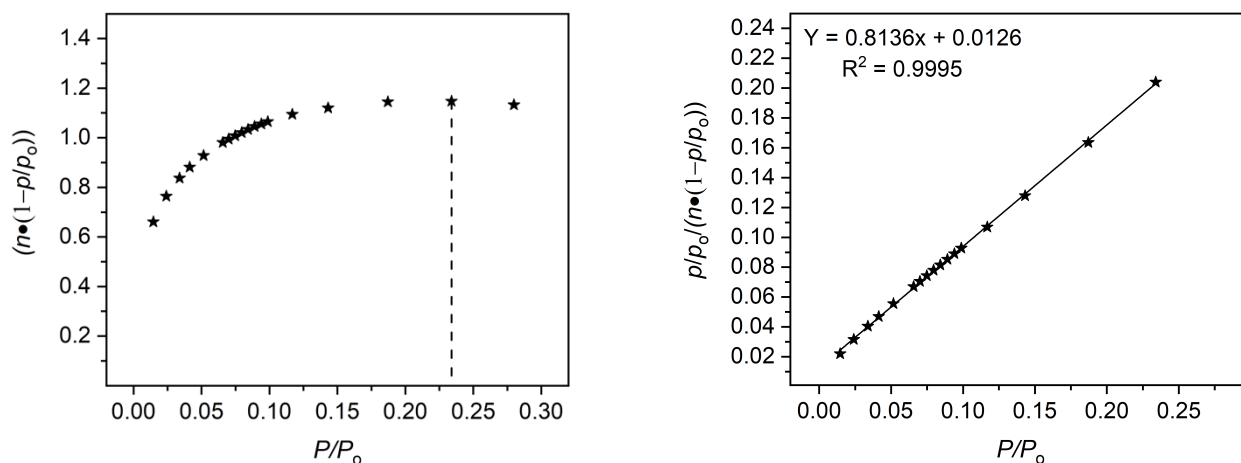


**Figure S83.** Top left: Plot of  $n(1-P/P_0)$  vs.  $P/P_0$  to determine the maximum  $P/P_0$  used in the BET linear fit according to the first BET consistency criterion for CO<sub>2</sub> adsorption at 195 K for the Co-ppgy-6AH). Top right: The slope of the best fit line for  $P/P_0 < 0.2340$  is 0.8136 and the y-intercept is 0.0126, which satisfies the second BET consistency criterion. This results in a measured surface area of 126 m<sup>2</sup>/g to CO<sub>2</sub>.



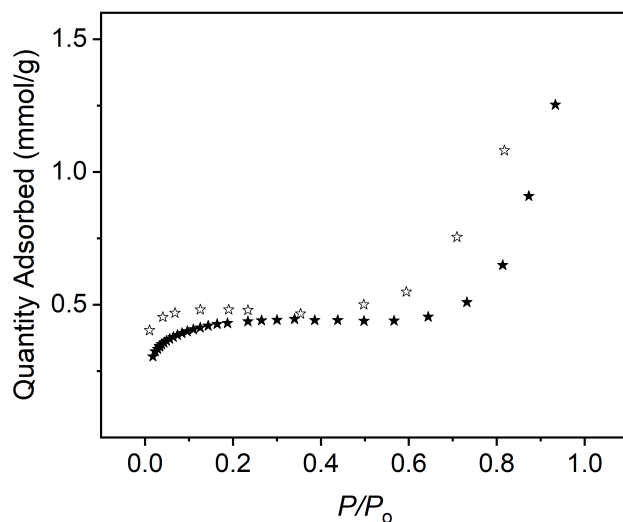


**Figure S84.** N<sub>2</sub> adsorption (solid black stars) and desorption (hollow black stars) at 77 K for Co-N<sub>3</sub>-PrOH.

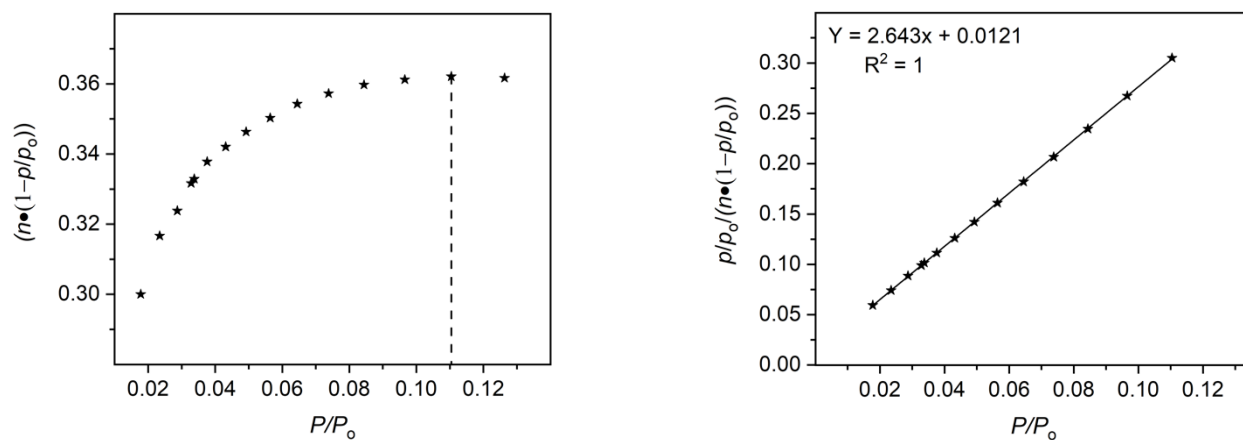


**Figure S85.** Top left: Plot of  $n(1-P/P_0)$  vs.  $P/P_0$  to determine the maximum  $P/P_0$  used in the BET linear fit according to the first BET consistency criterion for N<sub>2</sub> adsorption at 77 K for the Co-N<sub>3</sub>-PrOH). Top right: The slope of the best fit line for  $P/P_0 < 0.1099$  is 2.6409 and the y-intercept is 0.0121, which satisfies the second BET consistency criterion. This results in a measured surface area of 37 m<sup>2</sup>/g to N<sub>2</sub>.

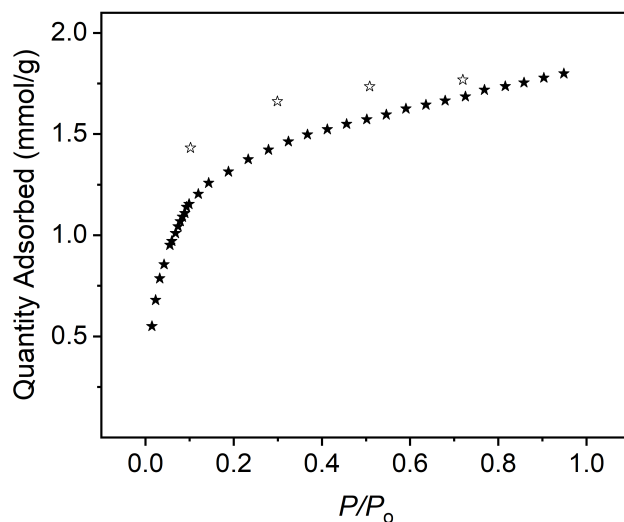


**Figure S86.** CO<sub>2</sub> adsorption (solid black stars) and desorption (hollow black stars) at 195 K for Co-N<sub>3</sub>-PrOH.

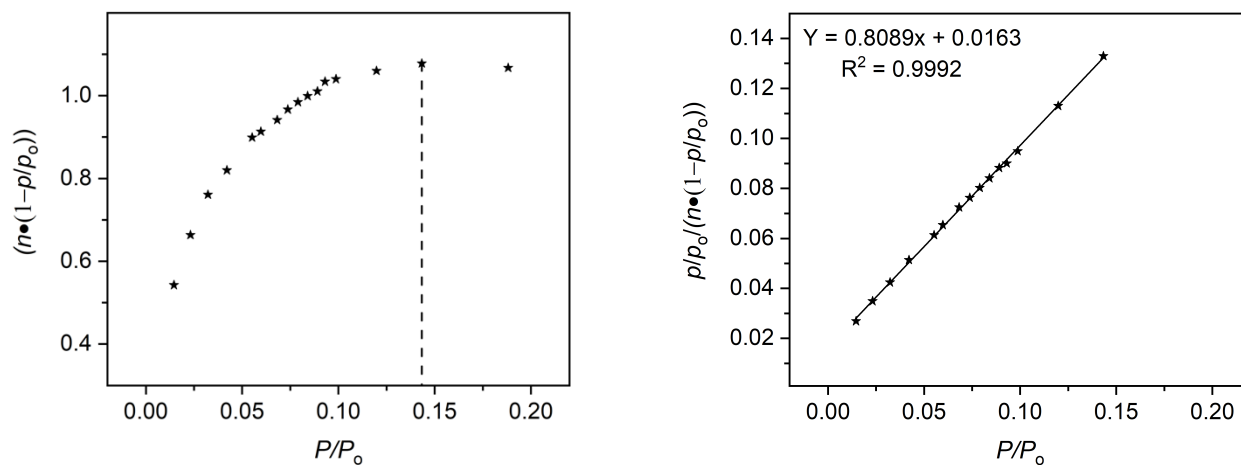


**Figure S87.** Top left: Plot of  $n(1-P/P_0)$  vs.  $P/P_0$  to determine the maximum  $P/P_0$  used in the BET linear fit according to the first BET consistency criterion for CO<sub>2</sub> adsorption at 195 K for the Co-N<sub>3</sub>-PrOH. Top right: The slope of the best fit line for  $P/P_0 < 0.1433$  is 0.8089 and the y-intercept is 0.0163, which satisfies the second BET consistency criterion. This results in a measured surface area of 127 m<sup>2</sup>/g to CO<sub>2</sub>.

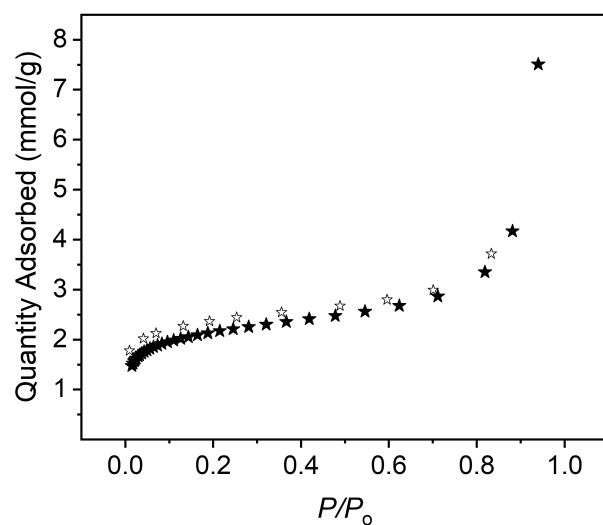


**Figure S88.** N<sub>2</sub> adsorption (solid black stars) and desorption (hollow black stars) at 77 K for Co-N<sub>3</sub>-EP.

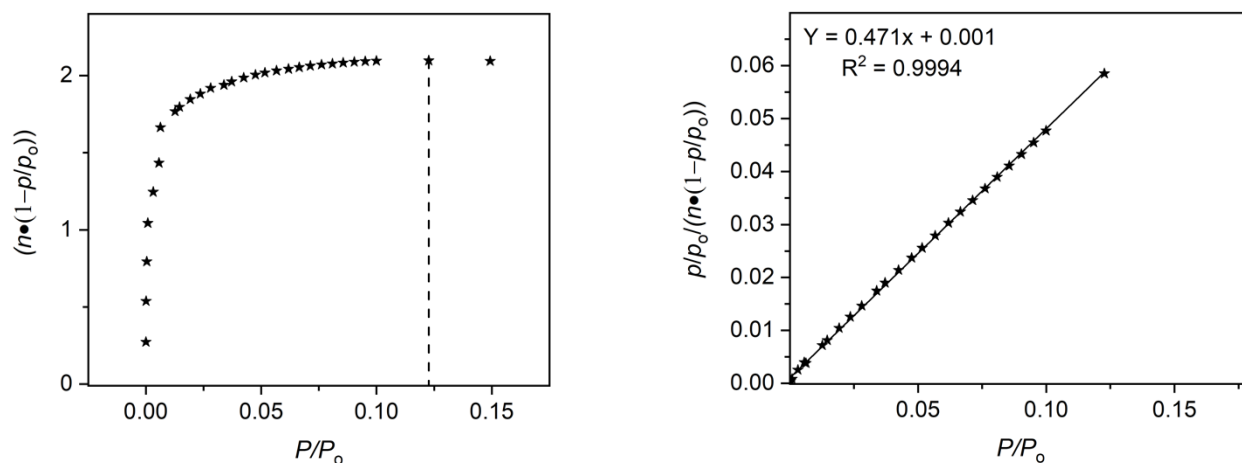


**Figure S89.** Top left: Plot of  $n(1-P/P_0)$  vs.  $P/P_0$  to determine the maximum  $P/P_0$  used in the BET linear fit according to the first BET consistency criterion for N<sub>2</sub> adsorption at 77 K for the Co-N<sub>3</sub>-EP). Top right: The slope of the best fit line for  $P/P_0 < 0.1099$  is 0.5452 and the y-intercept is 0.0021, which satisfies the second BET consistency criterion. This results in a measured surface area of 179 m<sup>2</sup>/g to N<sub>2</sub>.

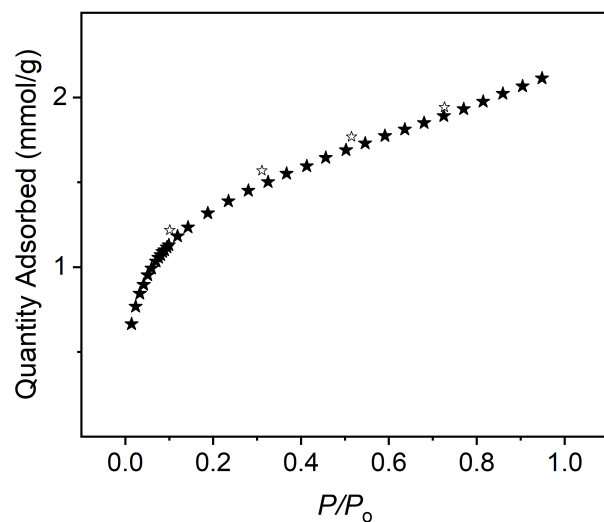


**Figure S90.** CO<sub>2</sub> adsorption (solid black stars) and desorption (hollow black stars) at 195 K for Co-N<sub>3</sub>-EP).

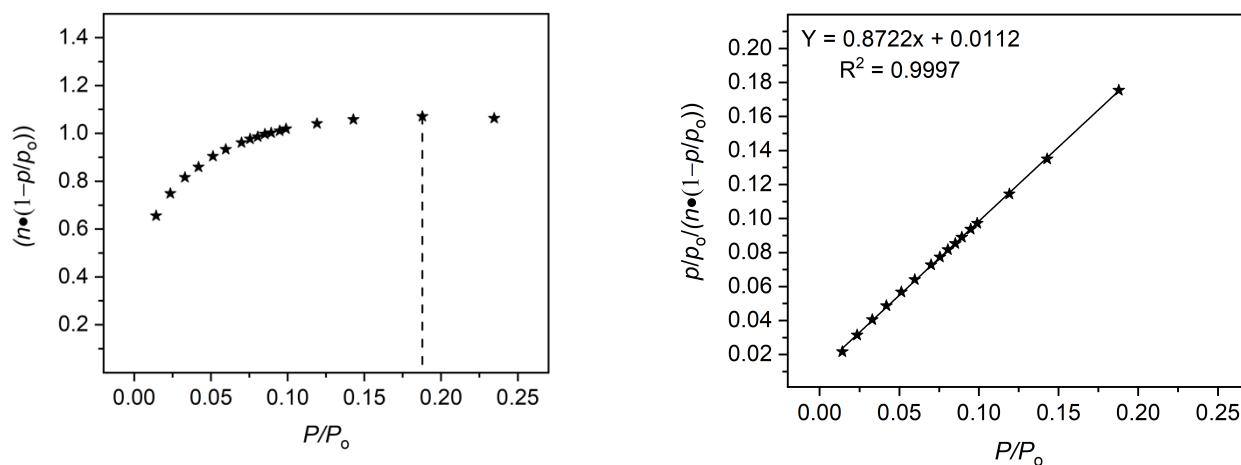


**Figure S91.** Top left: Plot of  $n(1-P/P_0)$  vs.  $P/P_0$  to determine the maximum  $P/P_0$  used in the BET linear fit according to the first BET consistency criterion for CO<sub>2</sub> adsorption at 195 K for the Co-N<sub>3</sub>-EP. Top right: The slope of the best fit line for  $P/P_0 < 0.1878$  is 0.8722 and the y-intercept is 0.0112, which satisfies the second BET consistency criterion. This results in a measured surface area of 117 m<sup>2</sup>/g to CO<sub>2</sub>.

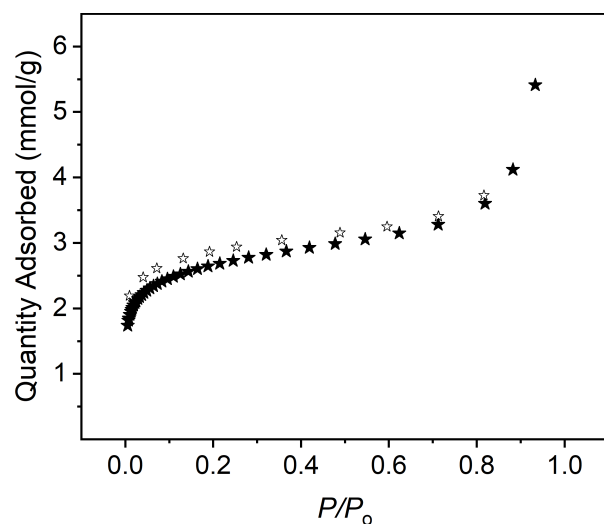


**Figure S92.** N<sub>2</sub> adsorption (solid black stars) and desorption (hollow black stars) at 77 K for Co-N<sub>3</sub>-PA.

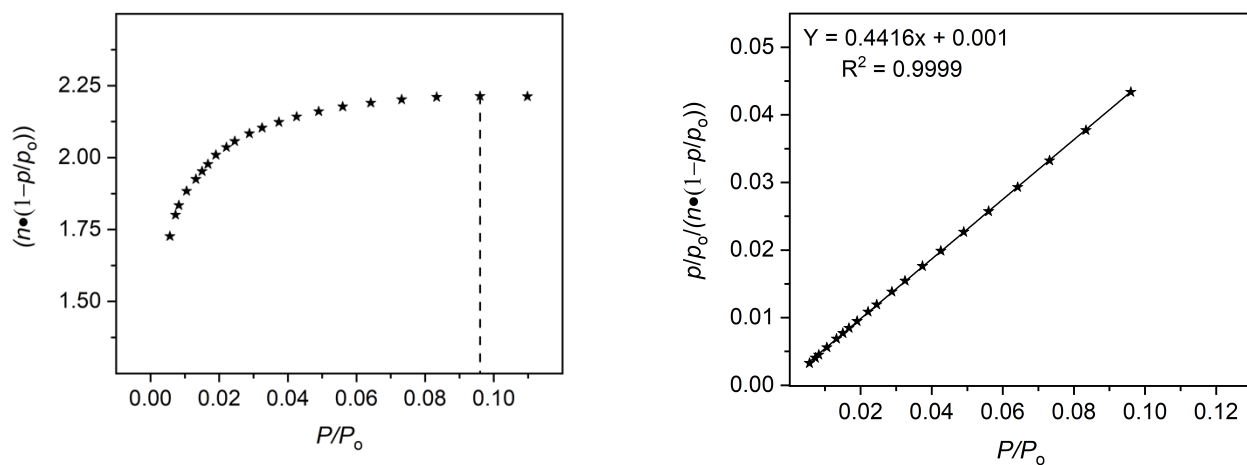


**Figure S93.** Top left: Plot of  $n(1-P/P_0)$  vs.  $P/P_0$  to determine the maximum  $P/P_0$  used in the BET linear fit according to the first BET consistency criterion for N<sub>2</sub> adsorption at 77 K for the Co-N<sub>3</sub>-PA. Top right: The slope of the best fit line for  $P/P_0 < 0.0960$  is 0.4416 and the y-intercept is 0.001, which satisfies the second BET consistency criterion. This results in a measured surface area of 221 m<sup>2</sup>/g to N<sub>2</sub>.

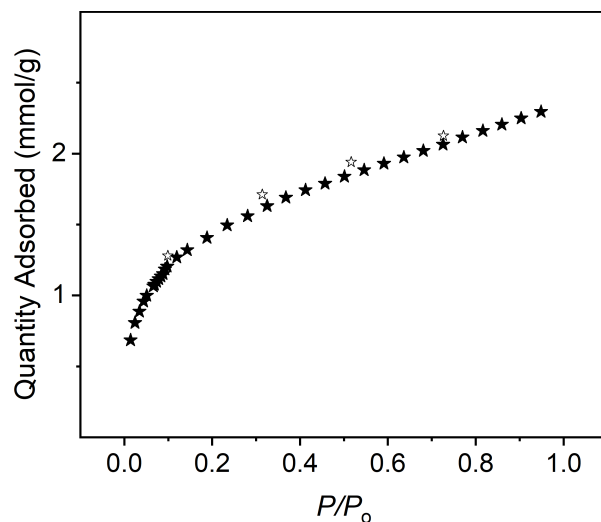


**Figure S94.** CO<sub>2</sub> adsorption (solid black stars) and desorption (hollow black stars) at 195 K for Co-N<sub>3</sub>-PA.

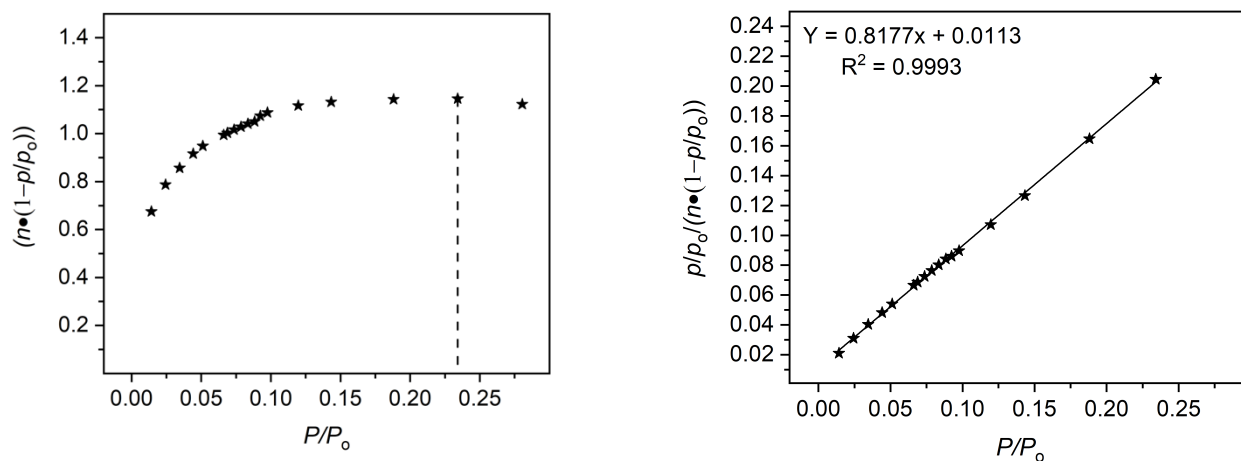


**Figure S95.** Top left: Plot of  $n(1-P/P_0)$  vs.  $P/P_0$  to determine the maximum  $P/P_0$  used in the BET linear fit according to the first BET consistency criterion for CO<sub>2</sub> adsorption at 195 K for the Co-N<sub>3</sub>-PA. Top right: The slope of the best fit line for  $P/P_0 < 0.1881$  is 0.8177 and the y-intercept is 0.0113, which satisfies the second BET consistency criterion. This results in a measured surface area of 125 m<sup>2</sup>/g to CO<sub>2</sub>.

**Table S2.** Surface areas of PCCs.

	N <sub>2</sub> Langmuir SA (m <sup>2</sup> /g)	N <sub>2</sub> BET SA (m <sup>2</sup> /g)	CO <sub>2</sub> Langmuir SA (m <sup>2</sup> /g)	CO <sub>2</sub> BET SA (m <sup>2</sup> /g)
Co-ppgy	-	-	902	308
Co-N <sub>3</sub>	-	-	491	240
Co-ppgy-3AP	426	207	310	153
Co-ppgy-6AH	613	196	287	126
Co-N <sub>3</sub> -PrOH	-	37	196	127
Co-N <sub>3</sub> -EP	-	179	240	117
Co-N <sub>3</sub> -PA	-	221	263	125

### Mass Spectrometry

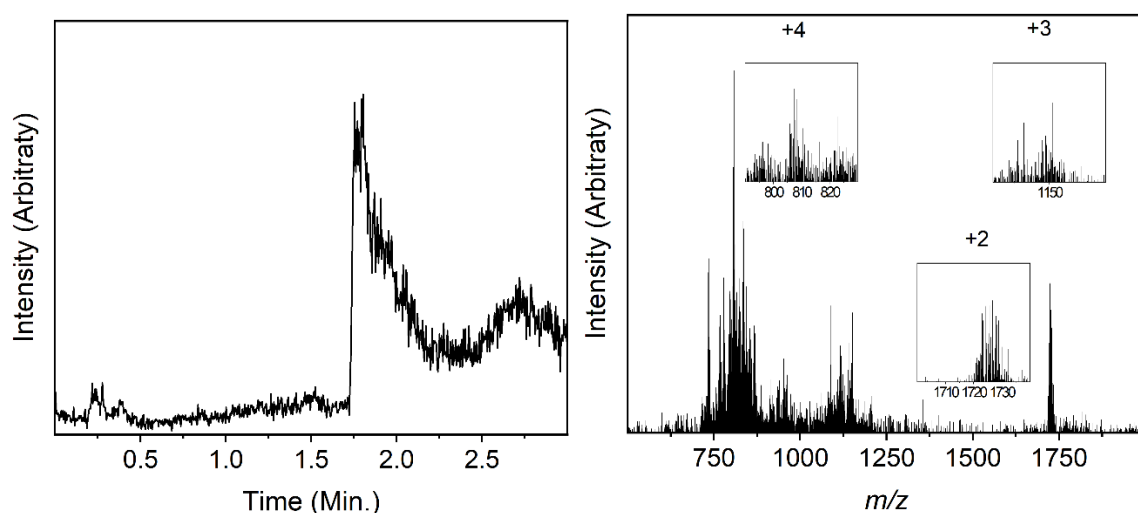


**Figure S96.** UPLC chromatogram (left) and mass spectrum (right) of Zr(5-ppgy) cage.

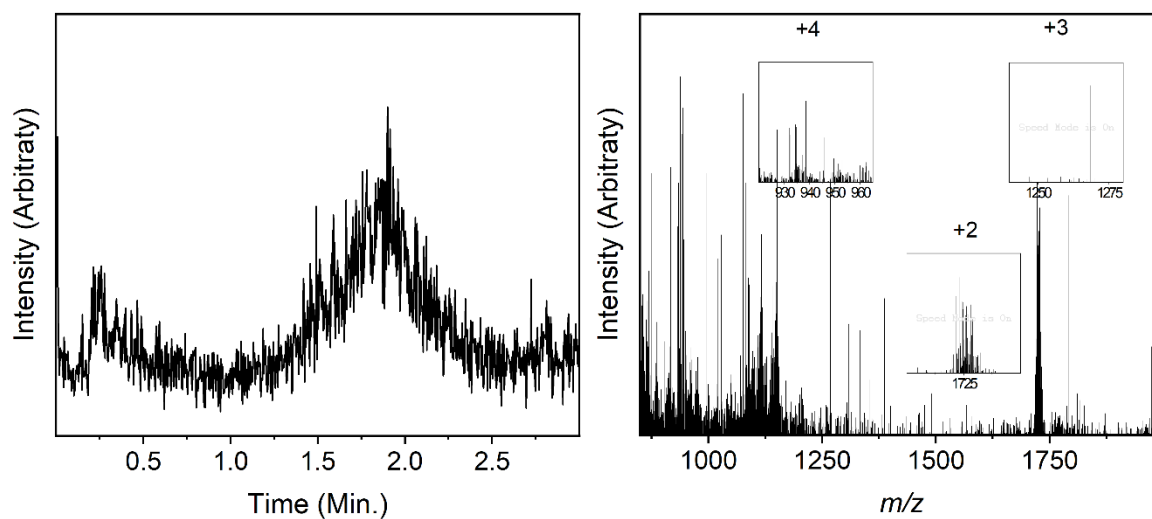


**Figure S97.** UPLC chromatogram (left) and mass spectrum (right) of Zr(2,5-dippgy) cage.

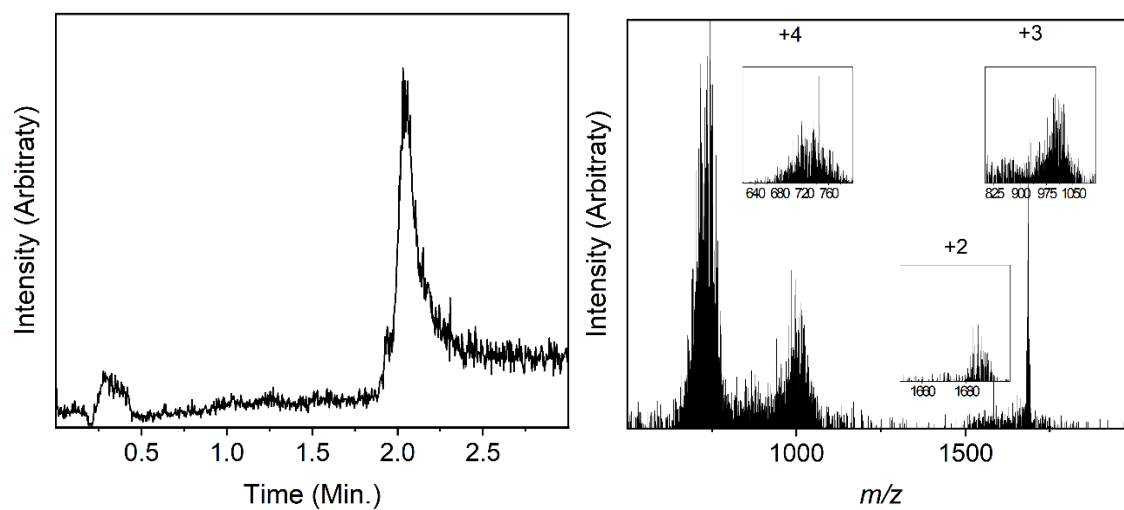


**Figure S98.** UPLC chromatogram (left) and mass spectrum (right) of Zr(5-N<sub>3</sub>) cage.

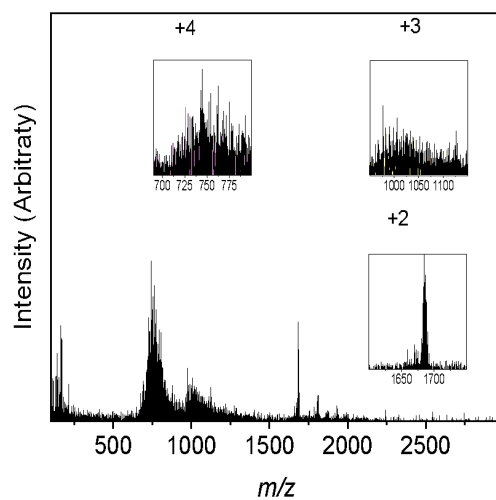


**Figure S99.** Mass spectrum of Zr(5-N<sub>3</sub>) cage exposed to click reaction conditions with triethylamine and CuI in acetonitrile.



## SEM Images

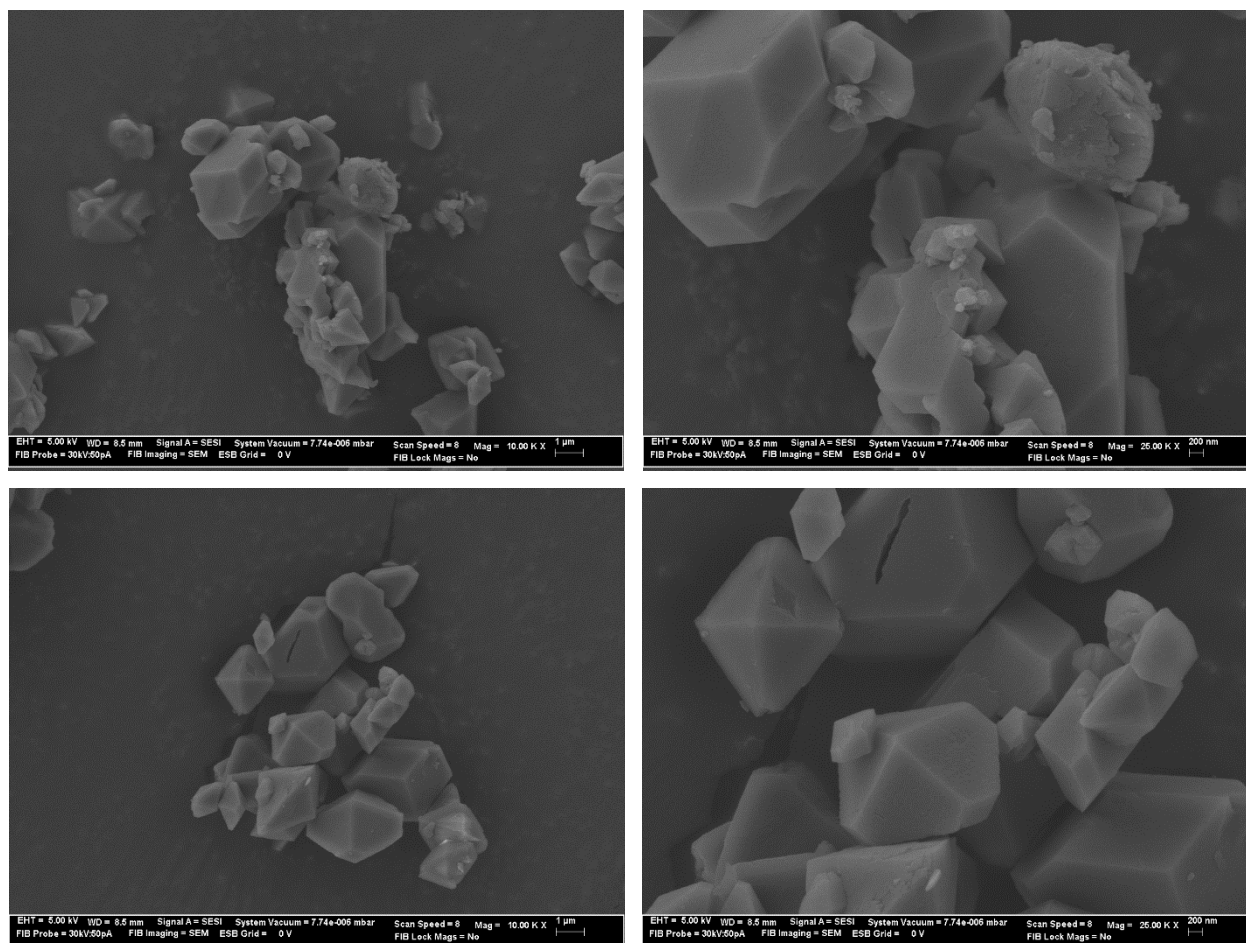


**Figure S100.** SEM images of Co-ppgy at 1  $\mu\text{m}$  (top left), 200 nm (top right), 1  $\mu\text{m}$  (bottom left), and 200 nm (bottom right).

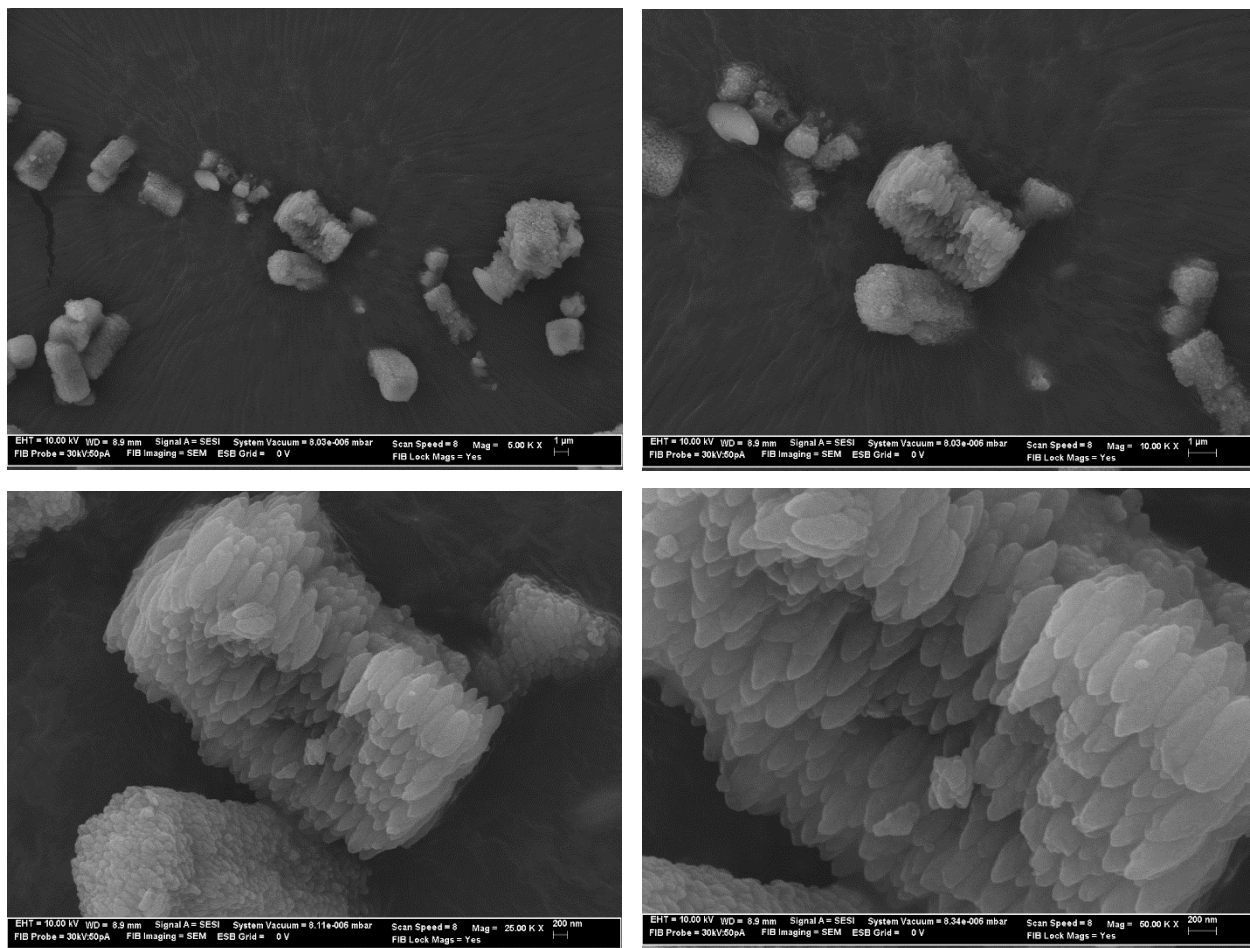


**Figure S101.** SEM images of Co-N<sub>3</sub> at 1 μm (top left), 1 μm (top right), 200 nm (bottom left), and 200 nm (bottom right).

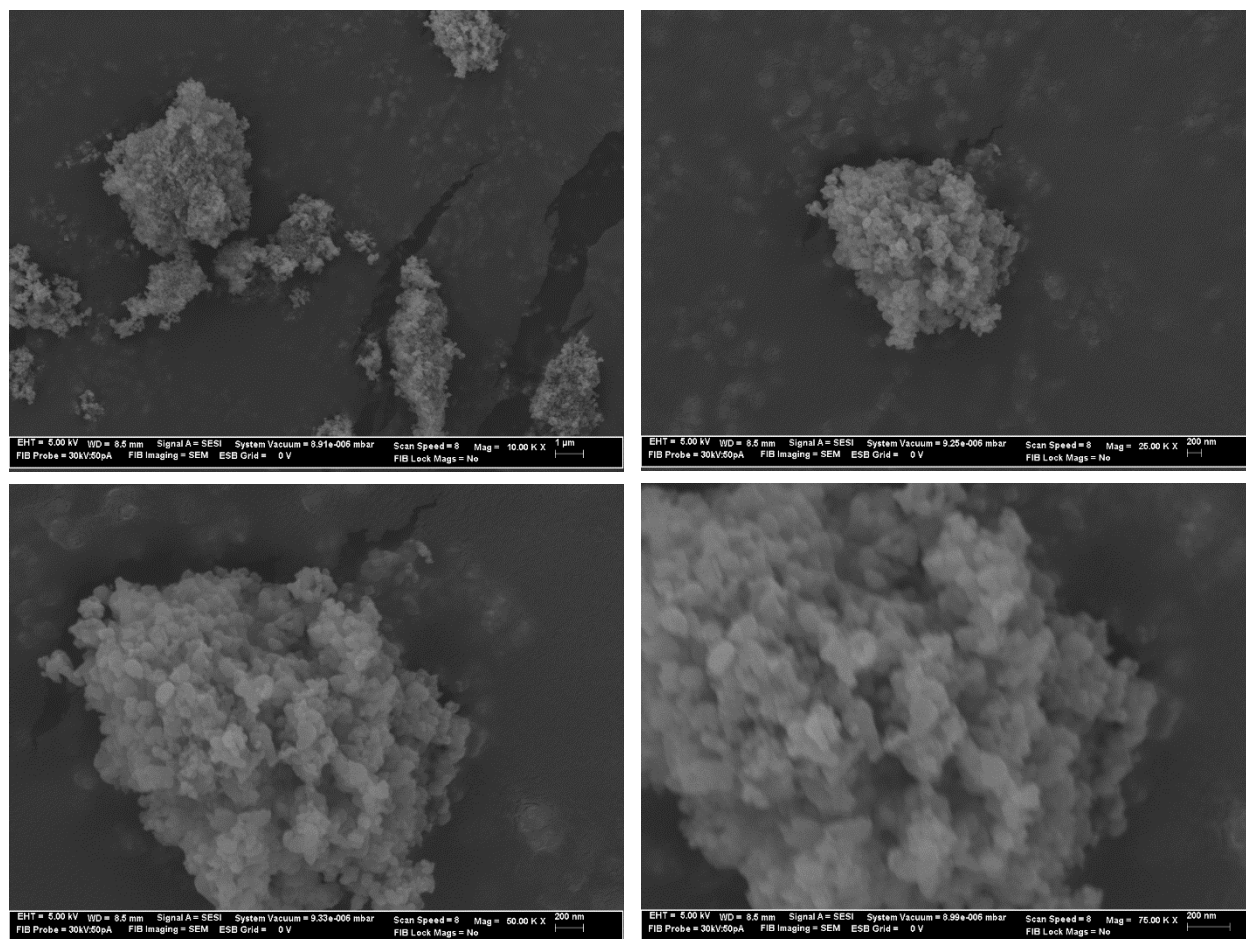


**Figure S102.** SEM images of Co-ppgy-3AP at 1  $\mu$ m (top left), 200 nm (top right), 200 nm (bottom left), and 200 nm (bottom right).

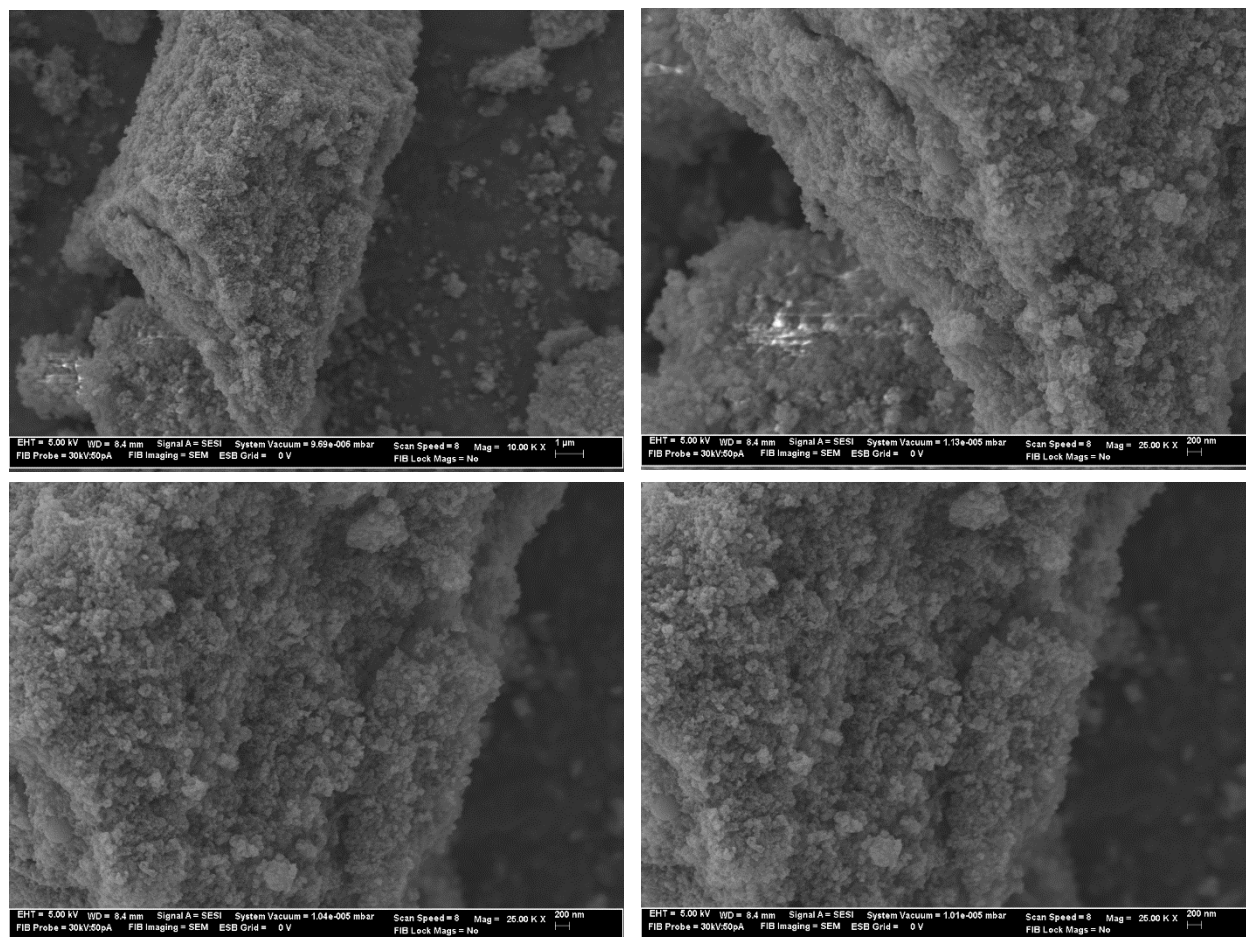


**Figure S103.** SEM images of Co-ppgy-6AH at 1  $\mu$ m (top left), 200 nm (top right), 200 nm (bottom left), and 200 nm (bottom right).

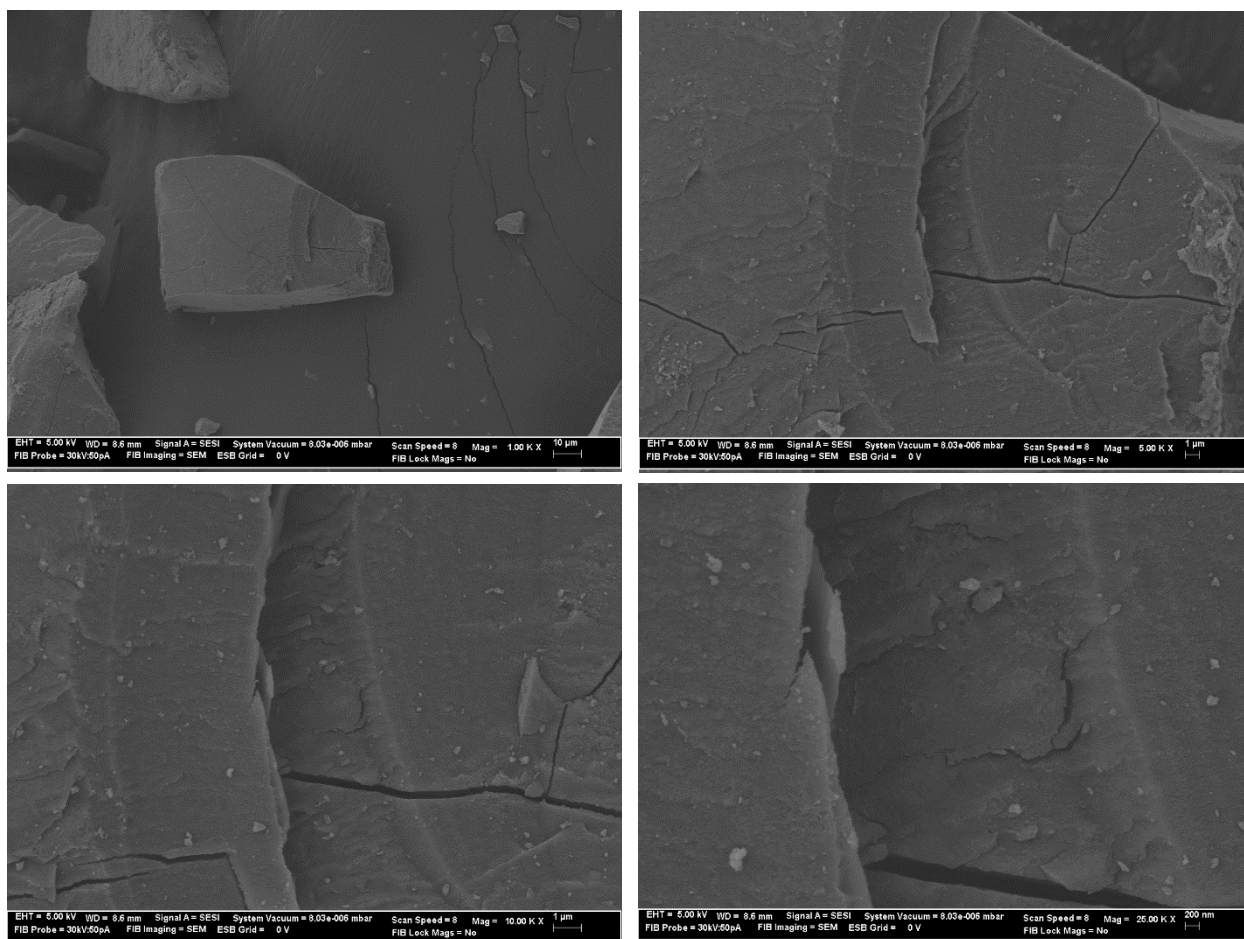


**Figure S104.** SEM images of Co-N<sub>3</sub>-PrOH at 10 um (top left), 1 um (top right), 1 um (bottom left), and 200 nm (bottom right).

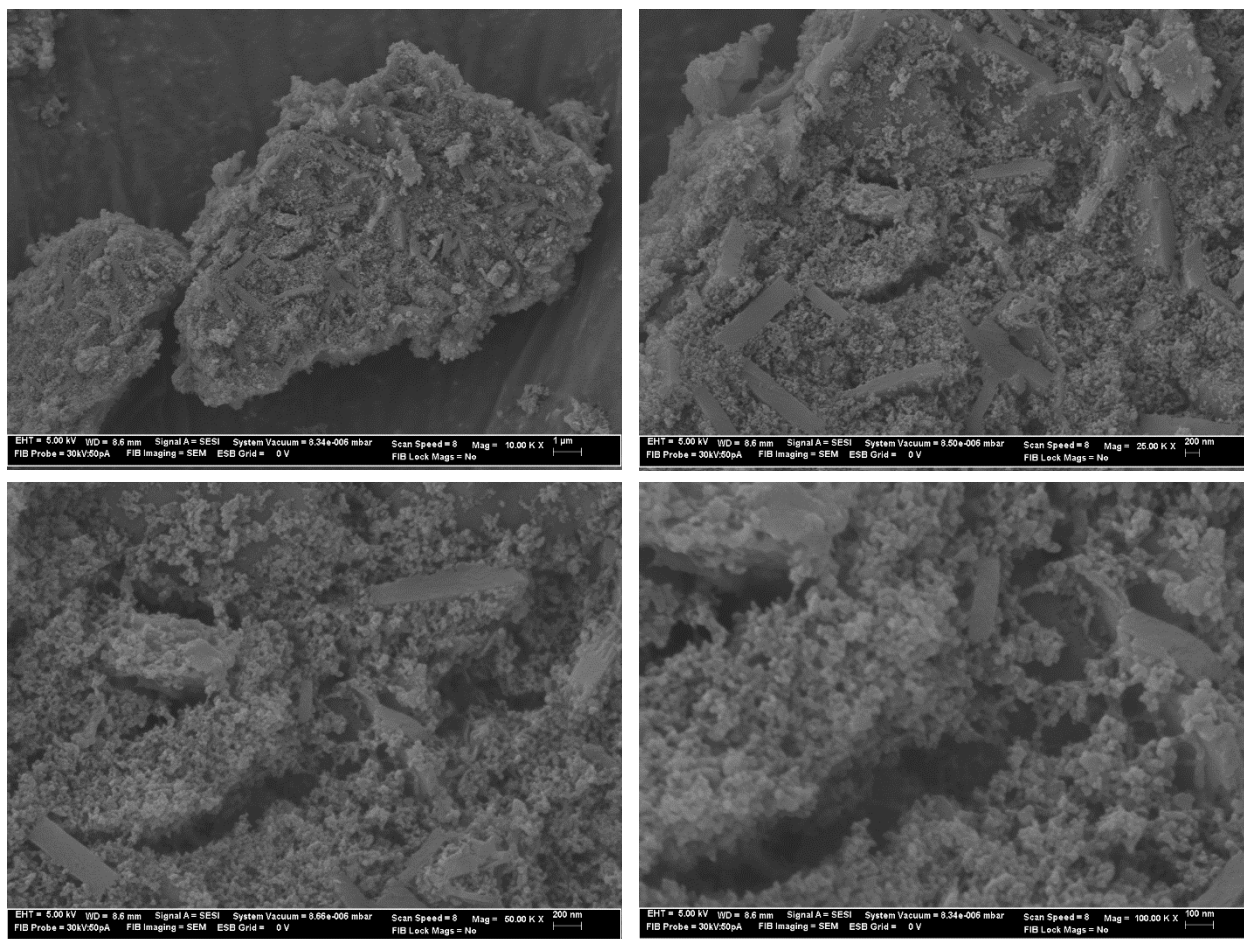


**Figure S105.** SEM images of Co-N<sub>3</sub>-EP at 1 μm (top left), 200 nm (top right), 200 nm (bottom left), and 100 nm (bottom right).



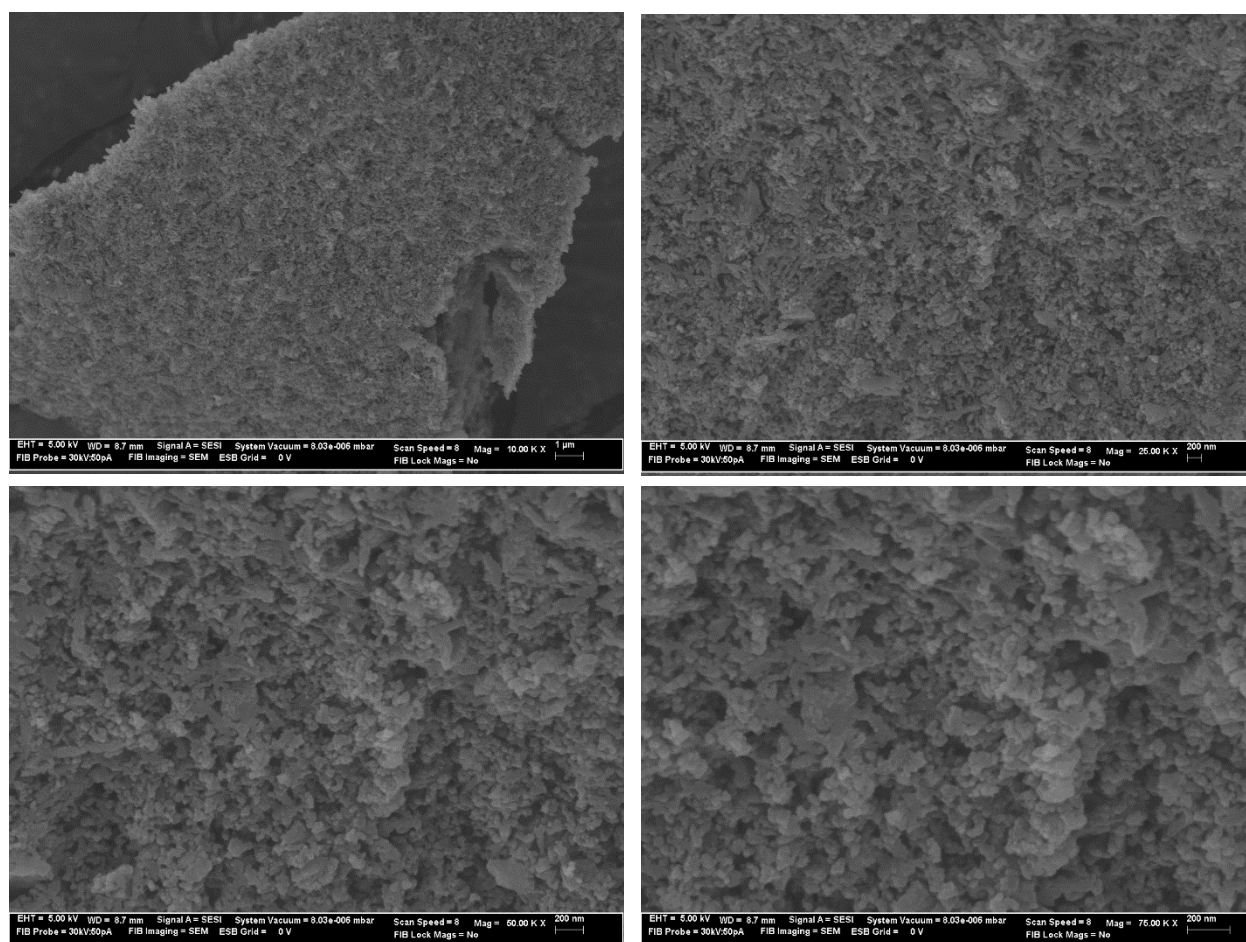


**Figure S106.** SEM images of Co-N<sub>3</sub>-PA at 1  $\mu$ m (top left), 200 nm (top right), 200 nm (bottom left), and 200 nm (bottom right).

## Crystal Structures

**X-ray structural analysis for Co-ppgy, Co-N<sub>3</sub>, Zr(5-N<sub>3</sub>), Zr(5-ppgy), and Zr(2,5-dippgy):** Crystals were mounted using viscous oil, perfluoroalkane or mother liquor onto a plastic mesh and cooled to the data collection temperature. Data were collected on a D8 Venture Photon III diffractometer with Cu-K $\alpha$  radiation ( $\lambda = 1.54178$  Å) focused with Goebel mirrors. Unit cell parameters were obtained from fast scan data frames, 1°/s  $\omega$ , of an Ewald hemisphere. The unit-cell dimensions, equivalent reflections and systematic absences in the diffraction data are consistent with *Cc* and *C2/c* for Zr(5-N<sub>3</sub>) and Zr(5-ppgy), and, uniquely, *I4<sub>1</sub>/a* for Zr(2,5-dippgy). No symmetry higher than triclinic was observed in Co-ppgy and Co-N<sub>3</sub>. Refinement in the centrosymmetric space group options for the non-unique cases yielded chemically reasonable and computationally stable results of refinement. The data were treated with multi-scan absorption corrections.<sup>6</sup> Structures were solved using intrinsic phasing methods<sup>7</sup> and refined with full-matrix, least-squares procedures on  $F^2$ .<sup>8</sup> These compounds apparently consistently deposited as weakly diffracting crystals and the data herein represent the best of several trials.

In each case the compound molecule is located at special positions: for Zr(5-N<sub>3</sub>) and Zr(5-ppgy), a two-fold rotation axis; for Co-ppgy, and Co-N<sub>3</sub>, an inversion center; and for Zr(2,5-dippgy), a four-fold rotoinversion axis. In each structure, presumably disordered solvent molecules and anions which could not be satisfactorily modeled were treated as diffused contributions with identities assigned based on the electron counts from the Squeeze results.<sup>9</sup>

Non-hydrogen atoms were refined with anisotropic displacement parameters. All hydrogen atoms were treated as idealized contributions with geometrically calculated positions and with  $U_{iso}$  equal to 1.2  $U_{eq}$  (1.5  $U_{eq}$  for methyl) of the attached atom.

Atomic scattering factors are contained in the SHELXTL program library.<sup>7</sup> The structures have been deposited at the Cambridge Structural Database under the following CCDC depositary numbers: CCDC 2191126-2191130.

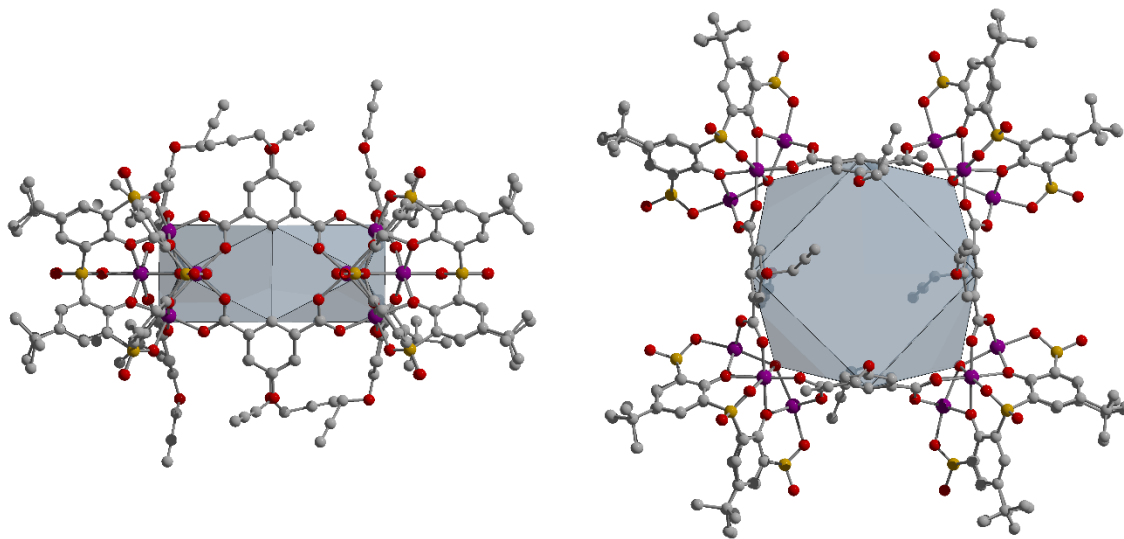


**Figure S107.** Single crystal structural depictions of Co-ppgy.



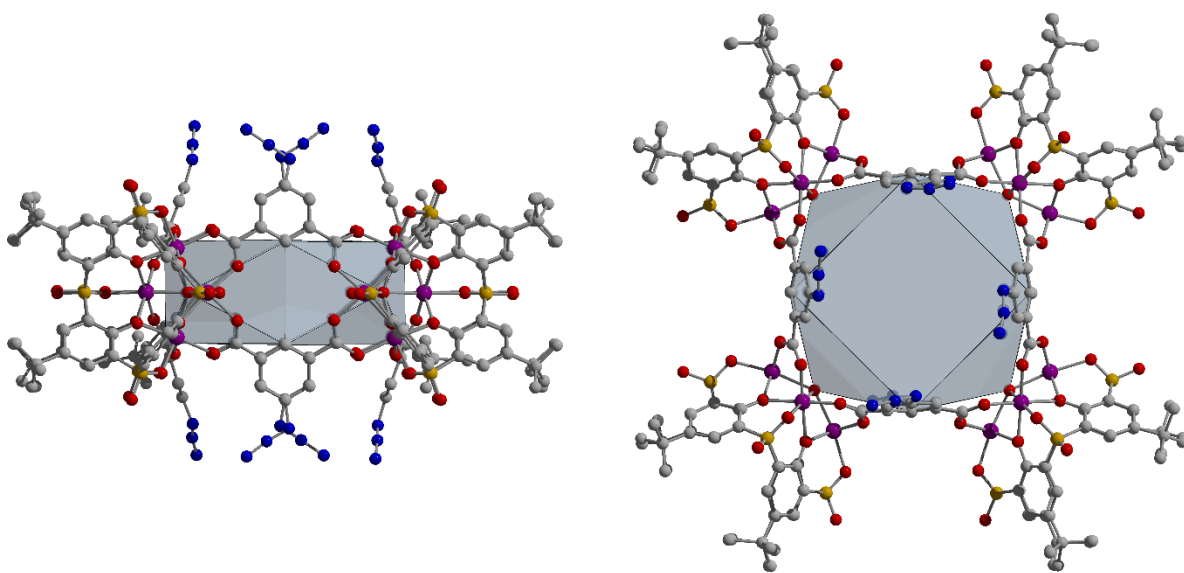


**Figure S108.** Single crystal structural depictions of Co-N<sub>3</sub>.

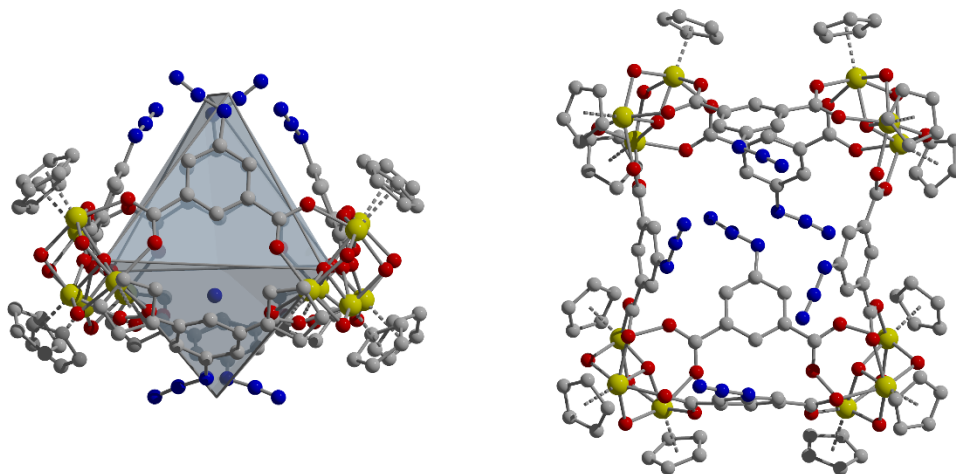


**Figure S109.** Single crystal structural depictions of Zr(5-N<sub>3</sub>).

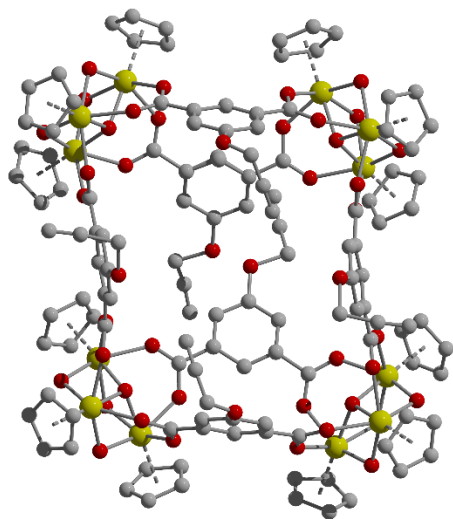


**Figure S110.** Single crystal structural depiction of Zr(5-ppgy).

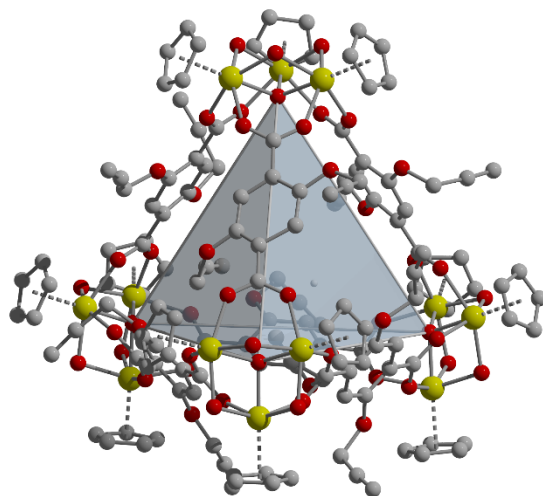


**Figure S111.** Single crystal structural depiction of Zr(2,5-dippgy).

**Table S4.** Crystal data and structure refinement details.

Compound	Co-ppgy	Co-N <sub>3</sub>	Zr(5-N <sub>3</sub> )
Sum Formula	C <sub>368</sub> Co <sub>16</sub> H <sub>508</sub> N <sub>40</sub> O <sub>132</sub> S <sub>16</sub>	C <sub>190</sub> H <sub>269</sub> N <sub>22</sub> Ni <sub>6</sub> O <sub>54</sub> S <sub>8</sub>	C <sub>108</sub> H <sub>94</sub> N <sub>18</sub> O <sub>40</sub> Zr <sub>12</sub> , 4(Cl), 20[C <sub>3</sub> H <sub>7</sub> NO]
Moiety Formula	C <sub>248</sub> H <sub>228</sub> Co <sub>16</sub> O <sub>92</sub> S <sub>16</sub> , 40[C <sub>3</sub> H <sub>7</sub> NO]	C <sub>224</sub> H <sub>200</sub> Co <sub>16</sub> N <sub>24</sub> O <sub>84</sub> S <sub>16</sub> , 50[C <sub>3</sub> H <sub>7</sub> NO]	C <sub>208</sub> H <sub>164</sub> N <sub>4</sub> Ni <sub>8</sub> O <sub>42</sub> S <sub>8</sub> , 2(C <sub>3</sub> H <sub>7</sub> NO), 14[C <sub>3</sub> H <sub>7</sub> NO]
Formula Weight, g/mol	9059.95	9682.69	4982.36
Temperature, K	150.0	120.0	150
Crystal system	triclinic	triclinic	monoclinic
Space group	<i>P</i> -1	<i>P</i> -1	<i>C</i> 2/c
Cell dimensions			
<i>a</i> , Å	20.642(2)	20.646(3)	29.144(3)
<i>b</i> , Å	20.651(3)	20.661(3)	26.347(3)
<i>c</i> , Å	28.167(4)	27.970(4)	29.344(3)
α, °	92.828(6)	96.343(5)	90
β, °	96.711(6)	92.698(5)	91.235(4)
γ, °	111.522	112.580(5)	90
Volume, Å <sup>3</sup>	11038(2)	10897(2)	22526(4)
<i>Z</i>	1	1	4
ρ <sub>calc</sub> , g/cm <sup>3</sup>	1.363	1.475	1.469
μ/mm <sup>-1</sup>	6.001	6.143	5.480
<i>F</i> (000)	4740.0	5072.0	10144.0
Reflections collected	103251	98463	26572
Independent reflections	20055	25929	6830
Data/restraints/parameters	20055/3300/1612	25929/3077/1511	6830/2195/710
Goodness-of-fit	1.746	1.067	1.049
<i>R</i> [ <i>I</i> ≥ 2σ ( <i>I</i> )] <i>R</i> <sub>1</sub> / <i>wR</i> <sub>2</sub>	0.1579/0.4143	0.1419/0.3661	0.0791/0.2258
<i>R</i> indexes [all data] <i>R</i> <sub>1</sub> / <i>wR</i> <sub>2</sub>	0.1038/0.4364	0.2120/0.3988	0.1076/0.2568
CCDC	2191126	2191127	2191128

**Table S4.** Crystal data and structure refinement details. (continued)

Compound	Zr(5-ppgy)	Zr(2,5-dippgy)
Sum Formula	C <sub>189</sub> Cl <sub>4</sub> H <sub>255</sub> N <sub>21</sub> O <sub>67</sub> Zr <sub>12</sub>	0.5(C <sub>144</sub> H <sub>120</sub> O <sub>52</sub> Zr <sub>12</sub> ),
Moiety Formula	C <sub>126</sub> H <sub>108</sub> O <sub>46</sub> Zr <sub>12</sub> , 4(Cl), 21[C <sub>3</sub> H <sub>7</sub> NO]	0.5(C <sub>144</sub> H <sub>120</sub> O <sub>52</sub> Zr <sub>12</sub> ), 2(Cl), 2 (C <sub>3</sub> H <sub>7</sub> NO), 2[C <sub>3</sub> H <sub>7</sub> NO], 2[H <sub>2</sub> O]
Formula Weight, g/mol	5129.56	2099.56
Temperature, K	150.0	150.0
Crystal system	monoclinic	tetragonal
Space group	C2/c	I4 <sub>1</sub> /a
Cell dimensions		
<i>a</i> , Å	28.889(5)	33.5754(18)
<i>b</i> , Å	27.244(5)	33.5754(18)
<i>c</i> , Å	29.476(5)	17.8640(11)
α, °	90	90
β, °	91.802(7)	90
γ, °	90	90
Volume, Å <sup>3</sup>	23189(7)	20138(2)
<i>Z</i>	4	8
ρ <sub>calc</sub> g/cm <sup>3</sup>	1.469	1.385
μ/mm <sup>-1</sup>	5.343	5.967
<i>F</i> (000)	10480.0	8384.0
Reflections collected	96695	72722
Independent reflections	12112	7988
Data/restraints/parameters	12112/1959/854	7988/344/576
Goodness-of-fit	1.063	1.046
<i>R</i> [ <i>I</i> ≥ 2σ ( <i>I</i> )] <i>R</i> <sub>1</sub> / <i>wR</i> <sub>2</sub>	0.0869/0.2392	0.0730/0.2028
<i>R</i> indexes [all data] <i>R</i> <sub>1</sub> / <i>wR</i> <sub>2</sub>	0.1009/0.2547	0.0939/0.2214
CCDC	2191129	2191130

<sup>1</sup> K. S. Walton and R. Q. Snurr, *J. Am. Chem. Soc.* 2007, **129**, 8552-8556.<sup>2</sup> H. Kumagai, M. Hasegawa, S. Miyanari, Y. Sugawa, Y. Sato, T. Hori, S. Ueda, H. Kamiyama and S. Miyano, *Tetrahedron Lett.* 1997, **38**, 3971-3972.<sup>3</sup> N. Iki, H. Kumagai, N. Morohashi, K. Eijma, M. Hasegawa, S. Miyanari and S. Miyano, *Tetrahedron Lett.* 1998, **39**, 7559-7562.<sup>4</sup> A. Mallick, B. Garai, D. D. Díaz and R. Banerjee, *Angew. Chem. Int. Ed.* 2013, **52**, 13755-13759.<sup>5</sup> N. Ahmad, H. A. Younus, A. H. Chughtai, K. Van Hecke, Z. A. K. Khattak, Z. Gaoke, M. Danish and F. Verpoort, *Catal. Sci. Technol.* 2018, **8**, 4010-4017.<sup>6</sup> Apex4 [Computer Software]; Bruker AXS Inc.: Madison, WI, USA, 2021.<sup>7</sup> G. M. Sheldrick, *Acta Cryst.* 2015, **A71**, 3-8.<sup>8</sup> G. M. Sheldrick, *Acta Cryst.* 2015, **C71**, 3-8.<sup>9</sup> A. L. Spek, *Acta Cryst.* 2015, **C71**, 9-18